Dendritic cell-specific function of OTUB1 in inflammation and infection

Dissertation

zur Erlangung des akademischen Grades

doctor rerum naturalium (Dr. rer. nat.)

genehmigt durch die Fakultät für Naturwissenschaften der Otto-von-Guericke-Universität Magdeburg

von **M.Sc. Floriana Mulas**

geb. am 09 September 1990 in Cagliari

Gutachter:

Prof. Dr. med. Dirk Schlüter

Prof. Dr. med. Roland Lang

eingereicht am: 20.02.2020

verteidigt am: 29.09.2020

This study has been published under the following title:

Floriana Mulas, Xu Wang, Shanshan Song, Gopala Nishanth, Wenjing Yi, Anna Brunn, Pia-Katharina Larsen, Berend Isermann, Ulrich Kalinke, Antonio Barragan, Michael Naumann, Martina Deckert, Dirk Schlüter. **The deubiquitinase OTUB1 augments NF-κB dependent immune responses of dendritic cells by stabilization of UBC13 in infection and inflammation.** **CELL MOL IMMUNOL** (2020). DOI: 10.1038/s41423-020-0362-6

Additional publication during the PhD:

Xu Wang, Floriana Mulas, Wenjing Yi, Anna Brunn, Gopala Nishanth, Sissy Just, Ari Waisman, Wolfgang Brück, Martina Deckert and Dirk Schlüter. **OTUB1 inhibits CNS autoimmunity by preventing IFN-γ-induced hyperactivation of astrocytes. EMBO J.** (2019). DOI: I*10.15252/embj.2018100947*

Table of Contents

Abbreviations

A

APC = Antigen Presenting Cell

ATM = Ataxia Telangiectasia Mutated

B

BAFF = B-cell Activating Factor

BAFFR = B-cell Activating Factor Receptor

BMDC = Bone Marrow-derived Dendritic Cell

BMDM = Bone Marrow-derived Macrophages

BSA = Bovine Serum Albumin

C

CBA = Cytometric Bead Assay

CCL = C-C Chemokine receptor Ligand

CCR = C-C Chemokine receptor

CD = Cluster of Differentiation

cDC = Conventional Dendritic Cell

CHX = Cycloheximide

CLR = C-type Lectin Receptors

CYLD = Cylindromatosis

D

DC = Dendritic Cell

DMSO = Dimethylsulfoxide

DPBS = Dulbecco's Phosphate-Buffered Saline

DUB = Deubiquitinase

E

ELKS = Protein rich in amino acids E (Glutamic acid), L (Leucine), K (Lysine) and S (Serine)

ER = Estrogen Receptor

ERAD = Endoplasmic Reticulum Associated Degradation

F

FcgRI = Fcgamma receptor 1

FCS = Fetal Bovine Serum

FLT3-L = Fetal Liver Tyrosine Kinase 3 Ligand

FN = Fibroblast growth factor-inducible

G

GBP = Guanylate Binding Protein

GM-CSF = Granulocyte Macrophage Colony Stimulating Factor

H

HECT = Homologous to E6-associated protein C-terminus

HIV = Human Immunodeficiency Virus

I

i.p. = Intraperitoneally

i.v. = Intravenously

IAA = Indole-3-acetic acid sodium

iDC = Inflammatory Dendritic Cell

IDO = Indoleamine 2,3-dioxygenase

IFN = Interferon

iGTP = Inducible Guanosine 5'-Triphosphate

IKB = Inhibitor of NF-κB

IKK = IKBα Kinase

IL = Interleukin

IMQ = Imiquimod

iNOS = Inducible Nitric Oxide Synthase

K

K = Lysine

L

LN = Lymph Node

LPS = Lipopolysaccharide

LRR = Leucine-Rich Repeat domain

LTβR = Lymphotoxin β Receptor

M

M = Methionine

MAPK = Mitogen-Activated Protein Kinase

MCMV = Murine Cytomegalovirus

M-CSF = Macrophage Colony Stimulating Factor

MHC = Major Histocompatibility Complex

moDC = Monocyte-derived Dendritic Cell

MOI = Multiplicity of Infection
MyD88 = Myeloid differentiation primary
      response gene 88
Mϕ = Macrophage

N

NEAA = Non-Essential Amino Acids
NEM = N-Ethylmaleimide
NEMO = NF-kB Essential Modulator
NF-κB = Nuclear Factor Kappa B
NIK = NF-κB Inducing Kinase
NK = Natural Killer Cell
NKT =   Natural killer T-cell
NLR = Nucleotide-binding oligomerization
      domain-like receptors
NLS = Nuclear Localization Sequence

O

ODN = Oligodeoxynucleotide
OTUB1 = Ovarian Tumor domain, ubiquitin
      aldehyde binding 1

P

p.i. = Post Infection
PAMP = Pathogen-associated Molecular
      Patterns
pDC = Plasmacytoid Dendritic cell
PGE2 = Prostaglandin E2
PGN = Peptidoglycan
PP = Phosphatases
PRR = Pattern Recognition Receptor
PTM = Post-Translational Modifications
pUb = Poly-Ubiquitin

R

RANK = Receptor Activator for the NF-κB
RHD = Rel Homology Domain
RING = Really interesting New Gene
RLR = RIG-1 like receptors
RNS = Reactive Nitrogen Species
ROS = Reactive Oxygen Species

S

SPF = Specific Pathogen-Free

T

T. gondii = *Toxoplasma gondii*
TE = *Toxoplasma* encephalitis
TgPFN = *Toxoplasma gondii* Profilin
Th = T Helper
TIR = Toll/IL-1 receptor homology
TLA = *Toxoplasma gondii* lysate antigens
TLR = Toll-like Receptor
TNF = Tumor Necrosis Factor
TNFR = Tumor Necrosis Factor Receptor
Treg = Regulatory T cell
TSLP = Thymic Stromal Lymphopoietin
TTP = Tristetraprolin

U

U-Box = UFD2 homology
UCH = Ubiquitin C terminal Hydrolases
USP = Ubiquitin-Specific Proteases
UV = Ultraviolet

W

WB = Western Blot

SUMMARY

Dendritic cells (DCs) are key sentinel and professional antigen-presenting cells (APCs) of the immune system. They bridge the innate and adaptive immune responses, and play indispensable roles in the host defence against invading pathogens including viruses, bacteria, and parasites, but may also contribute to immunopathology. Activation of DCs upon sensing of pathogens by Toll-like receptors (TLRs) is largely mediated by NF-κB signaling, which broadly depends on the appropriate ubiquitination of the respective signaling molecules. However, the involved ubiquitinating and deubiquitinating enzymes and their interaction are only incompletely understood. Here, we identified that the deubiquitinase OTU domain, ubiquitin aldehyde binding 1 (OTUB1) is upregulated in vivo and in vitro in DCs upon murine *Toxoplasma (T.) gondii* infection and lipopolysaccharide (LPS) challenge. Stimulation of DCs with the TLR11/12 ligand *T. gondii* profilin and the TLR4 ligand LPS induced an increased NF-κB activation in OTUB1-competent cells resulting in elevated IL-6, IL-12 and TNF production, which was also observed upon specific stimulation of TLR2, TLR3, TLR7, and TLR9. Mechanistically, OTUB1 promoted NF-κB activity in DCs by removing K48 ubiquitination and, therefore, by stabilizing the E2 conjugating enzyme UBC13 resulting in increased K63 ubiquitination of IRAK1 and TRAF6. Consequently, DC-specific deletion of OTUB1 impaired cytokine production, in particular IL-12, of DCs in the first two days of *T. gondii* infection resulting in diminished production of protective IFN-γ by NK cells, an impaired control of parasite replication and, finally, death from chronic *Toxoplasma* encephalitis, which all could be prevented by low-dose IL-12 treatment in the first three days of infection. In contrast, impaired activation and cytokine production of OTUB1-deficient DCs protected mice from LPS-induced immunopathology. Collectively, these experiments identified OTUB1 as a potent novel regulator of DCs during infectious and inflammatory diseases.

1. INTRODUCTION

1.1 DENDRITIC CELLS

Described for the first time in 1973 by Steinman and Cohn [1], the dendritic cell (DC) family has been revealed to be fundamental sentinels of the immune system and to play an unique role as a bridge between innate and adaptive immune response. The DC family is constituted of several different sub-populations, distributed in lymphoid and non-lymphoid organs. DCs originate from a common CD34^{+} precursor in the bone marrow and subsequentially differentiate in secondary lymphoid organs or peripheral tissues depending on the subset [2,3].

1.1.1 DC subsets

In mice, three major population of DCs exist that develop independently under control of unique masters of transcriptional regulation and that express different DC lineage markers:

(i)   conventional type 1 DCs (cDC1s) develop in a BATF3- and IRF8-dependent manner and express CD8α^{+} or CD103^{+} depending on their anatomic localization in lymphoid organs and tissues;

(ii)   conventional type 2 DCs (cDC2s), characterized by CD11b^{+} and CD172a^{+} expression, develop in an IRF4-dependent manner and represent the most abundant DC subset;

(iii)   plasmacytoid DCs (pDCs), characterized by high secretion of IFNα, are dependent on E2-2 and may arise from common DC and common lymphoid progenitors. [4–6]

All DC subpopulations share important characteristics, such as the high expression of CD11c, constitutive expression of MHC class II and their capability of processing antigens and activating naïve T cells. However, cDCs and pDCs differ in other important features and functions. Generally, cDCs are mainly located in secondary lymphoid organs such as spleen,

lymph nodes (LNs), Peyer's patches, but they can also migrate to non-lymphoid organs in response to inflammatory stimuli. cDCs are the most specialized antigen presenting cells (APCs) and they are fundamental to mediate the cross-talk to T cells. In addition, they have enhanced sensibility to tissue injuries and they are able to enforce self-tolerance due to their critical location in secondary lymphoid organs [7].

Although numbers of pDC are relatively small compared with other DC subsets, pDCs have been identified not only in spleen, LNs, and other lymphoid tissues, but also in liver, lung, skin, and other non-lymphoid organs. It has been widely demonstrated that pDCs are *in vivo* specialized producers of type I Interferon (IFN) in response to the recognition of DNA and RNA viruses via Toll-like Receptor (TLR) 9. Type I IFN secreted by pDCs mediates activation of NK cells, B cells, and may induce Th1 differentiation and subsequent IFN-γ production [8].

In addition to these three main DCs subsets, monocyte-derived DCs (moDCs), or inflammatory DCs (iDCs), have been identified as the forth important DC subtype [9]. As the name suggests, these cells originate from monocytes as a consequence of infiltration or inflammation. Phenotypically, it is difficult to distinguish this particular subtype from cDCs, because they both express DC antigens, such as class II MHC, CD11b$^+$, and CD11c^{hi}, and monocyte-lineage antigens such as CD64$^+$, Fcgamma receptor 1 (FcgRI) F4/80$^+$, and Ly6C$^+$. These DCs are characterized by high production of proinflammatory cytokines including IL-12 and IL-23 and by the capability of activating Th1 and Th17 phenotypes [10,11].

1.1.2 Functions of DCs

DCs play a unique and irreplaceable role in the activation of the immune response and they serve three main roles: (i) sentinels of the immune system, (ii) migration and transport of antigens, and (iii) activation of other cells of the immune system. DCs are appropriately

defined as "Sentinels of the Immunity and Tolerance" [12] for their capability to uptake and process virtually any types of endogenous and exogenous antigens, in both MHC I and MHC II context. DCs can present peptides that are derived from proteasomal degradation of endogenous proteins on MHC class I molecule. Besides, DCs can internalize extracellular material by macropinocytosis, phagocytosis, and receptor-mediated endocytosis. Antigens are then degraded in endosomes and the generated peptides are transported to the MHC II [13]. Interestingly, CD8+ DCs have the unique ability to present exogenous antigens by MHC I [14], in a process called "cross-presentation" that is still poorly understood today [15]. The DC's capability of presenting self-antigens is also crucial for the development of self-tolerance and thymic negative selection of CD4+ and CD8+ T cells [13].

Immature DCs slowly and randomly circulate in uninfected tissues scouting for pathogens. Once the pathogens are detected, DCs undergo a series of metabolic and morphological changes, which enable them to enter the lymphatic system from the peripheral tissues and finally reach the LNs where they can present the antigens to T cells [16]. The movement of activated DCs to LN is largely mediated by the C-C Chemokine receptor 7 (CCR7) expressed on activated DCs and CCL21, the ligand of CCR7 produced by lymphatic endothelial cells [17, 18, 19,20]. During infection, the local production of pro-inflammatory cytokines, such as interleukin-1 (IL-1), tumor necrosis factor (TNF) and prostaglandin E2 (PGE2), respectively, is additionally crucial for the initiation of DC migration [21].

The ability to stimulate the proliferation of both naïve CD4+ and CD8+ T cells and to induce a primary immune response are shared among all the DC subsets. Accordingly to the type of stimuli, DCs can express different antigens and initiate distinct T cell differentiations including CD40L-mediated Th1 differentiation and thymic stromal lymphopoietin (TSLP) triggered Th2 differentiation [22]. The secretion of cytokines by DCs is also a critical step for the maturation of

several cell types. For example DCs can promote Th17 differentiation by the secretion of transforming Growth Factor β (TGF-β), IL-23 and IL-1β [23]. In addition, DCs can also efficiently inhibit the immune response by inducing the generation of Tregs, which can block DC maturation, activation and proinflammatory cytokine production [24]. A study from Kim et al. (2007) described that the numbers of Tregs and DCs were closely correlated, and that, depletion of Treg resulted in a strong proliferation of DCs [25]. In fact, DCs and Tregs crossregulate each other to prevent uncontrolled immune responses [26, 27].

Of note, DCs also interact with other immune cells, such as B cells, NKT cells and all granulocyte subtypes, affecting the maturation stage of those cells and DC itself [28,29,30,30,31,32]. Therefore, DCs are indispensable for the delicate balance between activation and limitation of an immune response. Indeed, a complete suppression of CD11c$^+$ cells or of any DCs subsets results in devastating autoimmune diseases [33] or myeloproliferative disorders [34].

1.1.3 Molecular mechanisms of DC activation

DCs recognize pathogens by structures that are unique to pathogens and that are distinct from the ones expressed by host cells. These pathogen-specific structures are called Pathogen-associated Molecular Patterns (PAMPs) and are conserved among a great number of micro-organisms [35]. Common PAMPs include proteins from bacteria (e.g. flagellin), glycans from bacteria or fungi, cell surface molecules of bacteria such as LPS, and nucleic acids from viruses. The recognition of PAMPs by the innate immune system is mediated by particulars receptors named Pattern Recognition Receptors (PPRs). The PPRs are divided into 4 families:

- Toll-like receptors (**TLR**)
- Nucleotide-binding oligomerization domain-like receptors (**NLR**)
- C-type lectin receptors (**CLR**)

- RIG-1 like receptors (**RLR**)

These receptors are localized either on the cell surface to recognize extracellular PAMPs or in the endosomes to recognize intracellular micro-organisms. After activation by the specific ligands, PPRs activate various signaling pathways that eventually result in gene transcription, cytokine production (including IFN-α, IFN-β, IL-12, TNF, IL-6, and IL-1), DC maturation and, ultimately, the elimination of the pathogen. PPRs can also collaborate with each other to activate multiple and stronger responses [36]. Among all the PPRs, the most studied and best characterized is the TLRs family.

TLRs are a group of transmembrane proteins characterized by an extracellular leucine-rich repeat domain (LRR), a single transmembrane domain, and an intracytoplasmic domain crucial for signal transduction termed as the Toll/IL-1 receptor homology (TIR) domain. TLRs are highly expressed in both immune cells including DCs, mast cells, and Mφ, but also in non-immune cells such as fibroblast, epithelial cells and endothelial cells [37]. In 1997, Janeway identified the first human TLR, i.e. TLR4 [38]. Each of the 10 humand and 12 murine TLRs has major specificity for particular PAMPs as summarized in Table 1 [39,40].

HUMAN		MOUSE	
TLR1/ TLR2/ TLR6	Peptidoglycan *Neisseria meningitis* *Mycobacterium* Yeast *Trypanosoma cruzi*	TLR1/TLR2	Lipopeptide
		TLR2	Peptidoglycan *Staphylococcus aureus* Lipoteichoic Acid Glycolipid Phospholipomannan (*Candida albicans*) LPG (*Leishmania major*) GPI Anchors *Trypanosoma cruzi*
TLR3	Double-strand DNA (viruses)		
TLR4	LPS Lipoteichoic acid	TLR3	Double-strand RNA (viruses)
TLR7/TLR8	F protein (from respiratory syncytial virus) Synthetic compounds Single-strained RNA	TLR4	LPS Mannan Glycoinositolphospholipids GPI anchors
		TLR5	Flagellin
TLR9	*Influenza virus* CpG DNA *Herpes simplex virus*	TLR6	Mycoplasma *Saccharomyces cerevisiae* GPI Anchors
		TLR7/TLR8	Single-strand RNA (virus and non-viral origin) Guanine-rich ssRNA
		TLR9	CpG DNA Genomic DNA *Plasmodium falciparum*
		TLR11/TLR12	Profilin (*Toxoplasma gondii*)

Table 1 *Ligand specificity for TLRs in human and mouse (modified from [39,40])*

The binding of the TLRs with their specific ligand induces the recruitment of adaptor proteins in the TIR domain. The most common adaptor protein is MyD88, which is the adaptor protein for all the TLRs except for TLR3 [41]. The ligation of MyD88 with the TIR domain of TLRs stimulates the activation of intracellular signaling pathways including MAPK and NF-κB pathways. Studies with MyD88-deficient mice reveal that MyD88 plays an indispensable role in the activation of these signaling pathways, as in the absent of MyD88, Mφ and DCs are completely deficient in the production of pro-inflammatory cytokines in response to TLR ligands [42,43,44].
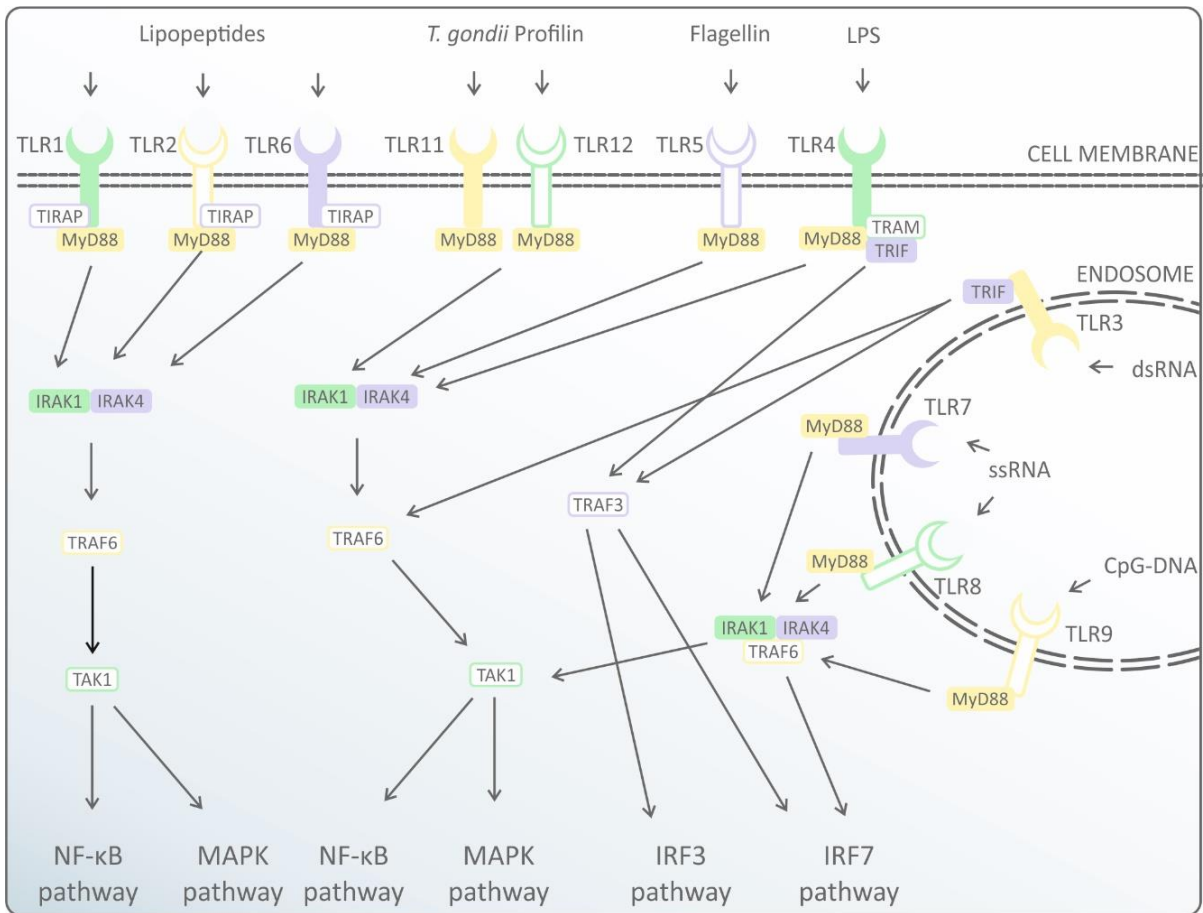
Figure 1 Summary of the pathways activated by TLRs.(modified from [42,43,44])

1.2 THE NF-κB PATHWAY

Since its first discovery in 1986 by Sen and Baltimore [45], the NF-κB pathway has been a central focus of investigation for the last 20 years. Nowadays, it is clearly evident that this tightly regulated pathway critically coordinates a wide range of immunological processes, is essential for the transcription of genes encoding pro- and anti-inflammatory cytokines, chemokines, costimulatory and adhesion molecules, and modulates cell death or proliferation [46]. In addition, a canonical, non-canonical and so called "atypical" NF-κB pathways have been described [47–53].

The NF-κB family consists of 5 members: NF-κB1 (p105/p50), NF-κB2 (p100/p52), RelA (p65),

RelB and c-Rel. NF-κB1 and NF-κB2 are synthesized as large precursors (p105 and p100), which are proteolytically processed to p50 and p52 respectively. These subunits form homo- and heterodimeric complexes that regulate NF-κB-specific genes [54]. In unstimulated cells, NF-κB members exist as homo- or heterodimers bound to inhibitory IκB family members (such as IκBα, IκBβ and IκBε) that maintain the associated NF-κB molecules in the cytoplasm. Two major stimuli lead to translocation of NF-κB dimers from the cytoplasm to the nucleus: pro-inflammatory cytokines (e.g. TNF) and PAMPs. These stimuli trigger ubiquitination and subsequent degradation of the inhibitor molecules. Finally, the free active NF-κB dimers migrate into the nucleus to activate gene target transcription [55,56].

1.2.1 Canonical NF-κB activation

The canonical NF-κB pathway requires the activation of the IKK complex. This complex consists of one scaffold/adaptor protein NEMO (also called IKKγ) and two IKK kinases: IKKα and IKKβ (also called IKK1 and IKK2, respectively). These molecules are so critical for immune responses and cell functions, that the loss of one of these kinases is not compatible with life [57]. A wide variety of activated receptors including TLRs, TNF receptor and IL-1 receptor can induce phosphorylation-dependent activation of the IKK complex. The phosphorylation of the IKK complex results in binding and phosphorylation of IκBα at specific serine residues in the N-terminal part. The phosphorylated IκBα is subsequently targeted by the E3 ligase β-TrCP-SCF, which adds K48 polyubiquitin (pUb) chains on IκBα leading to its degradation via the 26S proteasome [55]. The degradation of the inhibitor release NF-κB dimers, allowing them to translocate to the nucleus and to start gene transcription. The TLR-mediated activation of NF-κB is mostly dependent on MyD88 (except for TLR3, which uses TRIM as adaptor molecule). After the binding with the specific ligands, MyD88 is rapidly recruited to the receptor (within

minutes), and this adaptor recruits and activates several kinases from the IRAK family (IRAK1, IRAK4 and IRAK2) and other activator molecules (e.g. Pellino, UBC13, Tollip, etc.). This leads to the activation of the TAK/TABs complex that finally phosphorylates and activates the IKKs [55]. One interesting feature of NF-κB activity is the strong interaction with other signal transduction pathways such as the MAPK signaling. Indeed, phosphorylation of TAK1 leads not only to the activation of the IKK complex, but also to the activation of MAPKs [58]. A schematic representation of the canonical activation of NF-κB is shown in Figure 2 (left).

1.2.2 Non-canonical NF-κB activation

The non-canonical activation of NF-κB is independent of NEMO and IKKβ, but depends on the accumulation of NIK (NF-κB inducing kinase) and formation of IKKα homodimers. This type of activation is triggered mainly by signals that bind to several members of the TNF receptor family, such as the TNFR2, BAFFR (B-cells activator factor receptor), LTβR (Lymphotoxin β receptor), CD40R, RANK (receptor activator for the NF-κB), and FN-14 (fibroblast growth factor-inducible 14) [48]. In addition, the non-canonical NF-κB can also be induced by some pathogens including *Helicobacter pylori*, HIV1, *Influenza virus*, *Legionella pneumonia* and *Epstein-Barr virus*. [59].

In contrast to the activation of the canonical NF-κB pathway that requires the phosphorylation of the IKKs complex, the non-canonical pathway requires the stabilization and accumulation of NIK. Under resting condition, NIK is constantly bound by a complex comprising TRAF3 (TNFR associated factor 3), TRAF2 and cIAP, which mediates NIK K48 pUb and consequently, its proteasomal degradation. After stimulation, the TRAF3-TRAF2-cIAP-NIK complex is recruited to the receptor. The binding with the receptor induces the activation of cIAP, which, acting as E3 ligase, transfers K48 pUb chains on TRAF3, determining its proteasomal degradation and,

consequently, the disruption of the complex. As a result, NIK is no longer linked to TRAF3 and begins to accumulate in the cytoplasm and phosphorylates IKKα, which induces the proteasomal processing of p100 to p52 [48,59]. Heterodimers of mature p52 and RelB can finally migrate to the nucleus and start gene transcription (see Figure 2 (right)).
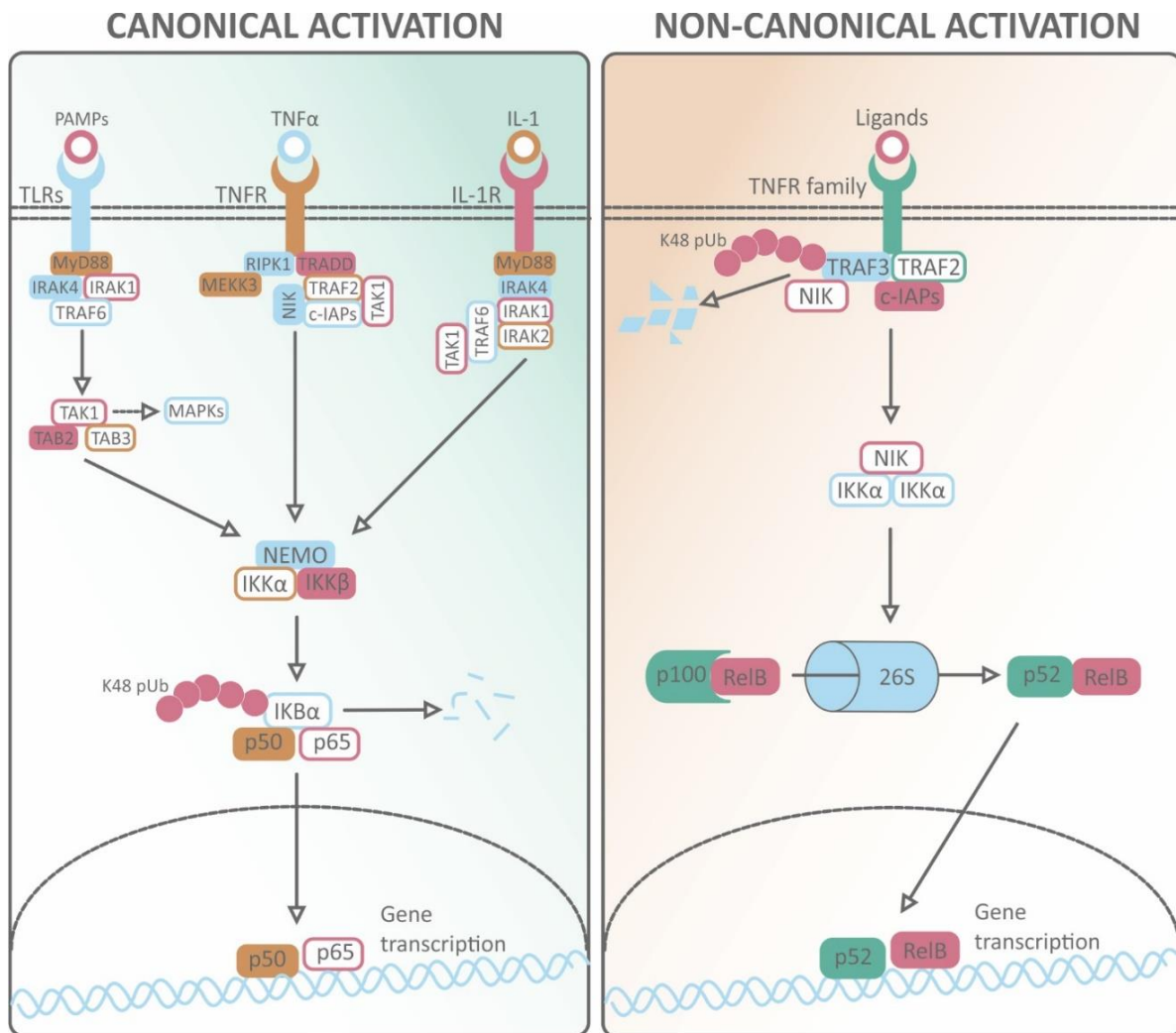
Figure 2 Regulation and activation of the NF-κB pathway. *Canonical activation of NF-κB is triggered by different stimuli and mediated by different receptors and pathways that all converge in the activation of the IKK complex, which catalyses the phosphorylation- and K48-ubiquitination-mediated degradation of IκBα. In resting condition TRAF3 binds to NIK, inhibiting its activation. Stimulation-induced degradation of TRAF3 leads to the release of NIK and activation of non-canonical NF-κB.*

1.2.3 Regulation of the NF-κB pathway

Since NF-κB plays crucial roles in many cellular processes, its activation is strictly regulated by intrinsic and extrinsic mechanisms, and, its dysregulation results in tumorigenesis [60,56,61] and autoimmune diseases [62,63]. The mechanisms of inactivation are mediated by: (i) protein-

protein inhibition, (ii) post-transcriptional inhibition, (iii) post-translational inhibition.

The binding of NF-κB with DNA induces the transcription of not only pro-inflammatory cytokines, but also several inhibitory factors to limit the activation and avoid uncontrolled cellular responses. One of the first produced negative factors is IκBα. Functionally, IκBα is able to block the binding of NF-κB with DNA and sequester it in the cytoplasm [64]. In addition to IκBα, several members of the IκB family act as negative regulators of the NF-κB pathway. p105, the precursor of p50, selectively binds to p50, RelA and c-Rel and segregates them in the cytoplasm. The IκB family member p100, the precursor of p52, may form high molecular weight complexes capable of binding to and inhibiting RelB [65]. IκBζ is a recently identified inhibitor molecule expressed in an inducible manner in response to LPS and it negatively regulates RelA [66]. Another unique molecule is IκB[NS], which is rapidly induced in case of ligation of the T cell receptor in thymocytes [67] and after LPS stimulation [68]. Mice deficient for IKB[NS] show constitutive activation of the NF-κB but the functional mechanism is still unclear [68].

IRAK family members are positive regulators of NF-κB. But the latest member of the IRAK family, IRAK-M (or IRAK3) [69], acts as an inducible negative regulator of the canonical NF-κB pathway [70]. IRAK-M, produced after TLR stimulation, has the capacity to bind to TRAF6 and inhibit its interaction with IRAK1, thereby suppressing downstream NF-κB activation [70].

Members of the nucleotide-binding domain and leucine rich repeat containing (NLR) family are molecules that create complexes to regulates several biochemical pathways, among which the most known is the inflammasome [71]. Interestingly, the last three defined members have been proved to act as inhibitory molecules of several pathways, including NF-κB.

Once the NF-κB-mediated gene transcription has been initiated, there are several post-transcriptional mechanisms that can be activated to attenuate the signaling. One efficient mechanism is the alternative splicing of inducible genes to block the signal propagation. For

instance, a truncated form of the protein MyD88 can be produced after stimulation. This protein is able to bind to TLR4 but fails to interact with IRAK4, resulting in a suppression of the signal [72].

In addition to the strategy of alternative splicing, the production of miRNA to target mRNA for degradation is also a highly effective negative feedback mechanism. For example, miR-146 is upregulated after TLR4 stimulation and it has been shown to bind mRNAs of both IRAK1 and TRAF6, either promoting their degradation or preventing their translation [73]. Another miRNA produced after TLR4 stimulation is miR-21. miR-21 is capable of target PDCD4 and suppress its effects of promoting IL-6 production and restraining the anti-inflammatory cytokine IL-10 [74]. miR155, produced in several cell types after TLR activation, was found to modulate NF-κB signaling through targeting IKKε, FADD, and RIPK1 transcripts [75].

Additionally, RNA-binding proteins (RBPs), are able to bind specific RNA molecules and recruit catalytic proteins to induce biochemical modifications of the substrate. The best characterized member of the RBPs is tristetraprolin (TTP), which can bind to mRNAs of proinflammatory proteins, such as TNF and IL-23, and induce their degradation [76].

Post-translational modifications (PTMs) refer to those chemical changes proteins may undergo after translation. Common PTMs include phosphorylation, ubiquitination, acetylation, sumoylation, nitrosylation and methylation. Among these modifications, phosphorylation, ubiquitination and recently discovered methylation are commonly observed in the NF-κB signaling cascade. Since phosphorylation is considered an activating PTM, phosphatases, such as PP6 and PP4, can function as negative regulators of the NF-κB signaling by dephosphorylating TAK1 and NEMO, respectively[77,78].

In the past few years, methylation of p65 emerged as a completely new mechanism of NF-κB regulation. It has been reported that p65 can be methylated at 6 different Lysine residues by

different histone-modifying enzymes. It appears that after stimulation-induced migration of p65 to the nucleus and the consequent binding to DNA, p65 becomes mono- and di-methylated and this leads to a decrease of its activity and to gene suppression. Therefore, methylation could be an internal negative feedback to reduce iper-activation of NF-κB pathway [79].

1.3 UBIQUITINATION AND DEUBIQUITINATION

Ubiquitination is an energy-dependent post-translational modification process in which one or more ubiquitin molecules are covalently attached to a substrate protein. Ubiquitin is a 76 amino acid protein, conserved across eukaryotic organisms, from yeast to humans. Ubiquitin has seven lysine residues, each of which can be used to forming a type of pUB chain, namely (according to the position) K6, K11, K27, K29, K33, K48 and K63, resulting in disparate effects [80]. In addition to the 7 lysine, a donor ubiquitin can also be attached to a recipient ubiquitin via the amino terminal methionine (M1) resulting in the formation of M1 or linear linkages.

The process of ubiquitination is a cascade consisting of three sequential steps known as: (i) activation, (ii) conjugation and (iii) ligation, which are catalysed by three different types of enzymes called E1, E2 and E3, respectively.

(i)   The first event is the activation of the ubiquitin molecule by the E1 ubiquitin-activating enzyme in an ATP-dependent manner, resulting in the formation of a thioester linkage between ubiquitin and the E1. There are only two E1 enzymes encoded in human's genome and they do not have any specificity for specific E2 enzymes.

(ii)   E2 ubiquitin-conjugating enzymes can bind ubiquitin with its catalytic cysteine residue. There are about 40 different E2 enzymes, whose primary function is to determine the type of

polyubiquitin chains that are catalysed by the E3 ligases.

(iii) Finally, E3 ubiquitin ligases, which bind to the E2 and the substrate, form an isopeptide bond between the C-terminal glycine of ubiquitin and a lysine residue of a target protein. The E3 ligase is responsible for the substrate specificity. Due to this reason, E3 ligases are the most abundant ubiquitin-catalysing enzymes in human cells. The number of E3 ligases exceeds 700, representing ≈5% of human genome. E3s can be divided into four major families: Really interesting New Gene (RING), Homologous to E6-associated protein C-terminus (HECT), UFD2 homology (U-box) and RING-in-between-RING (RBR) E3 ligases [81,82].

The ubiquitination process is reversible and ubiquitin molecules can be stripped from the substrate in a process called deubiquitination by deubiquitinating enzymes (DUBs). The mechanism of ubiquitination and deubiquitination is summarized in Figure 3.
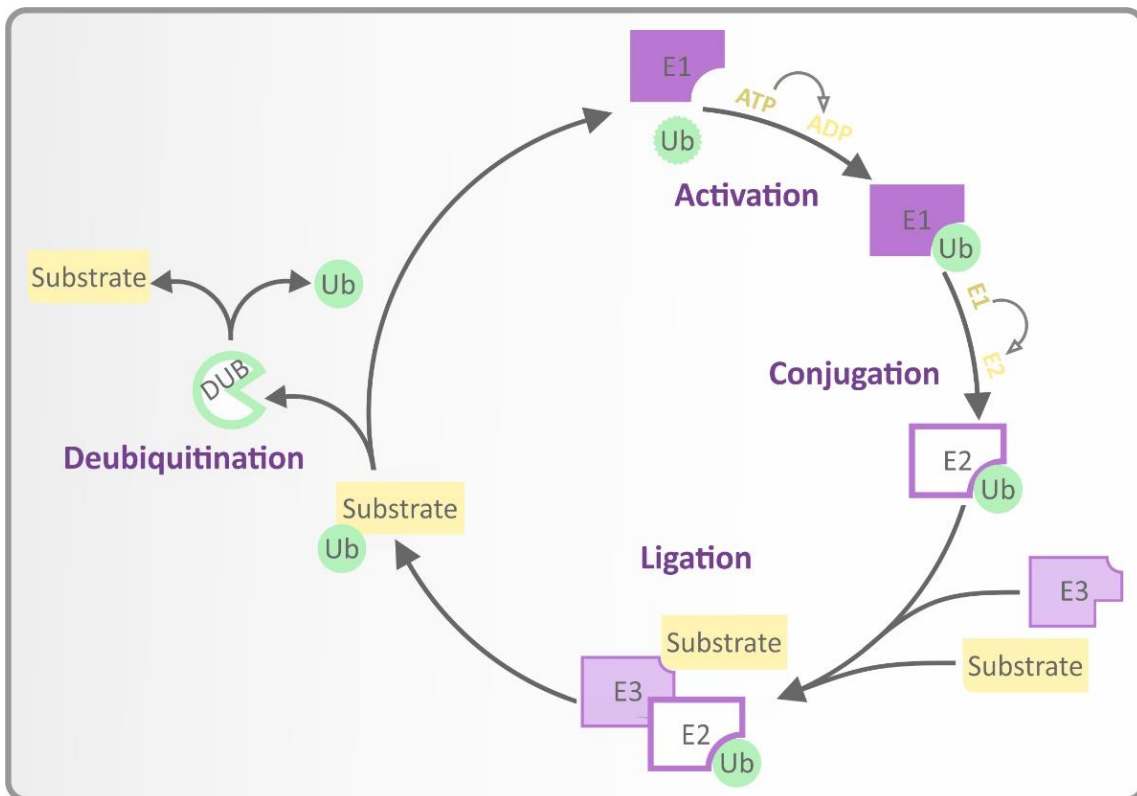
Figure 3. Activation of the ubiquitination system. *The process of ubiquitination is regulated by the subsequent activation of three classes of enzymes (E1, E2 and E3). The ubiquitin-activating enzyme (E1) activates the ubiquitin molecule, linking E1 with the ubiquitin. The ubiquitin molecule is transferred to the ubiquitin-conjugating enzyme E2. E2 conjugates with a substrate-specific ubiquitin ligase (E3). The E2-E3 complex binds to its target molecule and transfers the ubiquitin to the substrate protein. Polyubiquitin chains are formed by repeating this process multiple times. The process of ubiquitination is reversible and can be reverted by deubiquitinating enzymes, which remove ubiquitin molecules from the substrate.*

1.3.1 Types of Ubiquitination

Conjugation of ubiquitin to substrates generally occurs at lysine residues, but may also occur at cysteine, serine, threonine, and tyrosine residues. These particular types of ubiquitination are called "non-canonical ubiquitination" and are still not fully understood [83]. Otherwise, ubiquitination at lysine residues represents the most common and best studied forms of ubiquitination. For this reason, in this thesis I will only focus on this group of ubiquitination.

Residues can be modified with a single ubiquitin molecule (monoubiquitination), several single ubiquitin proteins (multi-monoubiquitination), or a chain of ubiquitin molecules (polyubiquitination). Polyubiquitin chains are usually formed through covalent binding of the C-terminal glycine of one ubiquitin molecule to an internal lysine residue of another ubiquitin molecule. Different ubiquitin linkages fulfil different physiological functions [84]. Among all the eight types of polyubiquitination, for many years, ubiquitin research was limited only to K48 and K63 pUb, but in the past few years, a plethora of novel data emerged regarding the remaining ubiquitin linkage types[85,86,87,88,89].

K6: The function of K6 is still largely unknown but it appears to be involved in the DNA damage response [90,91]. In addition, it is not associated with proteasomal degradation [92].

K11: K11 polyubiquitination has been associated with proteasomal degradation in cell cycle regulation [93], endoplasmic reticulum associated degradation (ERAD) [94], membrane trafficking [95] and TNF signaling [96,92].

K27: In 2014, the group of Wang [97] connected K27 linkages to host immune responses triggered by microbial DNA. In addition, K27 ubiquitination of the histone 2A is crucial for the activation of the DNA-damage response [89].

K29: Recently, K29 has been reported to be an inhibitor of Wnt signaling. The Wnt/β-catenin pathway plays essential roles in embryogenesis, but its deregulation has been associated with

tumorigenesis and multiple other human diseases. It has been shown that after Wnt activation, the E3 ligase Smad can induce K29 polyubiquitination of axin, which disrupts its interaction with the Wnt coreceptors, leading to the inhibition of Wnt/β-catenin signaling [98].

K33: K33-linked ubiquitin chains are negative regulators of T-cell antigen receptors (TCRs). Lys33-linked polyubiquitination of the signaling kinase Zap70 [99] or the TCR [100] affects the association between these two molecules by promoting their dephosphorylation. Recently, K33-linked polyubiquitination has also been implicated in post-Golgi protein trafficking, by facilitating the interaction between the proteins and their transport carriers [101].

K48: K48-polyubiquitin chains are the most abundant linkage in cells and the major signal for proteasome-mediated degradation [102]. Biochemical studies reveal that K48-linked chains directly interact with the 26S proteasome, binding the proteasome ubiquitin receptors Rpn10 and Rpn13 [103]. Under both resting and inflammatory conditions, K48-pUb plays a central role in the regulation of a plethora of cellular functions, such as: NF-κB signaling [104,105], TNF signaling [106], neuronal differentiation [107], cell death [106,108], DNA damage [109,110], T-cell tolerance [111] and, as recently shown, memory formation [112].

K63: Rather than triggering degradation, K63-linked chains serve as a molecular bridge that allows rapid and reversible formation of pivotal signaling complexes. K63 linkages are now known to regulate NF-κB activation [113,114], DNA repair [115,116], innate immune responses [117], clearance of damaged mitochondria [118], and protein sorting [119,120]. In addition, they can also guide assembly of large protein complexes that drive mRNA splicing or translation [121]. Interestingly, K63-linked chains are also able to perform their functions even if they are not attached to a substrate protein [122,85].

M1:. In 2006, the group of Iwai showed that M1-linked polyubiquitination was catalysed by a complex called LUBAC, consisting of two ubiquitin ligases, HOIL-1 and HOIP, and the accessory

protein SHARPIN [123]. M1 linear ubiquitination is required for inflammatory and immune responses by regulating the activation of NF-κB [124]. Other cellular functions related to M1 include the regulation of interferon production [125] and control of Wnt signaling [126]. Types of ubiquitination and their main functions are summarized in Table 2.

TYPE OF UBIQUITINATION	FUNCTION
Mono-ubiquitination	DNA replication and repair
	Endocytosis
	Signal transduction
	Protein localization
	Transcription regulation
Mono-multi-ubiquitination	Endocytosis
	Signal transduction
	Protein localization
K6 PolyUb	DNA repair
	Histone modification
	Cell cycle
K11 PolyUb	Cell cycle
	ERAD
	Hedgehog signaling
	TNF RI signaling
K23 PolyUb	Antiviral immunity
	Mitochondrial transport
	TGF-beta signaling
	Ubiquitin fusion degradation
K29 PolyUb	ER stress-mediated apoptosis
	Lysosomal degradation
	mRNP disassembly
	Wnt/beta-Catenin signaling
K33 PolyUb	Protein trafficking
	TCR signaling
K48 PolyUb	Proteasomal degradation
	TLR2/4 signaling
	TCR signaling
	Transcription regulation
K63 PolyUb	Autophagy
	Development
	DNA replication and repair
	Innate and adaptive immunity
	Neurodegeneration
	Signal transduction
	Spliceosome function
M1 PolyUb	Innate immunity

Table 2 *Types of ubiquitination and their functions*

1.3.2 Deubiquitination

The ubiquitination process can be reverted by particular enzymes named deubiquitinase (DUBs). There are about 100 DUBs in the human genome that play different roles in cellular processes. The DUBs are divided into 5 families: Ubiquitin C terminal hydrolases (UCHs), ubiquitin-specific proteases (USPs), ovarian tumour proteases (OTUs), Josephins and JAB1/MPN/MOV34 metalloenzymes. The first 4 families are cysteine proteases, while the last one is a metalloprotease [127]. A complete list of all the DUBs is shown in Figure 4.
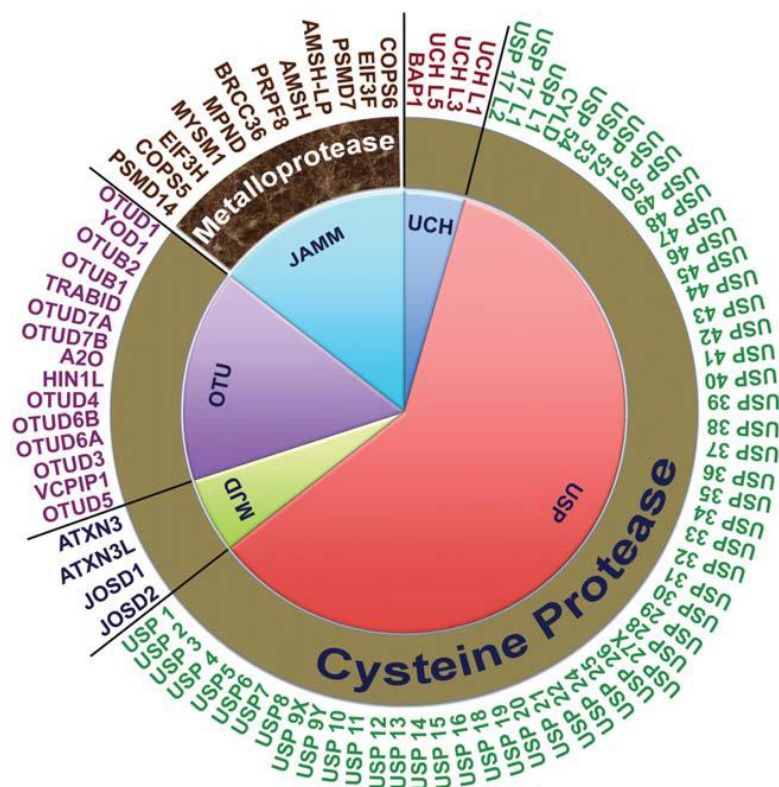
Figure 4 Members of the 5 DUB families. *Modified from* [128]

DUBs can remove Ubiquitin molecules from protein substrates to avoid their degradation or activation, edit the polyubiquitin signal to change the fate of the substrate, and disassemble polyubiquitin chains to free ubiquitin monomers to avoid the unnecessary degradation of ubiquitin [129]. Interestingly, some DUBs, called proteasome-associated DUBs, constantly interact with the 19S subunits to disrupt the bond between ubiquitin and the proteasome to remove the ubiquitin chains before degradation and free the ubiquitin binding receptors [130].

One of the important aspects of DUB specificity is its ability to discriminate between different chain linkages, for example studies have shown that the DUB Cezanne has a specificity to cleave K11 polyubiquitination [131], but A20 can specifically cleave K63 polyubiquitin chains. Functions of DUBs are tightly regulated either by substrate-induced conformational change, binding to adaptor proteins and proteolytic cleavage, or by PTMs, such as phosphorylation, monoubiquitination, SUMOylation and redox modification [128].

1.3.3 Ubiquitin as a regulator of NF-kB

Additionally ubiquitination and deubiquitination play critical roles in the regulation of NF-kB. Ubiquitination can be either an activating or an inhibitory signal, depending on the types of pUb linkage. Generally, if a target protein is modified by K48 or K11 pUb, it is destined for proteasomal degradation. Contrarily, addition of K63 pUb chains leads to the activation of tagged proteins. A20 (TNFAIP3) is an ubiquitin ligase inhibiting the canonical pathway by adding K48 pUb chains on RIP1, leading to its degradation [132]. In addition, A20 has been shown to block the E3 ligase function of TRAF6, TRAF2 and cIAP1 by preventing their interaction with the E2 Ub conjugating enzymes UBC13 and UBCH5c. A20 can add K48 pUb chains on UBC13 and UBCH5c to trigger their degradation [133]. Different from the mechanism of inhibition of A20, CYLD is a de-ubiquitinase (DUB) that suppresses NF-κB activation by removing K63 pUb chains from substrates to block their activation. Interestingly, the substrates of CYLD are the same as those of A20, i.e., RIP1, TRAF6, TRAF2 and cIAP1, confirming the predominant role of these molecules in the activation of this signaling pathway [134]. Additionally, the DUB OTUD7B (Cezanne) can negatively regulate NF-κB. Cezanne removes several types of Ub chains (branched, K48, K63, K11) and can suppress both canonical and non-canonical NF-κB pathways, despite the mechanisms have not been perfectly clarified [135,136].

1.3.4 OTUB1

Identified in 2002 by Borodovsky and colleagues, OTUB1 (Ovarian Tumor domain-containing Ubiquitin aldehyde-Binding protein 1, also called Otubain1) is the founding member of the ovarian tumour (OTU) domain family of DUBs [137]. OTUB1 is expressed in a variety of human tissues [138], with the highest expression observed in the brain. In mice, OTUB1 is also one of the most expressed DUB [139]. Full knockout of OTUB1 results in embryonic lethality in mice, suggesting a main role of OTUB1 during embryogenesis, while heterozygous knockout leads to a reduction in grip strength and a decrease in lean body mass [140]. Biochemical analysis determined that OTUB1 has a specificity for K48-linked ubiquitination, this means that it can bind and cleave only K48-linked polyubiquitin chains [141]. But, in addition to this canonical DUB activity, OTUB1 displays a catalytic-activity-independent, non-canonical activity by binding to E2 enzymes. When the E2 enzyme is charged, the donor ubiquitin (E2-linked) occupies the proximal site of OTUB1. In such setting, the E2 enzyme cannot participate in the ligation since that E2/OTUB1-binding surface overlaps with that of E2/E3-binding [142,143]. Therefore, OTUB1 can decrease a protein's ubiquitination status in two ways: 1. by removing already formed K48-linked polyubiquitin chains from a substrate (canonical activity) and 2. by preventing new polyubiquitin conjugation by inhibiting the E2 enzyme (non-canonical activity).

OTUB1 has been implicated in the regulation of different cellular processes:

➢ Enhancing CD4$^+$ T cell anergy by degradation of the ubiquitin ligase GRAIL [144];

➢ Reduction of virus-induced ubiquitination of TRAF3 and TRAF6, two ligases required for the activation of IRF3 and NF-κB pathways [145];

➢ Upon DNA double-strand breaks, binds to UBE2N and suppresses synthesis of K63-linked polyubiquitin chains, thereby reducing DNA damage response [146];

➢ Enhances TGFβ signaling by inhibiting ubiquitination and degradation of SMAD2/3 [147];

➢ Deubiquitinates and stabilizes the transcription factors FOXM1 [148], ERα [149] and RhoA [150];

➢ Regulates apoptosis by deubiquitinating the cellular inhibitor of apoptosis (cIAP1) [151];

➢ OTUB1 markedly stabilizes and activates p53 and induces p53-dependent apoptosis and cell growth inhibition [152];

➢ Involved in cancer development and progression (lung, ovarian, breast, glioma, colon, gastric, oesophageal, prostatic cancer) [153].

However, despite the growing literatures about OTUB1, many features of OTUB1 and its role in other cellular processes, especially during infection, remain unclear.

1.4 *TOXOPLASMA GONDII*

Toxoplasma (T.) gondii, an obligate intracellular parasite, is a member of the phylum *Apicomplexan*. The name originates from its particular curved shape (from the Greek word "*toxon*" = bow), and the animal from which it was first isolated (*Ctenodactylus gundi*, an African rodent). It can infect any warmblood animals, despite its definite hosts are the felines. It is distributed worldwide, with higher frequencies in countries with low-hygiene conditions [154]. Depending on the stage of its life cycle, *T. gondii* can convert into various cellular forms, which are characterized according to cellular morphology, biochemistry, and behaviour [155].

➢ **Tachyzoite:** The term "tachyzoite" derives from the Greek word "tachos", which means "speed", and therefore it indicates a *T. gondii* stage characterized by fast replication. The host cell ruptures when it can no longer support the growth of tachyzoites [156,157].

➢ **Bradyzoite:** The name bradyzoite derives from the Greek word "brady", which means "slow", indicating the slow replication rate of this organism. In this form, *T. gondii* may form

intracellular cysts, which contain hundreds of bradyzoites. The cyst wall is composed of parasitic materials and host cell's components and for this reason it cannot be recognized by the immune system. Although tissue cysts may develop in any organs, they are more prevalent in the brain, eyes and muscular tissue. Usually, intact tissue cysts do not cause any harm to the host and they are mostly silent for the entire life of the host without causing inflammatory responses [158].

Sporozoites: Sporozoites are the product of the sexual replication of parasites inside the definitive hosts (felines). They are contained inside the oocysts (4 sporozoites inside each oocyst). After shedding, oocysts are sporulated within 1-5 days depending upon the aeration and temperature. The wall of sporulated oocysts consists two layers and is extremely strong; therefore, oocysts can be preserved months and possibly years in the environment [159]. Several strains of *T. gondii* have been identified all over the world, but the most common and the best studied strains are the strain I, II, and III isolated in North America and Europa. Type I tachyzoites are the most virulent because they are less able to convert to bradyzoites, thereby causing mostly acute disease in their hosts. Type III strains, on the contrary, readily differentiate into bradyzoites causing their hosts to become chronically infected, but these strains are infrequently associated with clinical diseases in humans. Finally, the type II strain tend to be intermediate between types I and III in terms of differentiation competence and virulence [160,161].
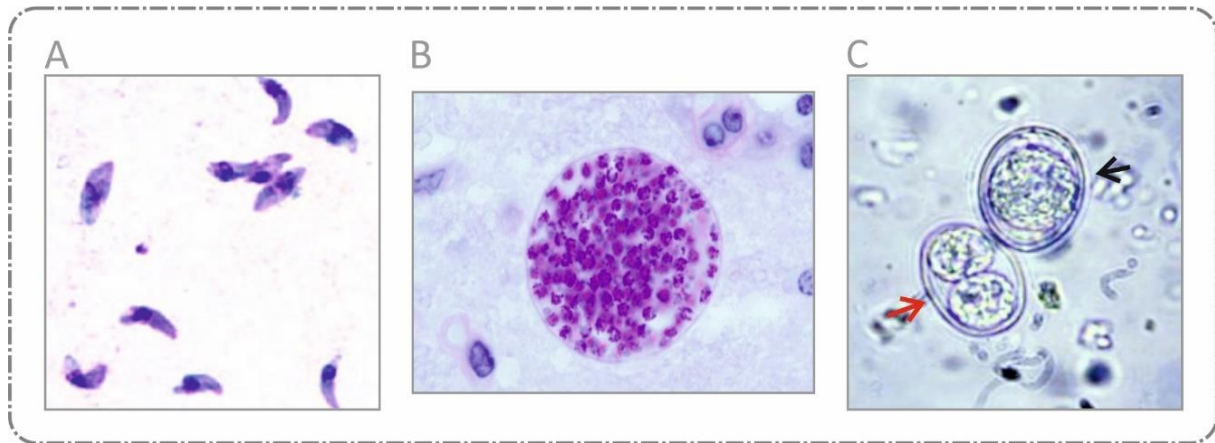
Figure 5 Three different stages of maturation of T. gondii. A. fresh released Tachyzoites (modified from [162]); B. Bradyzoites inside a tissue cyst in mouse brain (modified from [163]); C. Sporulated oocyst (red arrow) and unsporulated oocyst (black arrow) (modified from [164]).

1.4.1 Life cycle

Cats (and other Felidae) are the only host in which gametogony (sexual reproduction) can occur in the epithelial cells of the small intestine, leading to the production of unsporulated oocysts. Once shed with feline faeces in the environment, unsporulated oocysts become infectious sporulated oocysts. Sporulated oocysts can be ingested by intermediate hosts which could be any warm-blood animal. When bradyzoites or oocysts are ingested, they can transform into tachyzoites, which rapidly replicate and distribute in all the body [165]. The tachyzoite is responsible for the acute infection of *T. gondii*. It replicates every 6-8 hours in a process called endodyogeny within an intracellular compartment called parasitophorous vacuole, which protects the parasite and is essential for tachyzoite replication[166]. A few weeks after infection, most tachyzoites are eliminated by the immune system and the rest convert into the bradyzoite form. The vacuoles containing bradyzoites mature into cysts that can persist for years and even for the rest of the life of the host. The brain and muscle are the most common sites of the chronic, latent infection, although cysts have also been found in the lung, liver, kidney, and other visceral organs [167]. Tissue cysts are the terminal life-cycle stage in the intermediate host, but if they are ingested, they are immediately infective.
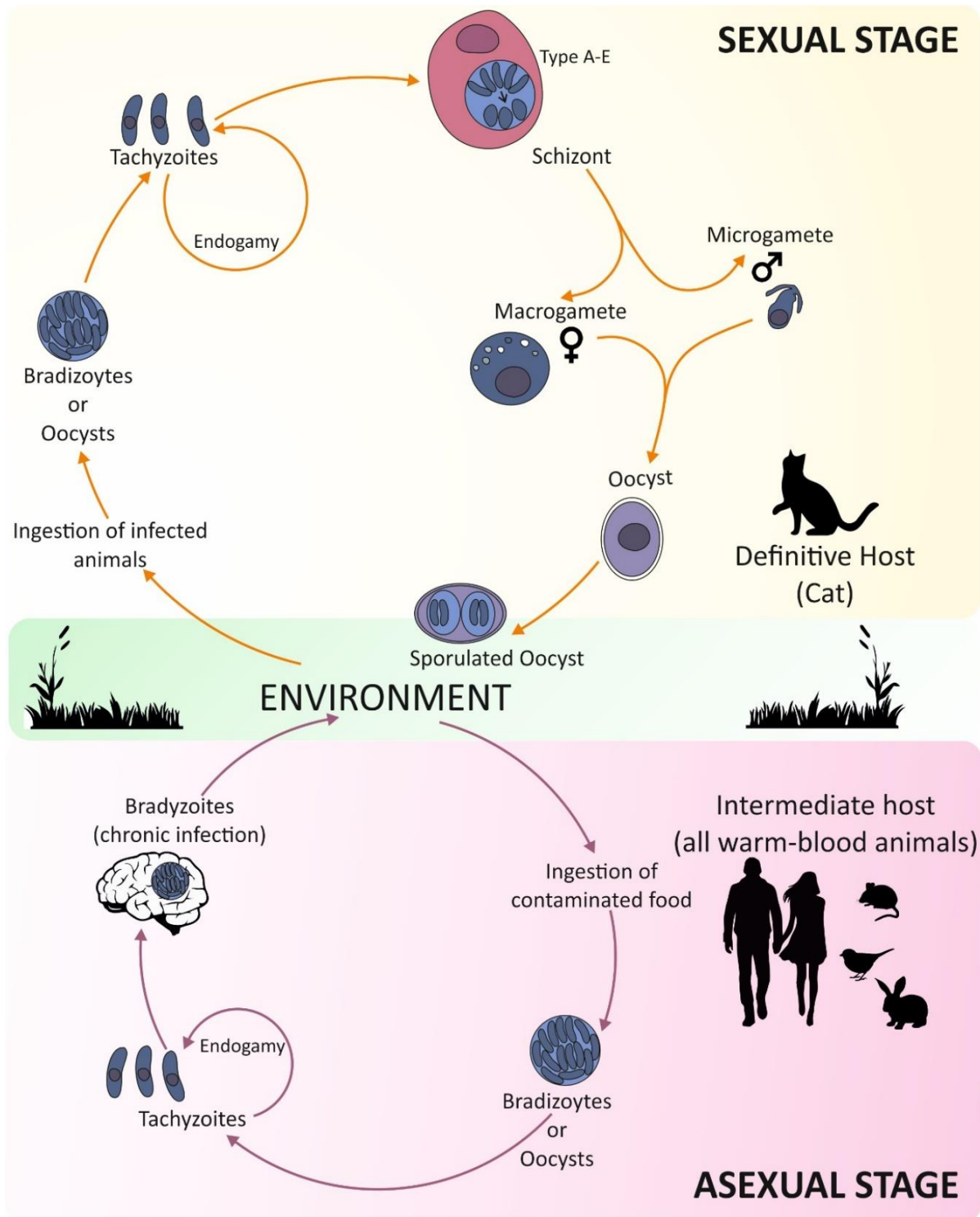
Figure 6 T. gondii life cycle. *T. gondii has 2 distinct life cycles. The sexual cycle occurs only in cats, the definitive host. The asexual cycle occurs in other mammals (including humans) and various strains of birds. A cat becomes infected with T gondii by eating contaminated raw meat, wild birds, or mice. The organism's sexual cycle then begins in the cat's gastrointestinal (GI) tract. Macrogametocytes and microgametocytes develop from ingested bradyzoites and fuse to form zygotes. The zygotes then become encapsulated within a rigid wall and are shed as oocysts. The zygote sporulates and divides to form sporozoites within the oocyst. Sporozoites become infectious 24 hours or more after the cat sheds the oocyst via faeces.*

T gondii oocysts, tachyzoites, and bradyzoites can cause infection in humans. Infection can occur by ingestion of oocysts following the handling of contaminated soil or cat litter or through the consumption of contaminated water or food sources (e.g., unwashed garden vegetables). Transmission of tachyzoites to the foetus can occur via the placenta following primary maternal infection.

1.4.2 Toxoplasmosis

Epidemiologic studies reported a seroprevalence of *T. gondii* in about one-third of the world's population. Prevalence is higher in countries with warm and wet climates as oocysts lose their virulence when dried or frozen. Transmission occurs predominantly via ingestion of oocysts from contaminated food or water [166]. Additionally, the parasite may spread to foetuses and cause congenital toxoplasmosis, if the mother is infected for the first time with *T. gondii* during pregnancy [168]. Transmission of *T. gondii* may also occur in organ transplantation, in particular if a cyst containing organ is transplanted to a seronegative recipient.

Infection in immunocompetent adult is usually asymptomatic. Only about 10% of the patients develop a toxoplasmosis with unspecific symptoms such as lymphadenopathy and fever, self-limited and rarely needs treatment. After 2 to 3 weeks of infection, due to an effective host immune response, tachyzoites are cleared from the host tissues and differentiation into bradyzoites occurs. Acute infection, in general, protects the host from symptomatic reinfection. In immunocompetent hosts, chronic infection is typically asymptomatic [166,168].

By contrast, toxoplasmosis can be a severe complication in immunocompromised patients. In these patients, toxoplasmosis is almost always caused by the reactivation of chronic infection. The CNS is the most typical site affected by *T. gondii* infection, and cerebral toxoplasmosis is the most common opportunistic and still a life-threatening disease in AIDS patients[169]. Clinical manifestations of cerebral toxoplasmosis include headache, fever, focal deficits, seizures, mental confusion, ataxia, lethargy, and visual alterations.

Another severe form of toxoplasmosis occurs when the primary infection takes place during pregnancy Indeed, infection of the foetus in the first trimester may lead to spontaneous abortion or severe neurological effects [159].

1.4.3 Immune responses to *T. gondii*

Upon oral infection, the first host defence against *T. gondii* is the single layer of epithelial cells lining the intestine. Intestinal epithelial cells are not only a target cell for T. gondii but may produce chemokines that coordinate recruitment of immune cells [170]. Recruited neutrophils, NK cells, monocytes, and dendritic cells contribute to the early defence against the parasite. One of the most critical functions of the innate immune response to *T. gondii* is the ability to sense the pathogen and initiate a Th1 response mediated by interleukin (IL)-12, which stimulates natural killer (NK) cells and T cells to produce the cytokine interferon-gamma (IFN-γ). IFN-γ is the major mediator of resistance to *T. gondii* and promotes multiple intracellular mechanisms to kill the parasite and inhibit its replication [171]. While infected inflammatory monocytes, macrophages and neutrophils are also able to produce and secrete IL-12, early IL-12 production by DCs is essential for inducing IFN-γ production by NK cells and T cells. Indeed, specific deletion of DCs or abrogation of IL-12 production in DCs by knocking out MyD88 resulted in lower systemic levels of IL-12 and increased sensitivity to *T. gondii* [172,173]. In particular, it has been revealed that CD8a$^+$ DCs are the main DC subset producing IL-12 [174,175]. The production of IL-12, and the subsequent IFN-γ response by NK cells (in acute stage) and T cells (in chronic stage), is critical for both stages of infection. IL-12 knockout mice die during acute *T. gondii* infection, but they can be rescued by administration of exogenous IL-12. However, if these mice stop receiving exogenous IL-12 after the establishment of chronic *T. gondii* infection, they display higher cyst burdens and succumb to toxoplasmic encephalitis (TE), proving that without continued production of IFN-γ during chronic infection, reactivation of bradyzoite cysts cannot be controlled in the brain [176]. The importance of IFN-γ is linked with its ability to stimulate gene transcription in immune cells as well as in non-immune cells such as fibroblasts, epithelial cells, endothelial cells and astrocytes [166]. These genes initiate a

multitude of host responses necessary for the parasite control, including immune cell proliferation, differentiation, and destruction of infected cells. In addition, IFN-γ induces the transcription of enzymes responsible for the destruction of the parasite, such as the Guanylate-binding proteins (GBPs) and GTPases. They target the parasitophorous vacuole to disrupt the membrane and cause the release of the parasite in the host cell cytoplasm, where it is destroyed. IFN-γ also limits parasite replication by mediating nutrient starvation. *T. gondii* is an obligate intracellular parasite and relies on the host cell for multiple resources that it is unable to synthesize, such as tryptophan. IFN-γ induces the production of indoleamine 2,3-dioxygenase (IDO), an enzyme that converts tryptophan into an unusable form for the parasite and thus limits its growth. In macrophages, a major function of IFN-γ during *T. gondii* infection is the production of reactive oxygen species (ROS) and reactive nitrogen species (RNS), which have potent antimicrobial activities and promote autophagy [166,176]. In spite of these *T. gondii*-eliminating functions, IFN-γ triggers the conversion of tachyzoites into bradyzoites, mediating the switch from acute to chronic infection [177].

Mechanistically, IL-12 production by DCs is mediated by TLR11 and TLR12 and their common ligand is an actin-binding protein called *T. gondii* Profilin (TgPFN), which is important for gliding motility, tissue migration, and host cell invasion. TgPFN is released by the parasite by an unknown mechanism. TLR11 and TLR12 are endosomal receptors that cooperate together to activate two distinct pathways via the adaptor molecule MyD88: NF-κB and IRF8. Mice lacking MyD88 are unable to produce IL-12 and thus cannot control acute *T. gondii* infection [178]. There are also other TLRs implicated in the immune response to *T. gondii* such as TLR2, TLR4 and TLR9. TLR2 and TLR4 have a specificity to recognize glycosylphosphatidylinositols on the surface of the parasite [179]. IL-12-production by DCs is summarized in Figure 7.
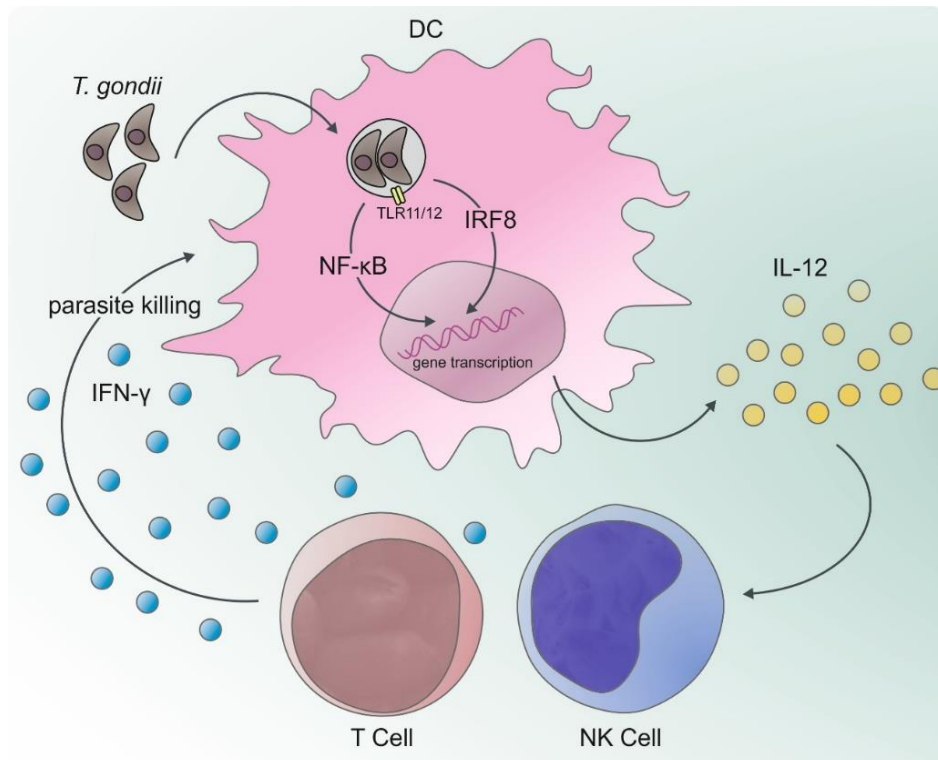
Figure 7 DC-mediated innate immune response to T. gondii. *DC are crucial participants in the immune response against T. gondii and one of the leading roles that they play in the production of IL-12, which, promotes the production of IFN-γ and thus deviates the immune response toward a Th1. The production of IL-12 induced by T. gondii in DC is dependent on MyD88, an adaptor molecule in TLR signaling pathways, which activates gene transcription via mainly two pathways: NF-κB and IRF8.*

DCs are generally considered to be the most crucial antigen-presenting cell (APC) population *in vivo*. Following infection with *T. gondii*, multiple populations of DCs undergo expansion and acquire an activated phenotype. A crucial feature of DCs as perfect APCs is their ability to migrate from the site of infection to the secondary lymphoid organs and to activate T and B cells by exposing *T. gondii* antigens. The mechanisms by which DCs acquire parasite antigens for presentation in the context of MHC II are unclear. Currently, there are two possible theories to explain how *T. gondii* antigens are internalized in DCs and they may both coexist at the same time. (i) In the first model, antigens may be acquired through the phagocytosis of infected cells, intact parasites, and parasite antigens, or through the endocytosis of parasite debris; otherwise, (ii) antigens may be acquired through active invasion mediated by the parasite. Interestingly, it has been also proved that *T. gondii*-infected DCs exhibit a

hypermigratory phenotype as a consequence of a parasite-derived molecule that mediates the actin cytoskeleton remodelling in DCs [180]. Thus, it is not a surprise that after oral ingestion of *T. gondii*, parasites can be found in mesenteric lymph nodes as early as 18 h post-inoculation and circulating in the blood by 24 h [181]. This rapid dissemination throughout the body is credited not only to the ability of *T. gondii* to invade migratory cells and influence their migratory behaviour (the so-called "Trojan Horse mechanism"), but also to the ability of the parasite to actively migrate cross epithelial barriers. By hijacking DCs, *T. gondii* can reach the brain and invade brain-resident cells. In the central nervous system (CNS), the tachyzoites will differentiate to the bradyzoite stage, form a cyst wall, and establish a chronic infection [176].

The success of *T. gondii* in survival and diffusion lies also in the evasion mechanisms that the parasite developed to escape from the immune response. There are several types of immune evasion mechanisms [176,177]:

➢ the parasitophorous vacuole enables it to escape the humoral immune defences such as enzymes, proteinases and complement;

➢ the various parasite stages ensure a constant renewal of the immunophenotype, requiring an adjustment of the host's immunological elimination process;

➢ the parasite shares some epitopes with its host, including cerebral epitopes, allowing it to remain undetectable in the brain tissues;

➢ *T. gondii* can interfere with the MyD88-dependent NF-κB pathway, which is indispensable for IL-12 production by DCs. In particular, type I and III strains of *T. gondii* have developed the ability to block the translocation of NF-κB to the nucleus, even after TLR-mediated phosphorylation of IκBα;

➢ *T. gondii* can block NO-mediated degradation in activated macrophages, by reducing the availability of intracellular Arginine;

➢ *T. gondii* can prevent the hyperactivation of the immune system by promoting the production of regulatory molecules including signaling suppressors like SOCS1, and inhibitory cytokines like IL-10 and IL-27;

➢ *T. gondii* can suppress the apoptosis of infected cells to guarantee their survival or induce the apoptosis of CD4$^+$ cells.

1.5 MURINE CYTOMEGALOVIRUS

Murine cytomegalovirus (MCMV) belongs to the genus cytomegalovirus (CMV) of the β-Herpesvirinae subfamily of the Herpesviridae family [182]. CMV virus species exist in essentially all mammalian host species, and have evolved in an intricate virus-host adaptation, resulting in a strict host-species specificity [182]. Despite Human Cytomegalovirus (HCMV) and MCMV exhibit some differences, e.g. the incapability of the latter of crossing the placenta, the infection with MVCM shares many features with HCMV infection, in particular regarding the neuro-pathogenesis of the disease and immune response of the host; therefore, the mouse model has been extensively used for studying the pathogenesis of acute, latent and recurrent virus infections [183,184]. Alike all the CMVs, MCMV has a tropism for hematopoietic tissue and secretory glands, and after the resolution of the acute infection, generally establish a persistent life-long infection characterized by alternate stages of virus productivity and latency [185].

In humans, HCMV infection is generally asymptomatic, even during primary infection. However, HCMV is an important opportunistic pathogen causing severe morbidity or death in immunocompromised patient such as AIDS patients, foetus and new-borns [184].

In mice, the course of the disease depends critically on the organs were MCMV have been isolated from. From example, infection of immunocompetent mice with MCMV isolated from

tissue culture is usually asymptomatic, and it is not associated with serious damage to organ systems. On the other hand, injection of a similar dose of salivary-gland isolated virus results in damage to multiple organs and tissues and high mortality even in fully immunocompetent hosts [182,183]. During acute infection, MCMV can infect hematopoietic cells, including DCs, but also many non-hematopoietic cells such as hepatocytes, endothelial cells or epithelial cells. Both innate and adaptive immune response are required for resistance to MCMV. Amongst innate immune lymphocytes, NK cells are the most critical defence against MCMV. NK cells can control MCMV replication by directly recognizing and killing infected cells. In addition, CD4 T cells play a key in the control of MCMV infection by production of both Th1 and Th17 cytokines; and through their IFN-γ secretion, CD4 T cells directly contribute to the control of viral replication in various organs. The activation of both NK and T cells heavily relies on the cytokine production by DCs and on their cross talk with them [185]. Indeed, once infected, DCs and in particular pDCs , are the main producers of IL-12, type I IFN and to lesser extent contribute also to the production of TNF, IL-6 and IL-18 [186]. Mechanistically, IL-12 production by DCs in MCMV infection is mediated by TLR3, TLR7, TLR9, RIG-I-like Receptors (RLR) [187], and cGAS/STING [187,188,71]. In addition, DCs are the main responsible for the spread of the virus during acute infection, as has been shown that most of the infected leukocytes in lungs, LN, blood and salivary glands are CD11c$^+$ [185].

2. AIM

DCs are indispensable for the host defence against pathogens and their activation is largely dependent on TLR-mediated activation of the MyD88 signaling pathway leading to the activation of NF-κB. OTUB1 has been shown to regulate numerous signaling pathways by stabilizing signaling molecules involved in NF-κB pathway; however, the *in vivo* function of OTUB1 in the immune system, and in particular in DCs, is still unclear.

To gain more insight into the role of DCs in infection and inflammation, we aimed to

1. Develop mice lacking OTUB1 specifically in CD11c$^+$ cells.

2. Define the *in vivo* and *in vitro* function of OTUB1 in the TLR11/12-dependent activation of DCs in murine toxoplasmosis.

3. Clarify the role of OTUB1 in TLR4-mediated activation of NF-κB in vitro and upon lethal in vivo LPS challenge of mice.

4. Elucidate the DC-specific function of OTUB1 in MCMV infection.

3. MATERIALS AND METHODS

3.1 Materials

<u>Materials for Animal Experiments</u>

2-methylbutane	Carl Roth, Karlsruhe, Germany
4% Paraformaldehyde (PFA)	Carl Roth, Karlsruhe, Germany
0.9% NaCl Sodium Chloride	Carl Roth (Karlsruhe, Germany)
Embedding medium	Sakura Finetek Europe BV, Zoeterwoude Netherlands (TissueOCTTM Tek ® compound)
Isoflurane (Forene ®)	Abbott, Wiesbaden, Germany
Heparin 5000U/ml	Biochrom AG (Berlin, Germany)

<u>Material for cell cultures</u>

Cell culture was performed under sterile conditions, inside a laminar flow hood. Before use all the cell culture media were pre-warmed at 37 °C in a water bath. Cells were maintained in culture in an incubator at 37 °C, 5% CO_2 and 60% of water vapor. Plastic consumables such as plates, plastic pipettes, and flasks, for cell culture were purchased from Greiner Bio-One (Frickenhausen, Germany) and Carl Roth (Karlsruhe, Germany).

RPMI 1640 medium	PAA Laboratories GmbH, Pasching, Austria
DMEM medium	PAA Laboratories GmbH, Pasching, Austria
10% Fetal Calf Serum	FCS, PAA Laboratories GmbH, Pasching, Austria
Penicillin/Streptomycin 100X	Gibco by Life Technologies (Darmstadt, Germany)
Sodium Pyruvate 100x	Gibco by Life Technologies (Darmstadt, Germany)
L-Glutamine	Gibco by Life Technologies (Darmstadt, Germany)
Dulbecco's Phosphate-Buffered Saline (DPBS)	PAA Laboratories GmbH, Pasching, Austria
Trypsin	PAA Laboratories GmbH, Pasching, Austria
Trypan Blue	Sigma-Aldrich, Steinheim, Germany
Dimethyl sulfoxide (DMSO)	Sigma-Aldrich (Steinheim, Germany)
Non-Essential Amino Acids (NEAA) 100X	Gibco by Life Technologies (Darmstadt, Germany)
B-Mercaptoethanol 50mM	Gibco by Life Technologies (Darmstadt, Germany)

GM-CSF 35ng/ml	Peprotech (Hamburg, Germany)
FLT3-L 400ng/ml	Peprotech (Hamburg, Germany)
M-CSF 35ng/ml	Peprotech (Hamburg, Germany)
IL-12 p40	Peprotech (Hamburg, Germany)
LPS	Sigma Aldrich (Steinheim, Germany)
TgPFN	Karolinska Institute (Stockholm Sweden)
TLA	Prepared in Lab
IMIQUIMOD	Invivogen (San Diego, California, USA)
PEPTIDOGLYCAN	Invivogen (San Diego, California, USA)
ODN	Invivogen (San Diego, California, USA)
POLY I:C	Invivogen (San Diego, California, USA)
IL-1β	Peprotech (Hamburg, Germany)
TNF	Peprotech (Hamburg, Germany)
Cycloheximide (CHX)	Sigma Aldrich (Steinheim, Germany)
MG132	Sigma Aldrich (Steinheim, Germany)
401486 IKK Inhibitor VII	Calbiochem (Merck KGaA, Darmstadt, Germany)
N-Ethylmaleimide (NEM)	Sigma Aldrich (Steinheim, Germany)
Indole-3-acetic acid sodium (IAA)	Sigma Aldrich (Steinheim, Germany)

Cell lines

VERO cells were cultured in RPMI medium supplemented with 10% (vol/vol) heat-inactivated fetal calf serum (FCS) and 1% (vol/vol) Pen/Strep solution in a cell incubator at 37 °C with 5% CO_2. NIH 3T3 cells were cultured in Dulbecco's modified Eagle's medium supplemented with 10% heat-inactivated FCS and 1% Pen/Strep in an incubator at 37 °C with 5% CO_2. Media were replaced every 2-3 days. Cells were subcultured when they reached 80% confluence.

Materials for molecular biology

Ethanol 70%, 100%	Fischer (Saarbrücken, Germany)
DNeasy Blood and Tissue Kit	Qiagen, Hilden, Germany
dNTP	Invitrogen, Karlsruhe, Germany
DTT	Invitrogen, Karlsruhe, Germany
EasyDNA kit	Invitrogen, Karlsruhe, Germany
Oligo-dT	Invitrogen, Karlsruhe, Germany
LightCycler 480 SYBR Green I Master Mix	Roche (Basel, Switzerland)
RNeasy Mini Kit	Qiagen, Hilden, Germany
Primers for PCR	Eurofins MWG Operon, Ebersberg, Germany

Primers for qRT-PCR	Applied Biosystems, Darmstadt, Germany
siRNAs	Invitrogen, Karlsruhe, Germany
Sterile distilled water	Berlin Chemie AG, Berlin, Germany
Superscript II Reverse Transcriptase	Invitrogen, Karlsruhe, Germany
TaqMan Universal PCR master mix	Applied Biosystems, Darmstadt, Germany
5x First Strand Buffer	Invitrogen, Karlsruhe, Germany
Lipofectamine 3000 transfection kit	Thermo Fisher Scientific (Waltham, USA)
Plasmids pCMV6-GFP, pCMV6-GFP-OTUB1, pCMV6-GFP-ΔN, and pCMV6-GFP-OTUB1-C91S	Origene (Rockville, Maryland, USA)

Genotyping Primers

Mouse strain	Primer sequence (5' → 3')
CD11c-Cre OTUB1$^{fl/fl}$ mice	
CD11c-Cre Sense	5' – ACT TGCCAGCTGTCTGCCA – 3'
CD11-Cre Antisense	5' – GCGAACATCTTCAGGTTCTG – 3'
OTUB1 Sense	5' – GAGGTAGGTGATGCTCAGGTG - 3'
OTUB1 Antisense	5' – CTTACTGGGAAAGAAGCTTGC – 3'

Materials for proteomics

Complete RIPA Buffer	50 mM Tris / HCl pH 7.5, 100 mM NaCl, 5 mM EDTA, 10 mM H_2PO4 (all from Carl Roth, Karlsruhe, Germany); 1% Triton X-100, 0.25% deoxycholic acid, Protease inhibitor cocktail, 20 mM sodium fluoride, 0.2 Mm phenyl methyl sulfonyl fluoride, 1mM Sodium molybdate, 20 mM glycerol-2-phosphate, 1 mM sodium phosphate buffer (all from Sigma-Aldrich, Steinheim,Germany); 10% glycerol (Calbiochem, Darmstadt, Germany); PhosStop (Roche, Mannheim, Germany); Protease Inhibitor Cocktail (25X) Sigma-Aldrich (Steinheim, Germany)
GammaBind G Sepharose Beads	GE Healthcare Bio-Sciences (Uppsala, Sweden)
TUBEs (UM402)	LifeSensors (PA, USA)
5 × Lane Marker Reducing Sample	Thermo scientific, MA, USA buffer
SDS-polyacrylamide separating gel	Distilled water, 8 to 10% acrylamide 30% (Applichem, Darmstadt, Germany), 0.4 M Tris, 0.1% Sodium dodecyl sulfate (both from Carl Roth, Karlsruhe, Germany), 0.1% ammonium persulfate, 0.1% TEMED (both from Sigma-Aldrich, Steinheim, Germany)

SDS-polyacrylamide stacking gel	Distilled water, 5% acrylamide 30% (Applichem, Darmstadt, Germany), 0.17 M Tris, 0.1% Sodium dodecyl sulfate (both from Carl Roth, Karlsruhe, Germany), 0.1% ammonium persulfate, 0.1% TEMED (both from Sigma-Aldrich, Steinheim, Germany)
PageRulerPrestained Protein Ladder (10-180 kDa)	Thermo Fisher Scientific (Waltham, USA)
Gel running buffer pH 8.3	25 mM Tris, 0.1% sodium dodecyl sulfate (both from Carl Roth, Karlsruhe, Germany), 250 mM glycine (Sigma Aldrich, Steinheim, Germany)
Polyvinylidene Fluoride (PVDF)	Millipore, Schwalbach, Germany Membrane Immobilon P
Filter paper	Carl Roth, Karlsruhe, Germany
Transfer buffer pH 8.4	25 mM Tris, 0.1% sodium dodecyl sulfate (both Roth, Karlsruhe, Germany), 500 mM glycine (Sigma-Aldrich, Steinheim, Germany), 20% Methanol (J.T. Baker, Deventer, Netherlands)
Blotting grade milk powder	Carl Roth, Karlsruhe, Germany
BSA	Sigma-Aldrich, Steinheim, Germany
TBS-Tween 20, pH 7.4	20 mM Tris, 140 mM NaCl (both from Carl Roth, Karlsruhe, Germany), 0.1% (v / v) Tween 20 (Sigma -Aldrich, Steinheim, Germany)
Anti-K63 Tube-Biotin	LifeSensors (Malvern, Pennsylvania, US)
HRP Avidin	BioLegend (San Diego, California, US)

Antibodies for western blot and immunoprecipitation

Antibody	SOURCE	IDENTIFIER
Rabbit polyclonal anti-OTUB1	Novus Biologicals, (Centennial, Colorado, US)	Cat# NBP1-49934
Rabbit monoclonal anti-GAPDH	Cell Signaling Technology, (Denver, Massachusetts, US)	Cat# 2118
Rabbit monoclonal anti-β-Actin	Cell Signaling Technology, (Denver, Massachusetts, US)	Cat# 8457
Rabbit polyclonal anti-P65	Cell Signaling Technology, (Denver, Massachusetts, US)	Cat# 3034
Mouse monoclonal βTUB	Cell Signaling Technology, (Denver, Massachusetts, US)	Cat# 86298
Mouse monoclonal HDAC-1	Santa Cruz Biotechnology, (Dallas, Texas, US)	Cat# Sc-81598
Rabbit monoclonal anti-IRF8	Cell Signaling Technology, (Denver, Massachusetts, US)	Cat# 5628S

Rabbit polyclonal anti-MyD88	Cell Signaling Technology, (Denver, Massachusetts, US)	Cat# 3699
Rabbit polyclonal anti-IRAK4	Cell Signaling Technology, (Denver, Massachusetts, US)	Cat# 4363
Rabbit polyclonal anti-phospho-IRAK4	Cell Signaling Technology, (Denver, Massachusetts, US)	Cat# 7652S
Rabbit polyclonal anti-IRAK1	Proteintech Group, (Manchester, UK)	Cat# 10478-2-AP
Rabbit polyclonal anti-phospho-IRAK1 (Thr209)	Sigma Aldrich, (Saint Louis, Missouri, US)	Cat#SAB4504246
Rabbit polyclonal anti-UBC13	Proteintech Group, (Manchester, UK)	Cat# 10243-1-AP
Mouse monoclonal anti-UBC13	Santa Cruz Biotechnology, (Dallas, Texas, US)	Cat# sc-58452
Mouse monoclonal anti-Uev1a	Santa Cruz Biotechnology, (Dallas, Texas, US)	Cat# sc-390047
Rabbit polyclonal anti-TAK1	Cell Signaling Technology, (Denver, Massachusetts, US)	Cat# 4505
Rabbit polyclonal anti-phospho-TAK1 (Ser412)	Cell Signaling Technology, (Denver, Massachusetts, US)	Cat#9339
Rabbit monoclonal anti-IκBα	Cell Signaling Technology, (Denver, Massachusetts, US)	Cat#4812
Rabbit monoclonal anti-phospho-IκBα (Ser32)	Cell Signaling Technology, (Denver, Massachusetts, US)	Cat#2859
Rabbit monoclonal anti-phospho-p65 (Ser536)	Cell Signaling Technology, (Denver, Massachusetts, US)	Cat# 4887
Mouse monoclonal anti-TRAF6	Santa Cruz Biotechnology (Dallas, Texas, US)	Cat# sc-8409
Rabbit polyclonal anti-TRAF6	Santa Cruz Biotechnology, (Dallas, Texas, US)	Cat# sc-7221
Mouse monoclonal anti-Pellino1/2	Santa Cruz Biotechnology, (Dallas, Texas, US)	Cat# sc-271065
Rabbit polyclonal anti-A20	Cell Signaling Technology, (Denver, Massachusetts, US)	Cat# 4625S
Rabbit polyclonal anti-cIAP1	Abcam (Cambridge, UK)	Cat# ab2399
Rabbit monoclonal anti-Lysine 48-specific polyubiquitin chains	Millipore (Burlington, Massachusetts, US)	Cat#05-1307
Rabbit polyclonal anti-P38	Cell Signaling Technology, (Denver, Massachusetts, US)	Cat# 9214S
Mouse monoclonal anti-Ubiquitin	Cell Signaling Technology, (Denver, Massachusetts, US)	Cat# 3936
Rabbit monoclonal anti-phospho-p38 (Thr180/Tyr182)	Cell Signaling Technology, (Denver, Massachusetts, US)	Cat#9215S
Rabbit polyclonal anti-ERK	Cell Signaling Technology, (Denver, Massachusetts, US)	Cat#9102S

Rabbit polyclonal anti- phospho-ERK (Thr202/Tyr204)	Cell Signaling Technology, (Denver, Massachusetts, US)	Cat# 9252
Rabbit polyclonal anti-SAPK/JNK Antibody	Cell Signaling Technology, (Denver, Massachusetts, US)	Cat#9101S
Rabbit monoclonal anti-Phospho-SAPK/JNK (Thr183/Tyr185)	Cell Signaling Technology, (Denver, Massachusetts, US)	Cat# 4668
Swine Anti-Rabbit Immunoglobulins/HRP Polyclonal	Dako (Glostrup, Denmark)	Cat#P0217
Rabbit Anti-Mouse Immunoglobulins/HRP Polyclonal	Dako (Glostrup, Denmark)	Cat#P0260
Rabbit polyclonal anti-*Toxoplasma gondii*	BioGenex Laboratories, (California, US)	Cat#PU125-5UP

Antibodies for flow cytometry

All antibodies were used at a concentration of 1μg/ $1x10^6$ cells

Antibody	Clone	Company
Anti-CD3 PECy7	145-2C11	BioLegend (San Diego, California, US)
Anti-CD11b PECy7	M1/70	BioLegend (San Diego, California, US)
Anti-CD8a PECy7	53-6.7	BioLegend (San Diego, California, US)
Anti-CD4 BV421	GK15	BioLegend (San Diego, California, US)
Anti-F4/80 BV421	BM8	BioLegend (San Diego, California, US)
Anti-B220 BV421	RA3-6B2	BD Biosciences (San Jose, US)
Anti-CD8 APC	53-6.7	eBioscience (Paris, France)
Anti-Ly6C APC	HK1.4	eBioscience (Paris, France)
Anti-PDCA-1 APC	927	BioLegend (San Diego, California, US)
Anti-CD11c APC	N418	BioLegend (San Diego, California, US)
Anti-IFN-γ APC	XMG1.2	Invitrogen (Carlsbad, California, US)
Anti-mouse IgG APC	M1-14D12	eBioscience (Paris, France)
Anti-IL-12 APC	C15.6	BD Biosciences (San Jose, US)
Anti-CD45 PerCP	30-F11	BioLegend (San Diego, California, US)
Anti-NK1.1 PE	PK136	eBioscience (Paris, France)
Anti-Ly6G PE	RB6-8C5	eBioscience (Paris, France)
Anti-CD11c PE	N418	eBioscience (Paris, France)
Anti-IL-12 PE	C17.8	eBioscience (Paris, France)
Anti-IL-6 PE	MP5-20F3	BD Biosciences (San Jose, US)
Anti-TNF PE	MP6-XT22	BioLegend (San Diego, California, US)
Anti-mouse IgG PE	MOPC-21	BioLegend (San Diego, California, US)
Anti-CD19 APCCy7	1D3	BD Biosciences (San Jose, US)
Anti-CD11c APCCy7	N418	BioLegend (San Diego, California, US)
Anti-NK1.1 APCCy7	PK136	BioLegend (San Diego, California, US)
Anti-CD3 APCCy7	17A2	eBioscience (Paris, France)
Anti-CD11b APCCy7	M1/70	BioLegend (San Diego, California, US)

Anti-B220 BV510	RA3-6B2	BioLegend (San Diego, California, US)
Anti-CD8 BV510	53-6.7	BioLegend (San Diego, California, US)

Kits used

EasySep™ Mouse CD11c Positive Selection Kit	STEMCELL Technologies (Cologne, Germany)
EasySep™ Mouse CD11b Positive Selection Kit	STEMCELL Technologies (Cologne, Germany)
EasySep™ Mouse CD3 Negative Selection Kit	STEMCELL Technologies (Cologne, Germany)
EasySep™ Mouse NK1.1 Positive Selection Kit	STEMCELL Technologies (Cologne, Germany)
EasySep™ Mouse CD19 Positive Selection Kit	STEMCELL Technologies (Cologne, Germany)
CBA Mouse Inflammation Assay	BD Biosciences, Heidelberg, Germany
NE-PER™ Nuclear and Cytoplasmic Extraction Reagents	Thermo scientific, MA, USA
DNeasy Blood & Tissue Kit	Qiagen, (Hilden, Germany)
RNeasy Mini Kit	Qiagen, (Hilden, Germany)
Pierce ECL Plus Western Blotting substrate	Thermo scientific, MA, USA

Instruments

Bacterial Incubator	Memmert (Schwabach, Germany)
Biometra Standard Power Pack P25	AnalytikJena (Jena, Germany)
Bio-Rad Mini protein system	Bio-Rad, California, USA
Bio Photometer	Eppendorf (Hamburg, Germany)
BD FACS Canto™ II Flow Cytometer	BD Biosciences (San Jose, Germany)
Centrifuge ROTANTA 460R	Hettich (Beverly, USA)
Centrifuge Mikro 22R	Hettich (Beverly, USA)
Chemo Cam Luminescent Image Analysis system	INTAS (Göttingen, Germany)
CO2 Incubator	Heraeus (Hanau, Germany)
EasySep Magnet	STEMCELL Technologies (Cologne, Germany)
Incubator shaker GFL 3032	Gesellschaft für Labortechnik (Burgwedel, Germany)
Laboratory balance	Sartorius (Göttingen, Germany)
Laminar flow hood	Heraeus (Hanau, Germany)
LightCycler 480 II	Roche Diagnostics (Mannheim, Germany)
Microscope Olympus-CX 41	Olympus (Hamburg, Germany)
Nanodrop ND-1000 Spectrophotometer	Thermo Fisher Scientific (Waltham, USA)
Neubauer Chamber (improved)	LO Laboroptik (Lancing, UK)

pH meter	Schott (Mainz, Germany)
PowerPac HC	Bio-Rad (California, USA)
Semi Dry Blotter	PEQLAB (Erlangen, Germany)
Thermocycler	PEQLAB (Erlangen, Germany)
Thermomixer	Eppendorf (Hamburg, Germany)
Tube Roller SRT9	Bibby Scientific (Staffordshire, UK)
Vortex Genius 3	IKA (Staufen, Germany)

Mice

C57BL/6J OTUB1$^{fl/fl}$ mice [189] were crossed with C57BL/6J CD11c-Cre mice [190] to obtain CD11c-Cre OTUB1$^{fl/fl}$ transgenic mice. Genotyping of new-borns was performed by PCR on tail DNA with primers targeting CD11c-Cre and OTUB1$^{fl/fl}$, respectively. Animals were kept under specific pathogen-free (SPF) conditions in the animal facility at Magdeburg University Hospital (Magdeburg, Germany). All mice were used at 8-12 weeks of age and were sex and age matched. Animal care and experiments were performed according to the European animal protection law and approved by local authorities (Landesverwaltungsamt Halle, Germany. Number of licence 2-1175). The regional Animal Research Ethical Board, Stockholm, Sweden, approved procedures and protocols involving extraction of cells from mice (N135/15, N78/16), following proceedings described in EU legislation (Council Directive 2010/63/EU).

3.2 Methods

Genotyping of the mouse strains

For genotyping of mice, genomic DNA from a tail tip was isolated using easyDNA kit (Invitrogen, Karlsruhe, Germany) according to the manufacturer's protocol. PCR was performed using primers indicated in the Materials session.

3. MATERIALS AND METHODS

Cell cultures and transfection

VERO cells were cultured in RPMI medium supplemented with 10% (vol/vol) heat-inactivated fetal calf serum (FCS) and 1% (vol/vol) Pen/Strep solution in a cell incubator at 37 °C with 5% CO_2. NIH 3T3 cells were cultured in Dulbecco's modified Eagle's medium supplemented with 10% heat-inactivated FCS and 1% Pen/Strep in an incubator at 37 °C with 5% CO_2. Control siRNA and OTUB1 siRNA (Thermo Fisher Scientific) were transfected into NIH 3T3 cells with Lipofectamine RNAiMAX transfection reagent (Thermo Fisher Scientific), respectively, according to manufacturer's instructions. Expression plasmids of pCMV6-GFP, pCMV6-GFP-OTUB1 (Origene), pCMV6-GFP-ΔN, and pCMV6-GFP-OTUB1-C91S (generated with Q5 Site-Directed Mutagenesis Kit, NEB) were transfected into NIH 3T3 cells, respectively, with Lipofectamine 3000 transfection reagent (Thermo Fisher Scientific) according to manufacturer's protocols.

Bone marrow-derived DCs (BMDCs) and bone marrow-derived macrophages (BMDMs)

BMDCs were obtained and cultured as described previously[12]. Cells were differentiated with 35 ng/ml GM-CSF (Peprotech Tebu-bio, Offenbach, Germany) or 400 ng/ml FLT3L (Peprotech Tebu-bio) for 8-10 days. The purity of BMDC cultures was >90%, as determined by flow cytometry for CD11c. To obtain BMDMs, bone marrow from femurs of CD11c-Cre OTUB1^{fl/fl} and OTUB1^{fl/fl} mice, respectively, was isolated and then incubated with 35ng/ml M-CSF (Peprotech Tebu-bio) for 8 days. Purity of BMDM cultures was >90% as determined by flow cytometry for CD11b and F4/80.

In vitro stimulation

After in vitro expansion, BMDCs were washed once with PBS and plated at desired

concentrations with appropriate medium. After 4h of incubation at 37°C, cells were stimulated as indicated. Samples for immunoprecipitation were always stimulated in the presence of the proteasome inhibitor MG132 (Sigma Aldrich). For the preparation of TLA, freshly released tachyzoites were isolated as described before and then freeze-thawed in liquid nitrogen for 5 times. Concentrations of TLA were quantified by the spectrophotometer. TgPFN was produced in the protein science core facility of the Karolinska Institute (Stockholm, Sweden). The purity of TgPFN was controlled by mass spectrometry and protein concentration was determined by Bradford assay. LPS (Sigma, St Louis, USA) was used at a working concentration of 500 ng/ml. PGN, ODN, IMQ and Poly I:C were purchased from Invivogen (San Diego, California, USA) and used at manufacturer's recommended concentrations. Recombinant murine IL-1β and TNF were purchased from PeproTech (Rocky Hill, USA) and used at working concentrations of 10 ng/ml and 20 ng/ml, respectively.

Cell isolation and flow cytometry

Leukocytes in the peritoneal cavity were isolated by lavage with PBS. Leukocytes in the spleen and brain were isolated by passing the organ through a 70 or 100 µm cell strainer, respectively. Erythrocytes from peritoneal cavity, brain and spleen samples were lysed by incubating the cells in lysis buffer at 4 ° C for 10 min. In addition, leukocytes from the brain and the liver were separated by Percoll (GE Healthcare) gradient centrifugation according to producer's protocol. Briefly, the cell pellet was resuspended in 10 ml Percoll at a density of 1.098 g. Density gradient was created by overlaying Percoll densities of 1.07 g, 1.05 g, 1.03 g, and 1.00 g. The cells were then centrifuged at 1.200 g for 20 min with rapid start-up, but without rotor brakes. The upper layers of densities 1.00 g and 1.03 g, containing lipids and debris, were carefully removed and discarded. The densities between 1.05 g, 1.07 g, and 1.098 g of Percoll gradients, where all the

leukocytes accumulated, were transferred to a fresh Falcon tube and washed with cell culture medium. Finally, the cell pellet was washed with FACS medium (PBS + 3% FCS). Cells were counted with the haemocytometer and then stained with specific fluorescent antibodies as indicated (BD Bioscience). For intracellular staining, cells were first stimulated for 6 hours with heat-killed (60 °C for 20 min) *T. gondii* (MOI = 3) in the presence of 1 µg/ml Brefeldin A (Thermo Fisher) to block cytokine secretion. Then, extracellular staining was performed and after that, intracellular antibodies were added in the presence of permeabilization buffer (Permeabilization Buffer 10x, Cat#00-8333-56, Invitrogen, Karlsruhe, Germany). Samples were acquired with the FACSCanto II (BD Biosciences), and data were analysed with the FlowJo® software. Cytokines from cell cultures and serum were measured using the BD CBA mouse inflammation kit (BD Bioscience). CBA data were acquired on the FACSCanto II and analysed with the BD CBA Software (BD Bioscience).

Quantitative and semi-quantitative PCR

DNA and mRNA were isolated from mouse organs or primary BMDCs. Tissues from mice were first mechanically homogenised with the QIAshredder kit (Qiagen), then isolation of DNA and mRNA was completed using the DNeasy or RNeasy kit (Qiagen), respectively. mRNA was reversely transcribed into cDNA using the SuperScript reverse transcriptase kit. Specific primers for *T. gondii* (Sense 5-gga act gca tcc gtt cat gag-3; antisense 5-tct tta aag cgt tcg tgg tc-3, Eurofins Scientific, Luxemburg), HPRT, iNOS, iGTP, GBP3 and GBP5 (Applied Biosystems, Foster City, California, US) were used. Quantitative and semi-quantitative PCR was performed on a Lightcycler 480 system (Roche).

3. MATERIALS AND METHODS

Protein isolation and Western Blot

Cells were stimulated as indicated and lysed for 30 minutes on ice with complete RIPA lysis buffer; proteins were then separated from insoluble fractions by centrifugation at 14.000 RPM at 4°C for 20 min. Nuclear and cytoplasmic fractions were separated using the Nuclear and Cytoplasmic Extraction Kit (Thermo Scientific). The protein content of the supernatant was determined photometrically using the Bradford reagent (Sigma Aldrich). Protein samples were diluted and boiled in lane marker reducing sample buffer (Thermo Scientific) at 95 °C for 5 min. Equal amounts of samples were separated on 8-10% SDS polyacrylamide gels and subsequently transferred through a semi-dry transfer system to polyvinylidene difluoride (PVDF) membranes. Membranes were blocked with 5% BSA and later incubated with specific antibodies as indicated. WB images were developed with an ECL plus kit (GE Healthcare) and captured on an INTAS image analysis system (INTAS). For quantification of protein intensities by densitometry, ImageJ software was used.

Immunoprecipitation

Proteins isolated from stimulated and unstimulated BMDCs were incubated under gentle shaking at 4 °C for 1 h with Sepharose G Beads (GE Healthcare) to remove proteins with aspecific binding to the beads. After removal of beads by centrifugation, equal amounts of lysates were then incubated with specific antibodies under gentle shaking at 4 °C overnight. The day after, Sepharose G beads were added to the lysates and incubated at 4 °C for 2 h with gentle shaking. To capture the immunocomplex, samples were centrifuged and beads were washed five times with PBS by pulse centrifugation. The beads were then resuspended in 2 x lane marker reducing sample buffer and boiled at 95 °C for 5 min. Then, samples were centrifuged at 14.000 g at 4°C for 1 min and the supernatant was harvested for WB analysis

as previous described.

Free ubiquitin assay

To test unanchored ubiquitin chains in FLT3L-expanded BMDCs we followed the protocol published by Gilda JE et al [191]. 1 mg of purified proteins from unstimulated and stimulated samples were depleted of substrate-conjugated ubiquitin chains using TUBEs (UM402, LifeSensors, PA, USA). TUBEs have been shown to be highly efficient at removing polyubiquinated proteins from lysates [192]. Two steps of incubation with TUBE probes were taken and significantly more bait (TUBEs) was used than required to ensure the lysate was depleted of ubiquitinated proteins. For every mg of total protein, 25 µl of resin was utilized and incubated for 1 h at 4°C in slow movement. TUBE-agarose was collected by low speed centrifugation (1.000 g, 4°C) for 2 min. The beads were washed with Tris-buffered saline containing 0.05% Tween-20 (TBST) and collected by low speed centrifugation. Supernatant was collected and subsequently analysed by western blot. After a pre-treatment with 0.5% glutaraldehyde, we used anti-ubiquitin VU-101 antibody (LifeSensors) to detect unanchored ubiquitin chains.

Magnetic sorting of leucocytes

Spleens from OTUB1$^{fl/fl}$ and CD11c-Cre OTUB1$^{fl/fl}$ mice were harvested and single cell suspension was obtained by passing the organs through 70 µm cell strainers. After lysis of erythrocytes, cells were pelleted by centrifugation at 1.200 rpm for 6 min. The cell pellet was resuspended in 40 µl of buffer (PBS supplemented with 0.5% bovine serum albumin (BSA) and 2 mM EDTA, pH 7.2) per 10^7 cells. DCs, Macrophages, NK cells, T cells and B cells were isolated with specific kits accordingly to the manufacturer's protocol. First the cells were incubated

with the fluorescent specific antibody for 15 minutes, then the Selection Cocktails, specific for the fluorochrome used was added for another 15 minutes. Finally, the magnetic beads were vigorously mixed and added to the solution for 10 minutes. The cell suspension was brought to a total volume of 2.5ml with medium. Tubes containing the cell suspension were placed inside an EasySep magnet (STEMCELL Technologies (Cologne, Germany) and set aside for 5 minutes. With one single movement, magnet containing tube was inverted and non-bonded cells were removed for the solution. Cells were then washed with medium and magnetic isolation was repeated for a total of 4 or 5 times. At the end of the last isolation tubes were removed from the magnet and cells were resuspended in PBS and harvested for western blot as previously described. The purity of cells was 90-95% as determined by FACS analysis.

Transduction of BMDCs

pLenti-C-Myc-DDK vector and pLenti-C-Myc-DDK-UBE2N plasmids were purchased from Origene. Lentivirus overexpressing UBC13 and control lentivirus were produced with the Lentiviral packaging kits (Origene). At 24 and 48 h after transfection, supernatant containing lentivirus was collected, filtered, aliquoted, and stored at -80°C.

After *in vitro* expansion for 7 d, FLT3L-BMDCs were transduced with lentivirus in the presence of polybrene (4 μg/ml). Plates containing BMDCs, lentivirus and polybrene were centrifuged at 1.000 g at 32 °C for 90 min to concentrate the cells and the lentivirus at the bottom of the wells, and further incubated at 37°C for 5 h. thereafter, medium containing lentivirus and polybrene was then removed and substituted by fresh BMDC culture medium. Transduced cells were incubated at 37°C in the presence of FLT3L for 2 more days, after which cells were stimulated with TgPFN as indicated.

Motility assays

Motility assays were performed by the group of Barragan (Department of Molecular Biosciences, Stockholm University, 10691 Stockholm, Sweden). DCs were cultured in chamber slides (Lab-Tek®, Nalge Nunc International) with complete medium ± freshly egressed GFP-expressing *T. gondii* tachyzoites (type II PTG-GFP, MOI = 3, 4 h incubation). Bovine collagen I (1 mg/ml, Life Technologies) was added and then loaded onto a Labtech chamber slide (Nalge Nunc International) where the medium chambers were removed, but the gaskets were left intact. The slide was spun at 1.000 rpm for 5 s to concentrate the cells to the bottom of the slide. Live cell imaging was performed for 1 h, 1 frame/ min, at 10 x magnification (Z1 Observer with Zen 2 Blue v. 4.0.3, Zeiss). Time-lapse images were consolidated into stacks and motility data was obtained from 30 cells/condition (Manual Tracking, ImageJ) yielding mean velocities (Chemotaxis and migration tool, v. 2.0). GFP+ cells harbouring tachyzoites were defined as infected cells. Motility patterns were compiled using ImageJ (image stabilizer software and manual tracking plugins).

Histology

Histology was performed with the collaboration of the group of Prof. Dr. Martina Deckert (Department of Neuropathology, Faculty of Medicine and University Hospital Cologne, University of Cologne, 50931 Cologne, Germany). At day 30 p.i. with *T. gondii*, mice were anesthetized and intracardially perfused with 0.9 % NaCl; brains were dissected and snap-frozen in isopentane (Flika, Neu-Ulm, Germany), pre-cooled on dry ice, and stored at -80°C until preparation of 10 μm frozen sections. Immunohistochemistry was performed with polyclonal rabbit anti-*T. gondii* (BioGenex, Fremont, CA, USA) using an ABC protocol with 3,3' diaminobenzidine (Merck, Darmstadt, Germany) and H_2O_2 as co-substrate.

MCMV infection

Seven to ten weeks old CD11c-Cre OTUB1^{fl/fl} and OTUB1^{fl/fl} control mice were i.v. infected with 106 murine Cytomegalovirus (MCMV) 3DR87. After 36 h, mice were perfused with PBS and lymph nodes, lungs, spleens and livers were removed and organ homogenates were plated in serial log10 dilutions on primary murine embryonic fibroblasts. Centrifugal enhancement was performed (2000 rpm, 15 min) and after 2 h of incubation at 37°C and 5% CO_2 the cells were overlaid with 1% methylcellulose. Plaques were counted after 4 days of culture under a light microscope (Zeiss). In addition, leukocytes were isolated from the spleen and liver, and analysed by flow cytometry. Intracellular staining for IL-12 was performed after 4 h incubation at 37°C with Golgi plug™ (BD Bioscience). Serum was collected from infected animals to measure cytokines.

Quantification and statistical analysis

Quantification of western blot was performed using NIH ImageJ software. Statistical analysis and graphic design were performed using GraphPad Prism 6. For Student's t test, P values <0.05 were considered statistically significant: * indicates a P value <0.05, ** indicates a P value <0.01, *** indicates a P value <0.001. All experiments were performed at least twice.

4. RESULTS

4.1 OTUB1 is up-regulated in DCs during *T. gondii* infection and LPS challenge

Since OTUB1 has been reported to interact with molecules that are critical for the activation of the immune system and DCs are key immune cells protecting the host from various infectious diseases including toxoplasmosis [28,193] but also contributing to immunopathology in sepsis [145,151,194,195], we asked if DC-specific OTUB1 is regulated during murine toxoplasmosis and LPS-induced sepsis.

OTUB1 protein was constitutively expressed in splenic CD11c$^+$ cells, which comprise all major populations of DCs [4], but its levels were significantly increased during *T. gondii* infection and LPS challenge (Fig. 8a and 8b).
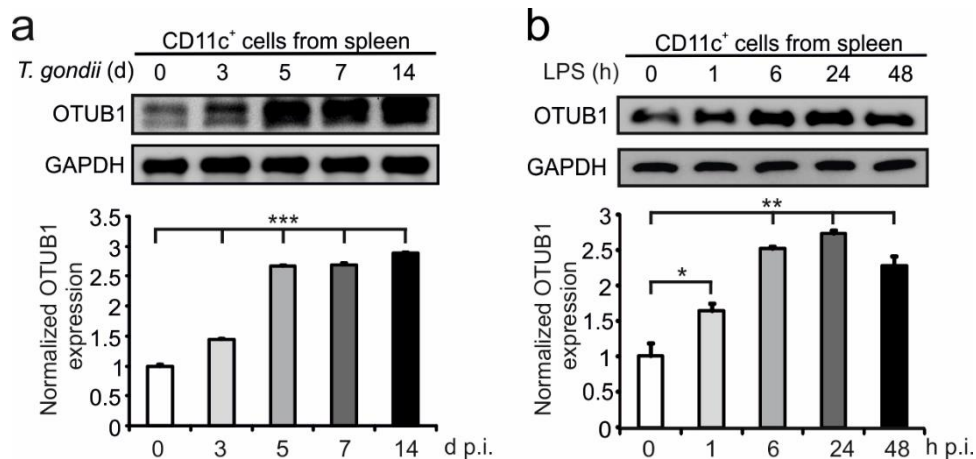
Figure 8 OTUB1 is up-regulated in CD11c+ cells during toxoplasmosis and LPS challenge. Mice were infected with T. gondii (a) or challenged with LPS (b) for the indicated time points. CD11c+ cells were isolated from spleens by magnetic sorting and OTUB1 expression was measured by WB (upper panels). The lower panels show the relative expression of OTUB1 (n = 3 for each group).

To substantiate the *in vivo* findings, *in vitro* expanded BMDCs were stimulated with *T. gondii*, which activates TLR2, TLR4, TLR7, and TLR11/12 [179], TgPFN, or LPS, which binds to TLR4, for the indicated time and analyzed by WB for OTUB1 expression. Consistent with the *in vivo* data, all three stimuli significantly increased OTUB1 protein in *in vitro* stimulated GM-CSF- and FLT3L-expanded BMDCs (Fig. 9a-9f).
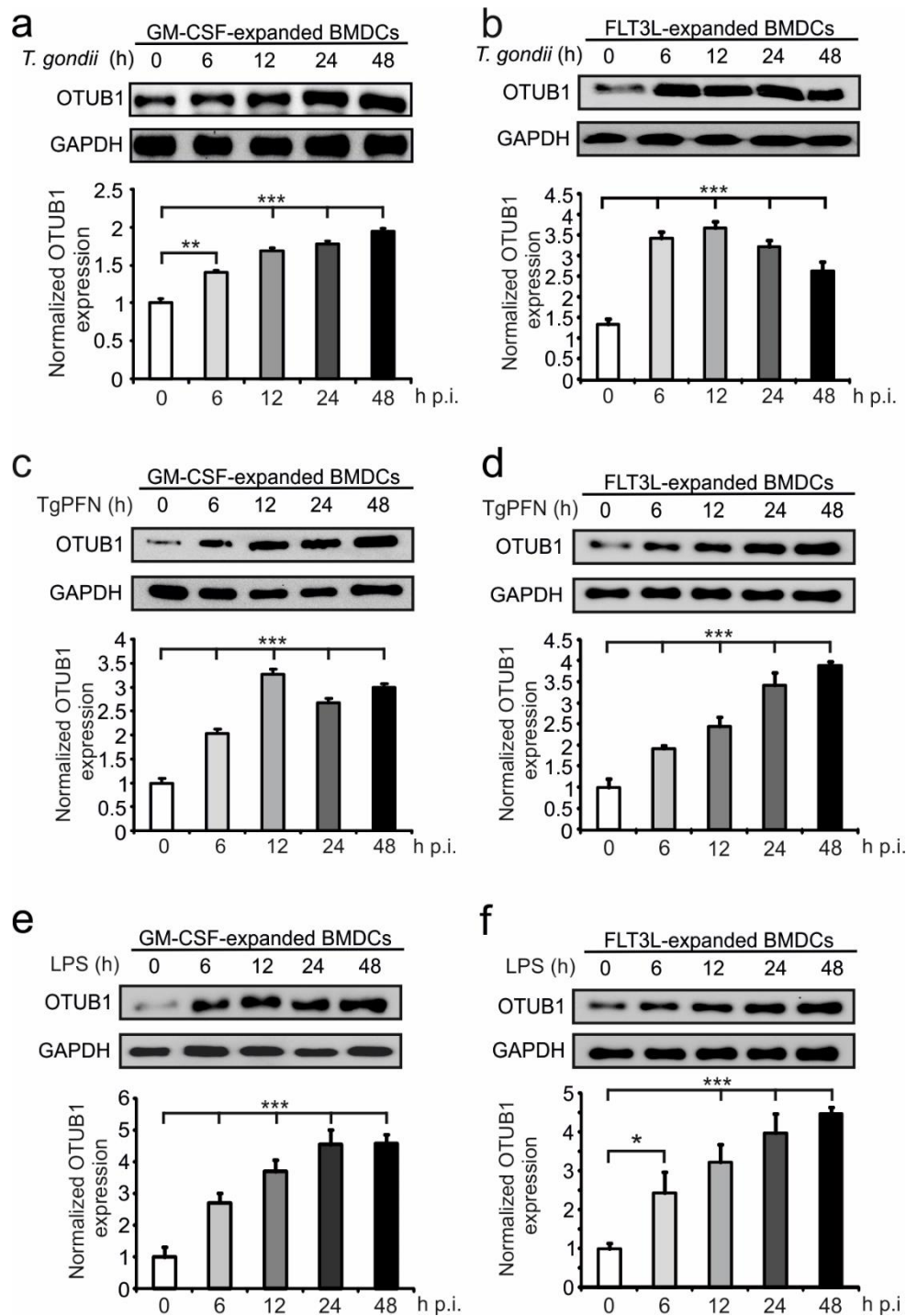
Figure 9 *OTUB1 is up-regulated after T. gondii in vitro infection and in vitro stimulation with T. gondii antigen TgPFN and LPS. GM-CSF-expanded (a, e and g) and FLT3L-expanded (d, f and h) BMDCs generated from C57BL/6 OTUB1$^{fl/fl}$ mice were stimulated in vitro with tachyzoites at an MOI of 3 (c and d), 1 μg/ml TgPFN (e and f), and 500ng/ml LPS (g and h) for the indicated time points. OTUB1 expression in BMDCs was analysed by WB (upper panels). The lower panels show the relative expression of OTUB1 (n = 3 for each group).*

The identification of the upregulation of OTUB1 in *T. gondii*-infected, TgPFN and LPS-stimulated DCs raises the question whether OTUB1 is not only induced upon stimulation of the TLR/MyD88/NF-κB signaling but may also act as a feedback regulator of this signaling

pathway.

4.2 OTUB1 positively regulates pro-inflammatory NF-κB signaling in DCs

To determine the functional role of OTUB1 in DCs, we crossed CD11c-Cre mice [190] with

OTUB1^{fl/fl} mice [189] to generate CD11c-Cre OTUB1^{fl/fl} mice. WB analysis of DCs, macrophages,

NK cells, T cells, and B cells isolated from spleens of OTUB1^{fl/fl} and CD11c-Cre OTUB1^{fl/fl}

mice showed that OTUB1 was specifically and efficiently deleted from DCs of CD11c-Cre

OTUB1^{fl/fl} mice (Fig. 10a). In addition, OTUB1 expression was strongly reduced in *in vitro*-

expanded BMDCs but not in bone-marrow-derived macrophages (BMDMs) (Fig. 10b).
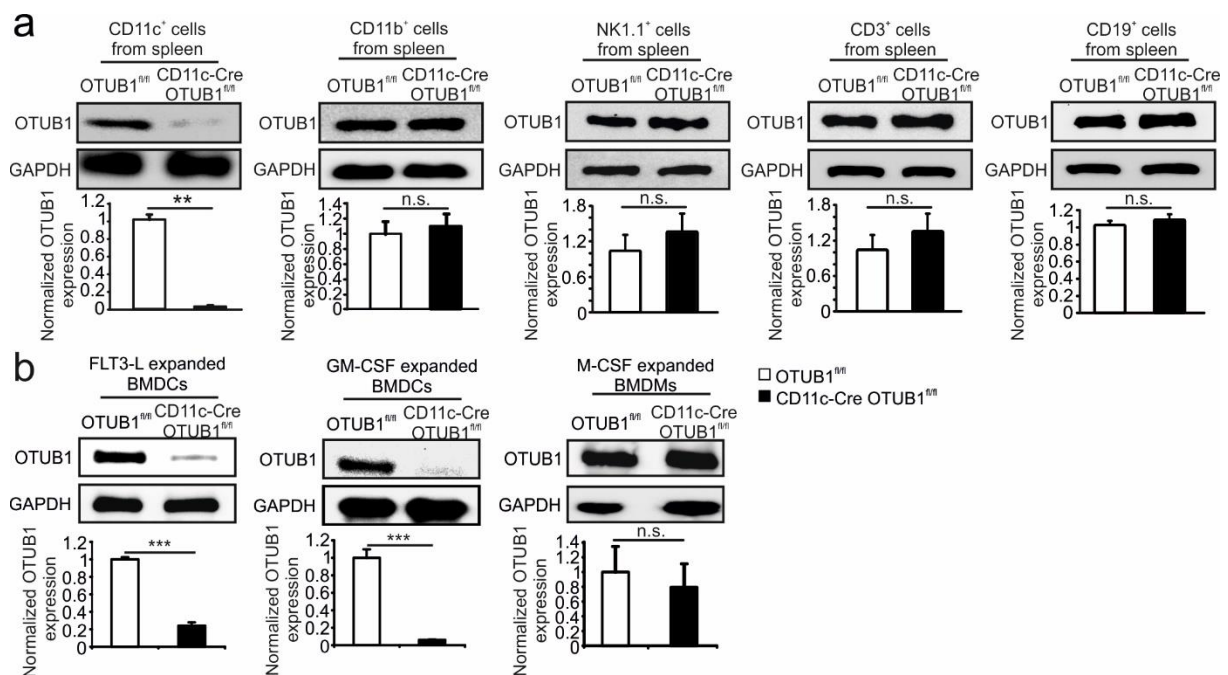
Figure 10 OTUB1 is specifically deleted in CD11c+ cells in vivo and in vitro. (a) CD11c+, CD11b+, NK1.1+, CD3+ and CD19+ cells were magnetically isolated from spleens of CD11c-Cre OTUB1fl/fl and control OTUB1fl/fl mice, and analysed by WB for OTUB1 expression. The lower panels show the relative expression of OTUB1 normalized to GAPDH (n = 3). (b) OTUB1 expression in GM-CSF-expanded BMDCs, FLT3L-expanded BMDCs, and M-CSF-expanded BMDMs was analysed by WB (upper panels). The lower panels show the relative expression of OTUB1 normalized to GAPDH (n = 3).

The CD11c-Cre OTUB1^{fl/fl} mice were born in a normal Mendelian ratio, did not develop any

clinical signs of disease, and preserved a normal immune system as revealed by flow

cytometry (Fig. 11a-11e).
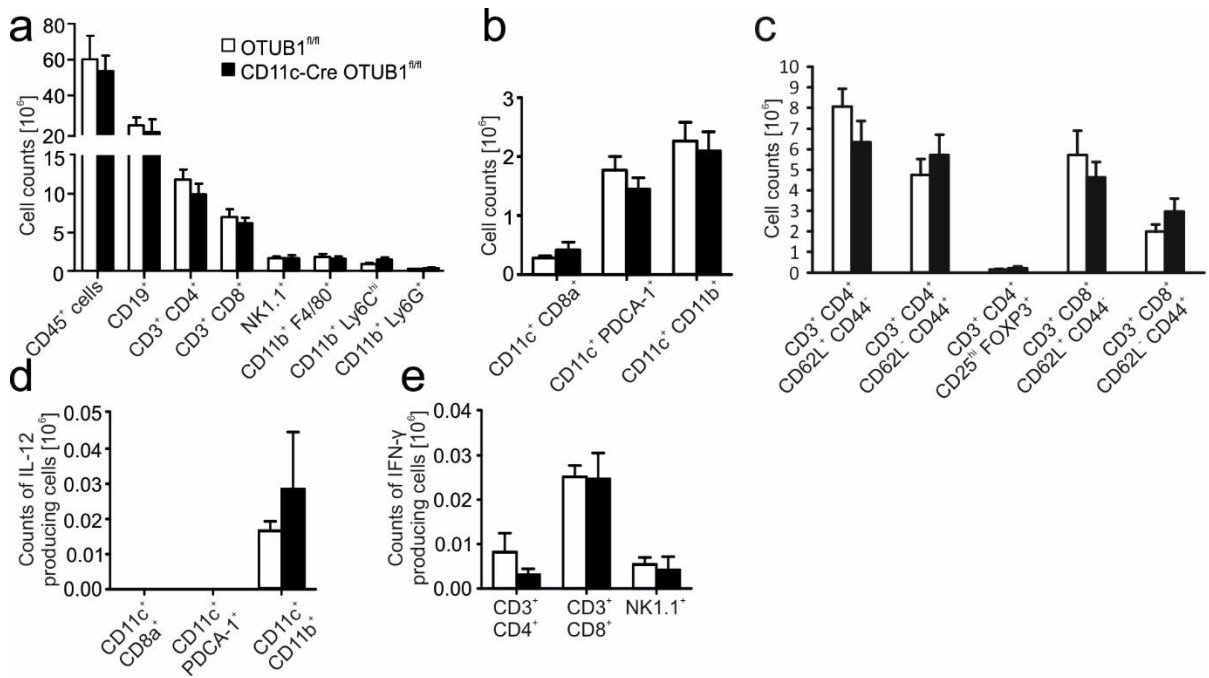
Figure 11 CD11c-Cre OTUB1$^{fl/fl}$ mice exhibit a normal immune system in physiological condition. *Absolute numbers of leukocytes (a), DC (b) and T cell (c) subpopulations in the spleen of OTUB1$^{fl/fl}$ and CD11c-Cre OTUB1$^{fl/fl}$ mice were determined by flow cytometry. (d and e) Absolute numbers of IL-12-producing DCs (d) and IFN-γ-producing T and NK cells (e) were calculated based on flow cytometry results.*

Consistent with the finding that OTUB1 had no impact on DC differentiation *in vivo* (Fig. 11b), OTUB1 did not interfere with the *in vitro* development of FLT3L- and GM-CSF-expanded BMDC subpopulations including CD8$^+$ CD11c$^+$ cDC1, CD11b$^+$ CD11c$^+$ cDC2, and PDCA1$^+$ CD11c$^+$ pDC (Fig 12).
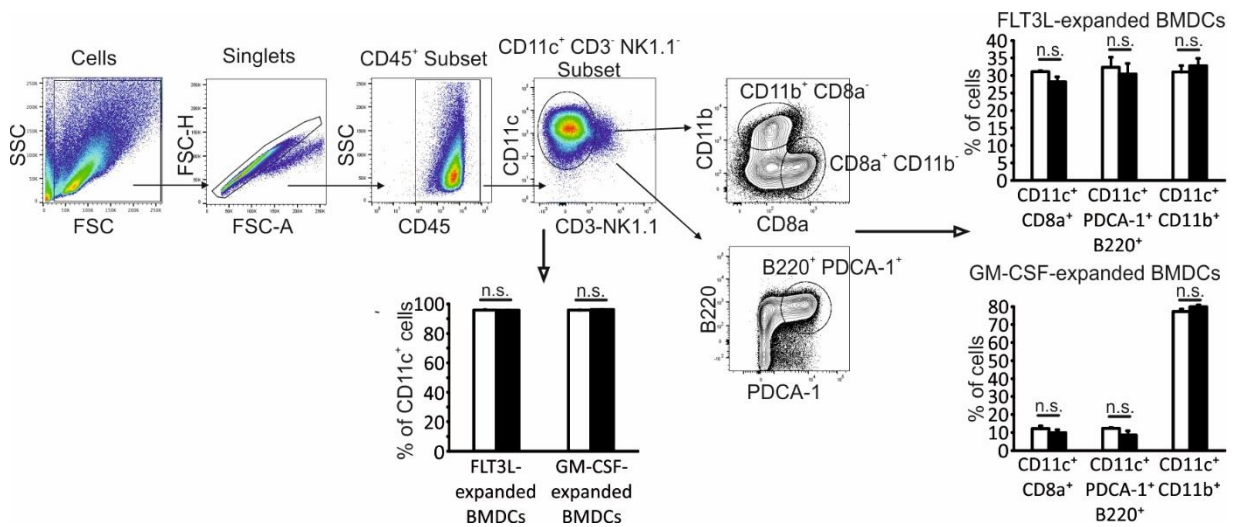
Figure 12 OTUB1 does not play a role in BMDC in vitro development. *Gating strategy for BMDC subpopulations. After in vitro FLT3L and GM-CSF expansion, BMDCs were stained for DC markers and measured by flow cytometry. Percentages of total CD11c+ cells (lower panel) and CD8a$^+$, CD11b$^+$ and PDCA-1$^+$ B220$^+$ subtypes (right panels) were analysed by FlowJo software. (n = 3).*

To clarify the role of OTUB1 in DCs after TLR engagement, we stimulated *in vitro* FLT3L-expanded BMDCs with different TLR ligands. As shown in Fig. 13a and 13b, OTUB1-deficient BMDCs produced significantly less IL-12, TNF, and IL-6 after stimulation with *T. gondii*, *T. gondii* lysate antigen (TLA), TgPFN, which all signal via MyD88 [175] (Fig. 13a), and LPS (Fig. 13b).
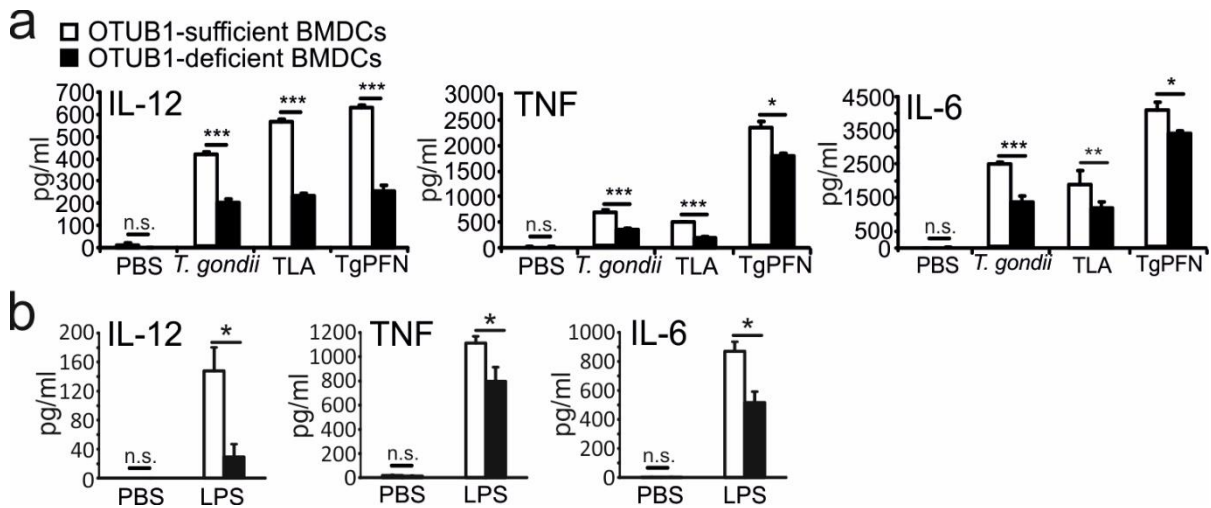

Figure 13 OTUB1 deletion impairs cytokine response by BMDCs during T. gondii antigens and LPS stimulations. OTUB1-sufficient and -deficient BMDCs were left untreated or stimulated with T. gondii tachyzoites (MOI = 3), different antigens (TLA and TgPFN) or LPS for 24h. Concentrations of cytokines in the supernatant were analysed by ELISA (n = 4).

In addition, engagement of TLR2, TLR7, and TLR9 , which all signal via MyD88, and of TLR3, which signals MyD88-independent through TRIF [51], resulted in significantly reduced IL-12, TNF, and IL-6 production of OTUB1-deficient BMDCs (Fig. 14) illustrating a stimulatory role of OTUB1 in pro-inflammatory TLR signaling.
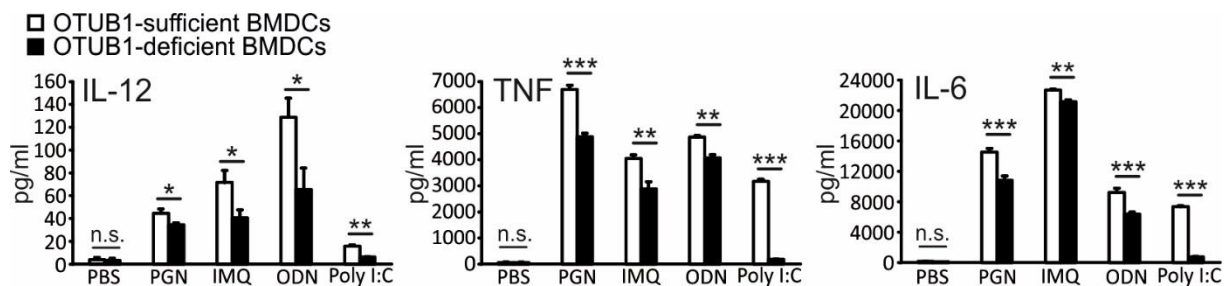
Figure 14 OTUB1 deletion impairs cytokine productions during TLR2, TLR7, TLR9 and TLR3 stimulation. FLT3L-expanded BMDCs were stimulated with PGN (TLR2 agonist), Imiquimod (IMQ) (TLR7 agonist), CpG ODN (TLR9 agonist) and Poly I:C (TLR3 agonist) for 24 h. Cytokines in the supernatant were analysed by ELISA (n = 7).

To understand how OTUB1 promotes cytokine production in DCs, we stimulated FLT3L-expanded BMDCs with TLA (Fig. 15a), TgPFN (Fig. 15b) and LPS (Fig. 15c), respectively, and analyzed signaling molecules by WB. WB analysis of cytoplasmic and nuclear fractions of

untreated and stimulated OTUB1-sufficient and -deficient BMDCs revealed that after 30 minutes of stimulation, nuclear translocation of NF-κB p65 was reduced in OTUB1-deficient BMDCs (Fig. 15a-15c), suggesting that OTUB1 augments NF-κB activation.
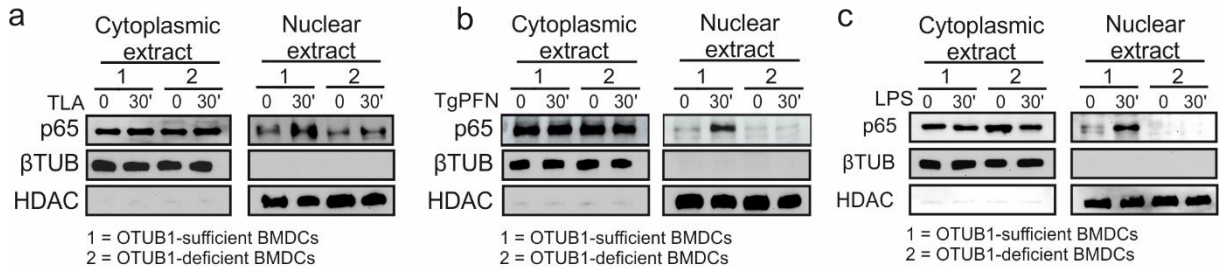

Figure 15 OTUB1 regulates NF-kB activation. *FLT3L-expanded BMDCs were left untreated or stimulated with TLA (a), TgPFN (b) or LPS (c) for 30 min. Levels of p65 in cytoplasmic and nuclear fractions were analysed by WB.*

In murine DCs, recognition of TgPFN by TLR11 and TLR12 induces IL-12 production by activating two signaling pathways: NF-κB and IRF8 [196,197]. In contrast to NF-κB, stimulation of BMDC with TgPFN resulted in an equal nuclear accumulation of IRF8 in both genotypes indicating that OTUB1 only regulates the MyD88/NF-κB signaling (Fig. 16).
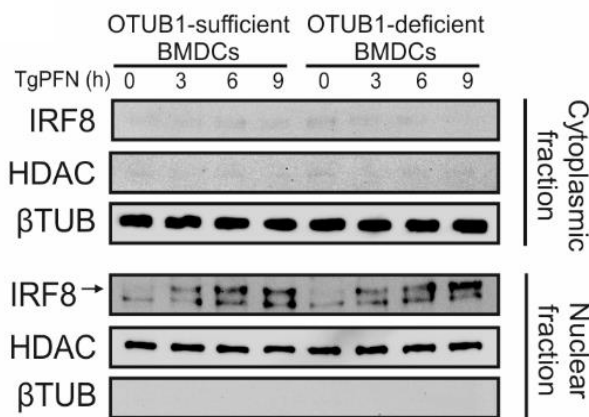
Figure 16 OTUB1 does not regulate IRF8 pathway. *FLT3L-expanded BMDCs were stimulated with TgPFN for indicated time points. IRF8 in cytoplasmic and nuclear extracts was detected by WB.*

Next, we analyzed the MyD88-mediated signaling upstream of p65. Reduced phosphorylation of TAK1, IκBα and p65 was detected in OTUB1-deficient BMDCs upon stimulation with TgPFN (Fig. 17a), suggesting that OTUB1 is required for the full-fledged activation of NF-κB. To reinforce the contention that OTUB1 promotes IL-12 production by increasing NF-κB activity, we studied the effect of IKK inhibition on TgPFN-induced cytokine production in OTUB1-sufficient and -deficient BMDCs. Abolishment of NF-κB activity by the inhibitor dramatically

reduced IL-12 production in both OTUB1-sufficient and -deficient BMDCs and blunted the difference between the two cell populations (Fig. 17b).
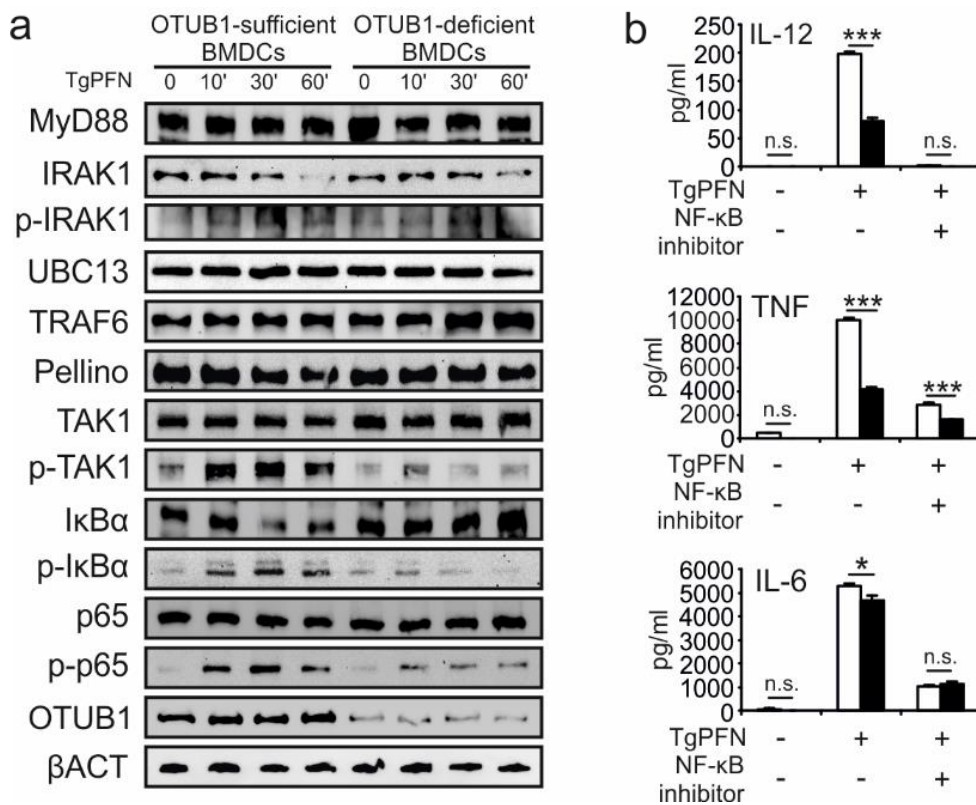

Figure 17 OTUB1 is required for the full-fledged activation of NF-κB pathway. *(a) FLT3L-expanded BMDCs were stimulated with TgPFN for indicated time points. Whole cell lysates were analysed by WB with indicated antibodies. (b) FLT3L-expanded BMDCs were left untreated or stimulated with TgPFN in the presence or absence of NF-κB inhibitor for 24 h. Cytokine levels in the supernatant of cell cultures were measured by ELISA (n = 4).*

Since phosphorylation of TAK1 is a crucial step for the activation of the NF-κB pathway in TLR-initiated signaling pathways [198], we determined the phosphorylation of TAK1 following stimulation of TLR2, TLR3, TLR4, TLR7, and TLR9 with their specific ligands. In good agreement with the increased TAK1 phosphorylation of OTUB1-competent BMDCs upon TLR11/12 stimulation (Fig. 17a), phosphorylation of TAK1 was strongly increased in OTUB1-competent BMDCs upon engagement of TLR2, TLR4, TLR7, TLR9 and also TLR3, respectively (Fig. 18).
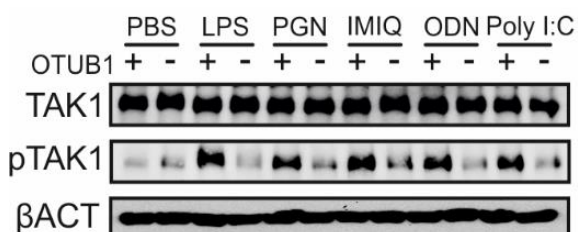

Figure 18 OTUB1 regulates TLR-mediated activation of NF-κB pathway. *FLT3L-expanded BMDCs were stimulated with LPS, PGN, IMIQ, ODN and Poly I:C, respectively, for 30 min. Whole cell lysates were analysed by WB with indicated antibodies. Data are shown as mean + SD. * p < 0.05, ** p < 0.01, *** p < 0.001.*

Stimulation of TLR3 activates NF-κB by RIP1-mediated TAK1 phosphorylation [199]. Therefore, we further explored whether the increased MyD88-independent TLR3/TRIF-mediated activation of TAK1 in OTUB1-competent BMDCs also resulted in an enhanced activation of NF-κB. In fact, stimulation with Poly I:C induced augmented IκBα and p65 phosphorylation in OTUB1-competent DCs as compared to OTUB1-deficient DCs (Fig. 19a). Likewise, stimulation with TNF, which also induces RIP1-dependent TAK1 activation [200], and with IL-1β, which activates TAK1 via MyD88 and TRAF6 [201], induced an increased phosphorylation of IκBα and p65 in OTUB1-competent BMDCs (Fig. 19b and 19c, respectively), further illustrating that OTUB1 supports NF-κB activation in DCs upon stimulation with both MyD88-dependent and -independent proinflammatory stimuli.
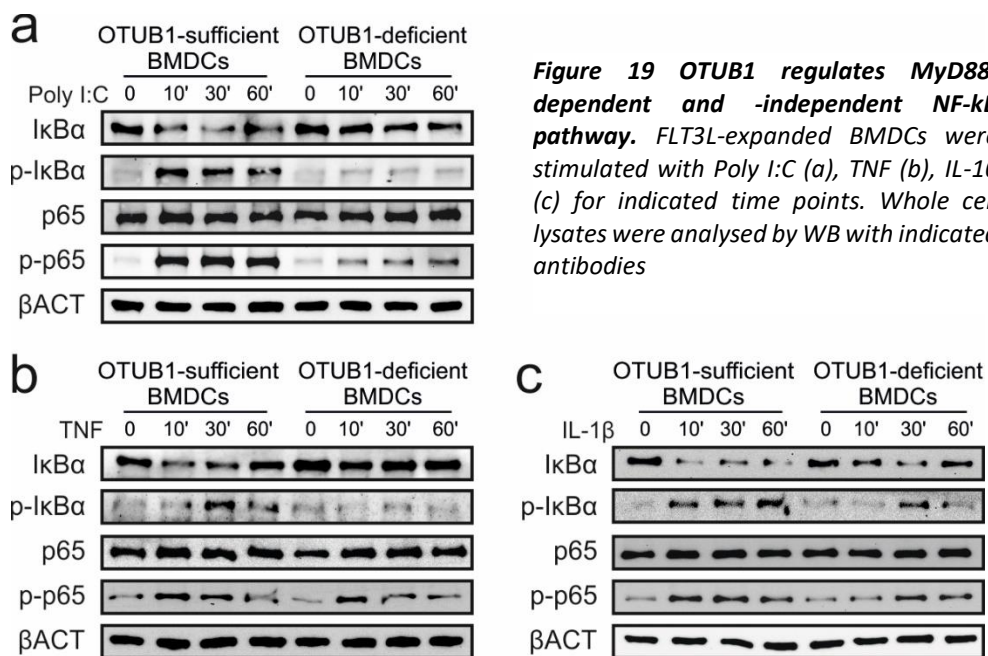

Figure 19 OTUB1 regulates MyD88-dependent and -independent NF-kB pathway. FLT3L-expanded BMDCs were stimulated with Poly I:C (a), TNF (b), IL-1β (c) for indicated time points. Whole cell lysates were analysed by WB with indicated antibodies

Beside activation of NF-κB, engagement of TLR4 and TLR11/12 results in activation of the MAPKs p38, ERK1/2, and JNK, which induce genes associated with innate immunity, inflammation, and cell survival [202]. The NF-κB and MAPK pathways cross-regulate each other and share some signaling molecules including TAK1, UBC13 and TRAFs [198,203,204]. Therefore, we studied the impact of OTUB1 on MAPK activation upon TLR11/12 and TLR4 stimulation.

Stimulation of OTUB1-competent BMDCs with both TgPFN and LPS resulted in increased p38, ERK1/2 and JNK phosphorylation as compared to OTUB1-deficient BMDCs (Fig. 20a and 20b) demonstrating that OTUB1 augments activation of both NF-κB and MAPK upon engagement of TLR4 and TLR11/12.
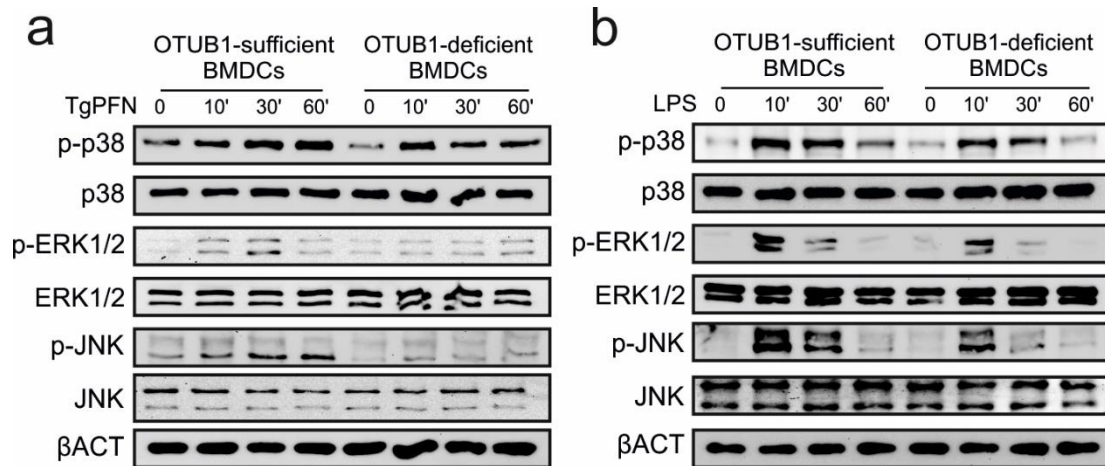

Figure 20 OTUB1 regulates MAPK pathway during TgPFN and LPS stimulation. *FLT3L-expanded BMDCs were stimulated with TgPFN (a) or LPS (b) for indicated time points. Whole cell lysates were analysed by WB with indicated antibodies. Intensity of p-p38, p-ERK1/2 and p-JNK was quantified and normalized to unstimulated samples (data not shown). (n=4)*

4.3 OTUB1 regulates NF-κB activity via deubiquitinating and stabilizing UBC13

To investigate the mechanism how OTUB1 promotes NF-κB activation, we performed a screening for OTUB1-interacting signaling molecules of the NF-κB pathway by immunoprecipitation (IP) and WB. In this screening, UBC13 (UBE2N) emerged as a promising target of OTUB1 because it was co-immunoprecipitated with OTUB1 upon stimulation with TgPFN (Fig. 21a and 21b) and LPS (Fig. 21c and 21d) and a previous study reported nuclear OTUB1 and UBC13 interaction in the context of DNA double-strand breaks [205]. Functionally, UBC13 acts as an E2 conjugating enzyme in the NF-κB pathway. In cooperation with the E3 ligase Pellino, UBC13 can add K63-linked polyubiquitin chains on phosphorylated IRAK1, which enables IRAK1 to activate NEMO directly [206]. Additionally, phosphorylated but not ubiquitinated IRAK1 induces the recruitment of TRAF6, which is subsequently K63

ubiquitinated by itself to activate NEMO through TAK1. In this process, the E2 activity of

UBC13 is indispensable for the self-ubiquitination and activation of TRAF6. Therefore, UBC13

can positively regulate the NF-κB signaling via ubiquitinating IRAK1 and TRAF6. In good

agreement, we detected an interaction of UBC13 with TRAF6 and Pellino in TgPFN-stimulated

BMDCs (Fig. 21d). On the contrary, we did not detect any interaction between OTUB1 and

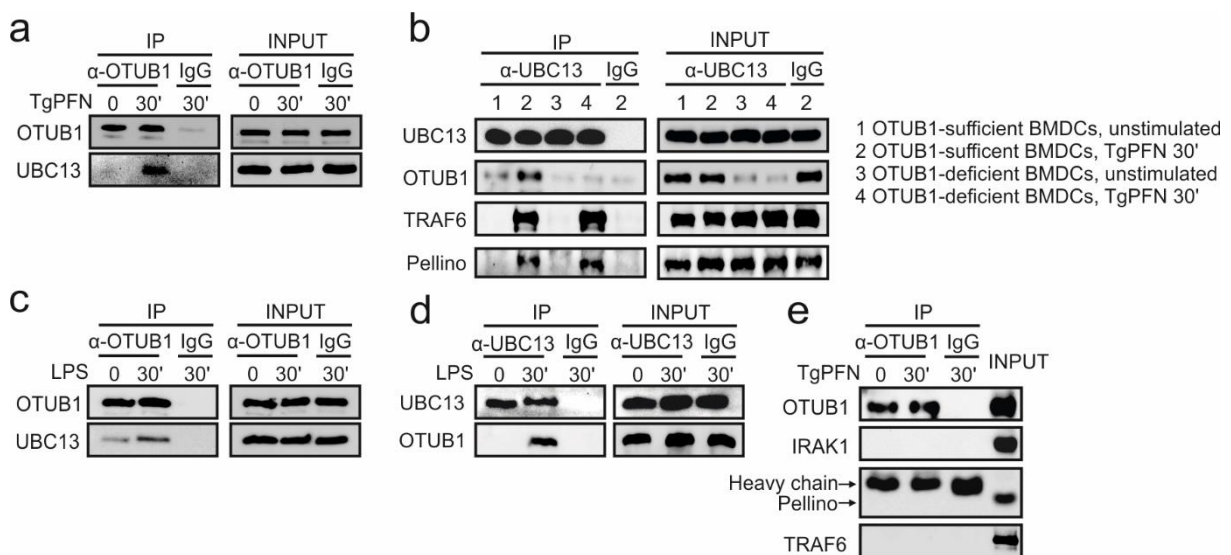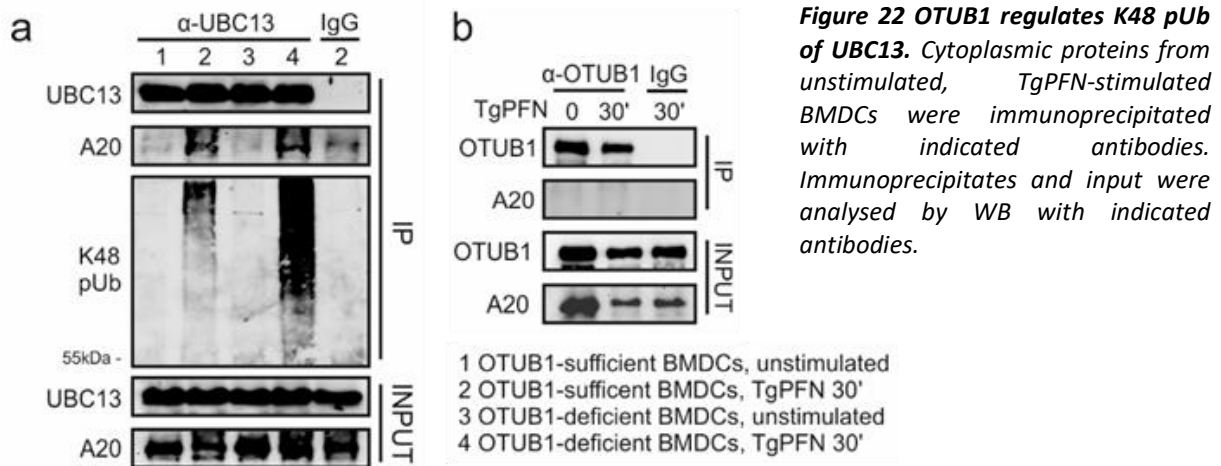IRAK1, Pellino or TRAF6, respectively (Fig. 21e).

Figure 21 OTUB1 interacts with UBC13. *Cytoplasmic proteins from unstimulated, TgPFN-stimulated (a, b and e) and LPS-stimulated (c and d) BMDCs were immunoprecipitated with indicated antibodies. Immunoprecipitates and input were analysed by WB with indicated antibodies.*

It has been reported that UBC13 protein stability is controlled by the E3 ligase A20, which adds

K48 polyubiquitin chains on UBC13 to induce its proteasomal degradation [207]. Since (i) OTUB1

interacts with UBC13, (ii) UBC13 can be K48 ubiquitinated [207], and (iii) OTUB1 is a K48-specific

DUB [208], we explored the effect of OTUB1 on the K48 ubiquitination status of UBC13. As shown

in Fig. 22a, OTUB1 reduced K48 ubiquitination of UBC13 in TgPFN-stimulated BMDCs. This

reduced K48 ubiquitination of UBC13 is due to the deubiquitinating activity of OTUB1 on

UBC13 but not by an interaction of OTUB1 with A20 (Fig. 22b), the E3 ligase mediating K48

ubiquitination of UBC13 [207].

Figure 22 OTUB1 regulates K48 pUb of UBC13. *Cytoplasmic proteins from unstimulated, TgPFN-stimulated BMDCs were immunoprecipitated with indicated antibodies. Immunoprecipitates and input were analysed by WB with indicated antibodies.*

1 OTUB1-sufficient BMDCs, unstimulated
2 OTUB1-suffcient BMDCs, TgPFN 30'
3 OTUB1-deficient BMDCs, unstimulated
4 OTUB1-deficient BMDCs, TgPFN 30'

Since K48 ubiquitination is associated with protein degradation, we studied the impact of OTUB1 on UBC13 protein stability using a cycloheximide (CHX) chase assay. Consistent with Fig. 22a, the decreased K48 ubiquitination of UBC13 in the presence of OTUB1 resulted in reduced protein degradation (Fig. 23a). Of note, the influence of OTUB1 on UBC13 was only restricted to post-translational modification and protein degradation, as mRNA expression of UBC13 was independent of OTUB1 (Fig. 23b). In addition, accelerated degradation of UBC13 was also observed in OTUB1-siRNA treated NIH 3T3 cells (Fig. 23c), ruling out the possibility that the enhanced UBC13 degradation in OTUB1-deficient BMDCs was cell type-specific or was due to a genotoxic effect of the CD11c-Cre transgene. In contrast to UBC13, protein stability of Uev1a, the non-catalytic E2-like partner protein of UBC13 [142,209–212], was OTUB1-independent in TgPFN stimulated BMDCs (Fig. 23d).
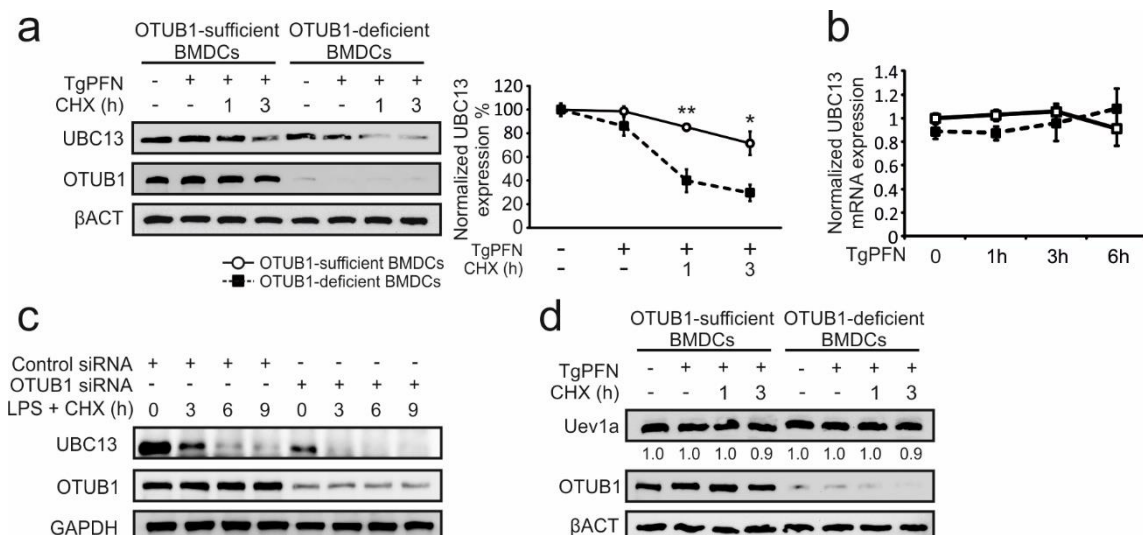
Figure 23 OTUB1 regulates UBC13 stability. (a and d) OTUB1-sufficient and -deficient FLT3L-expanded BMDCs were pre-treated with TgPFN (1 µg/ml) for 1h or left unstimulated. Then, cycloheximide (CHX, 100 µg/ml) was added for the indicated time points. Protein levels of UBC13 and Uev1a in whole cell lysates were analysed by WB. (b)) FLT3L-expanded BMDCs were stimulated with TgPFN for indicated time points. UBC13 mRNA expression was determined by qPCR (n = 4). Data are shown as mean + SD. (c) NIH 3T3 cells were transfected with siRNA for 24 h. Thereafter, cells were stimulated with LPS and CHX for 0, 3, 6 and 9 h. Protein levels of UBC13 were analysed by WB.

OTUB1 can reduce ubiquitination of substrates by two mutually non-exclusive mechanisms. First, OTUB1 can cleave polyubiquitin chains from substrates by its catalytic activity, which is mainly depending on the C91 residue and has specificity for K48 polyubiquitin chains. Second, OTUB1 can prevent K48 and K63 polyubiquitination of substrates by binding to the respective E2/E3 complex and blocking ubiquitin transfer by its N-terminal ubiquitin binding domain [153,208,213]. To clarify which mechanism is responsible for the deubiquitination and stabilization of UBC13, we transfect 3T3 fibroblasts where OTUB1 was suppressed with siRNA with (i) a catalytically inactive OTUB1-C91S-GFP mutant, (ii) an OTUB1-ΔN-GFP mutant, lacking the ubiquitin-binding N-terminus, responsible for non-catalytic inhibition of substrate ubiquitination mechanism, and (iii) wild type OTUB1-GFP plasmids. Expression of UBC13 in wild type OTUB1-transfected 3T3 cells was strongly preserved and after 3h of stimulation with LPS in combination with CHX was still detectable (Fig. 24). However, UBC13 was undetectable in 3T3 fibroblasts transfected with OTUB1-C91S-GFP and OTUB1-ΔN-GFP mutants, respectively, illustrating that both the C91 residue and the N-terminus of OTUB1 play a critical role in the stabilization of UBC13.
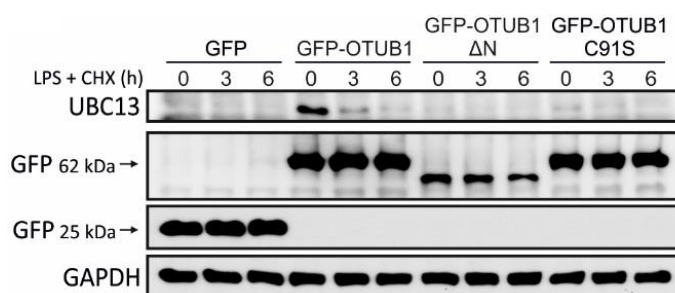

Figure 24 Full OTUB1 is required to stabilize UBC13. NIH 3T3 cells were transfected with OTUB1 siRNA for 36 h. After that, cells were transfected with GFP, GFP-OTUB1, GFP-OTUB1 ΔN, or GFP-OTUB1 C91S plasmids. Twenty-four hours later, cells were treated with CHX + LPS for 0, 3, and 6 h. Whole cell lysates were then isolated and analysed with indicated antibodies.

Since UBC13 was stabilized by reduced K48 ubiquitination in OTUB1-competent BMDCs, we inspected the impact of OTUB1 on the ubiquitination status of IRAK1 and TRAF6. In response

to TgPFN, total and K63 ubiquitination of IRAK1 and TRAF6 were increased in the presence of

OTUB1 (Fig. 25a-25d). In contrast, K48 polyubiquitination of TRAF6 was only weakly induced

by TgPFN in OTUB1-competent and -deficient BMDCs (Fig. 25e). Interestingly, K48

polyubiquitination of IRAK1 was also increased in OTUB1-competent BMDCs (Fig. 25d), which

is consistent with the sequential K63 and subsequent K48 polyubiquitination of IRAK1 in TLR-

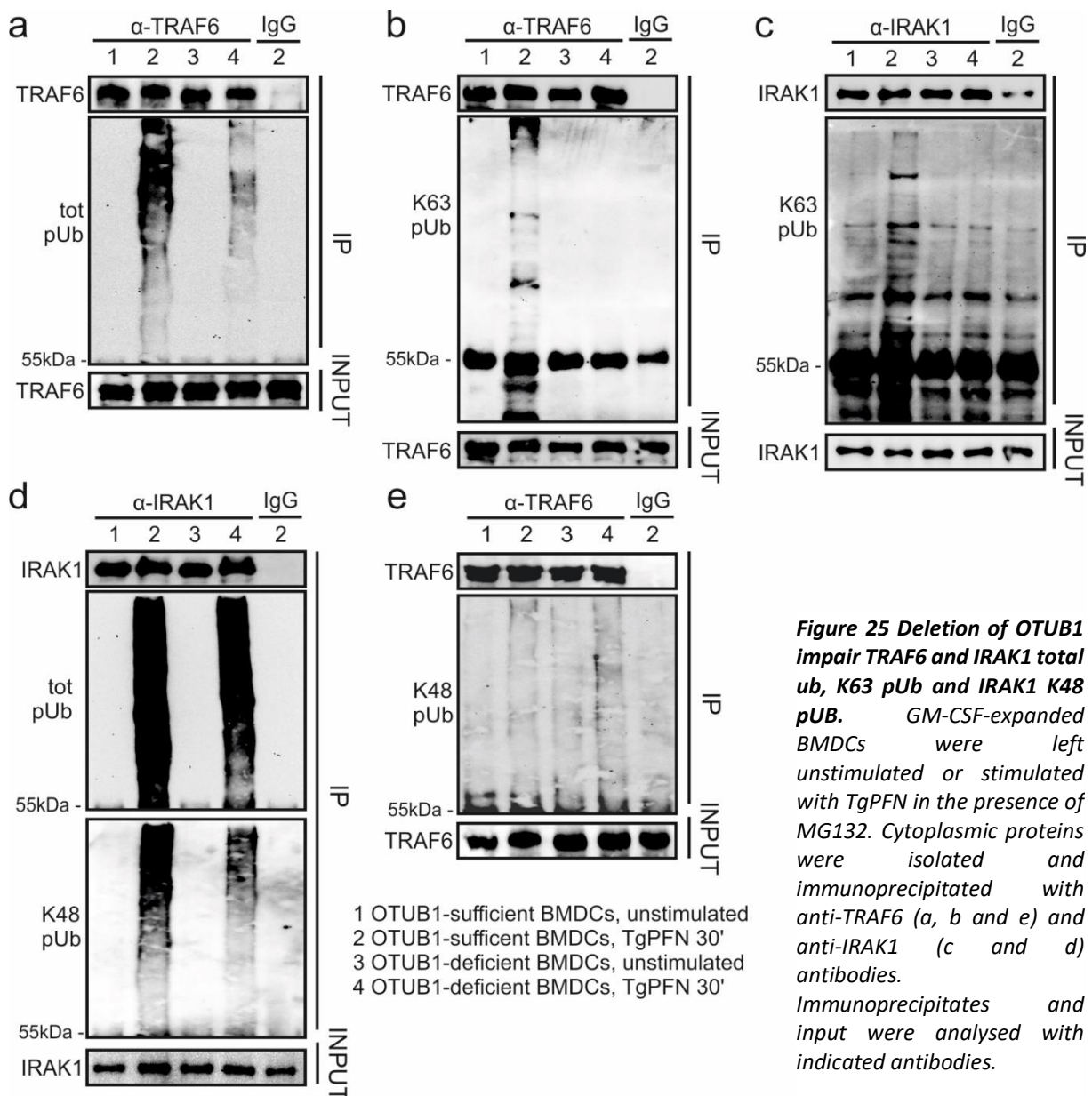induced MyD88-dependent NF-κB activation [206,214].

Figure 25 Deletion of OTUB1 impair TRAF6 and IRAK1 total ub, K63 pUb and IRAK1 K48 pUB. GM-CSF-expanded BMDCs were left unstimulated or stimulated with TgPFN in the presence of MG132. Cytoplasmic proteins were isolated and immunoprecipitated with anti-TRAF6 (a, b and e) and anti-IRAK1 (c and d) antibodies. Immunoprecipitates and input were analysed with indicated antibodies.

1 OTUB1-sufficient BMDCs, unstimulated
2 OTUB1-sufficent BMDCs, TgPFN 30'
3 OTUB1-deficient BMDCs, unstimulated
4 OTUB1-deficient BMDCs, TgPFN 30'

To directly verify that the reduced production of pro-inflammatory cytokines in OTUB1-

deficient BMDCs was a consequence of the rapid degradation of UBC13, we overexpressed

UBC13 with lentivirus (Fig. 26a). As shown in Fig. 26b, untransduced and mock-transduced

OTUB1-deficient BMDCs, respectively, produced significantly lower amount of IL-12, TNF, and

IL-6 in comparison to OTUB1-sufficient BMDCs, whereas OTUB1-deficient BMDCs transduced

with UBC13 produced similar amounts of pro-inflammatory cytokines as compared to UBC13-

transduced OTUB1-sufficient BMDCs. This demonstrates that restoration of UBC13 corrects

the defect in cytokine production in OTUB1-deficient cells. Taken together, OTUB1 promotes

T. gondii-induced NF-κB activation and cytokine production in DCs by directly deubiquitinating
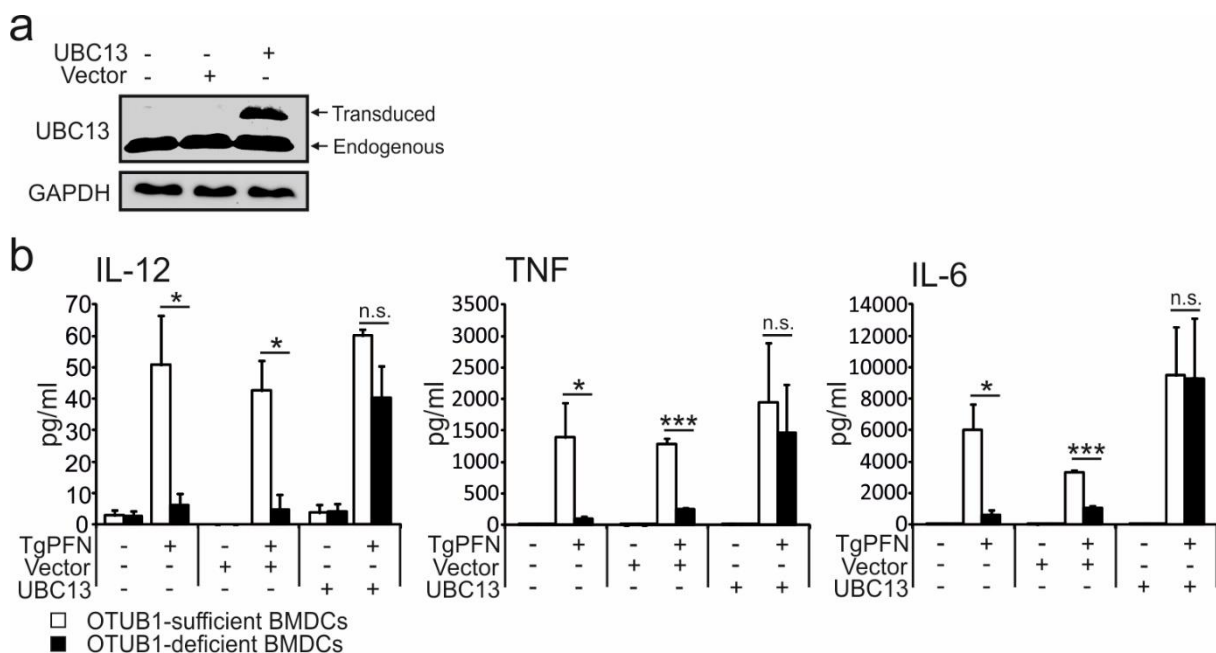
and stabilizing the E2 enzyme UBC13.

Figure 26 Restoration of normal levels of UBC13, corrects the cytokine production defect in OTUB1-deficient BMDCs. *FLT3L-expanded BMDCs were left untreated or transduced with UBC13-expressing lentivirus or vector lentivirus for 72 h followed by stimulation with TgPFN for 24 h. (a) UBC13 expression was measured by WB. (b) Cytokines in the supernatant of cell cultures were measured by flow cytometry (n = 4).*

Ubiquitinated TRAF6 induces the activation of its downstream kinase TAK1, which is essential

for NF-κB and MAPK activity. In addition to TRAF6, unanchored ubiquitin chains can also

directly activate TAK1 [215]. Unanchored ubiquitin chains can originate from the DUB-dependent

release of ubiquitin from substrates during proteasomal degradation or they can be

synthesized *de novo* using monomeric ubiquitin as a substrate [216]. Since, first, OTUB1 is a DUB

and, second, UBC13 in cooperation with UEV1A and TRAF6 mediates the formation of unanchored ubiquitin [211,215,217,218], we hypothesized that unanchored ubiquitin is increased in TgPFN-activated OTUB1-competent DCs. We performed a free ubiquitin assay [191], and discovered that 30 minutes after TgPFN stimulation accumulation of unanchored ubiquitin monomers, dimers and polyubiquitin chains was strongly increased in OTUB1-sufficient as compared to OTUB1-deficient BMDCs (Fig. 27). Thus, in OTUB1-competent BMDCs, the increased amount of free ubiquitin may further contribute to the activation of TAK1 and the stronger NF-κB activation.
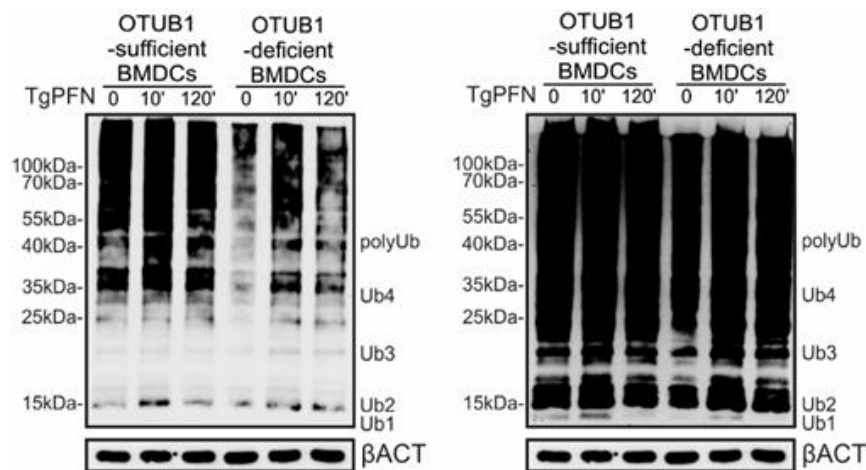

Figure 27 OTUB1 regulates free-ubiquitin chains production. GM-CSF-expanded BMDCs were left untreated or stimulated with TgPFN for 30 min. Whole cell lysate were incubated for two times with TUBE-ubiquitin for 1 h and only unbonded proteins were used for WB analysis. Short exposure (left) and long exposure (right) are shown.

4.4 OTUB1 is required for a strong cytokine production by CD11c$^+$ cells and subsequent IFN-γ responses in early toxoplasmosis.

To determine the functional role of OTUB1 in DCs *in vivo*, we induced toxoplasmosis in CD11c-Cre OTUB1$^{fl/fl}$ and control mice. CD8$^+$ cDC1 are the main source of IL-12 within a few hours after infection [193,219], and, shortly thereafter, IFN-γ-primed CD11b$^+$ cDC2 and PDCA1$^+$ pDC additionally contribute to IL-12 production [196]. Therefore, we explored the impact of OTUB1 on DC-mediated IL-12 production during *T. gondii* infection. CD11c-Cre OTUB1$^{fl/fl}$ and OTUB1$^{fl/fl}$ control mice were i.p. infected with 50.000 tachyzoites expressing GFP (PTG-GFP strain, type II strain) and cells in the peritoneal cavity were collected at 12 and 24h post

infection (p.i.) for further analysis. In good agreement with OTUB1-dependent cytokine production *in vitro* (Fig. 14a), CD8$^+$ cDC1 of CD11c-Cre OTUB1$^{fl/fl}$ mice showed significantly reduced percentage and absolute number of IL-12-producing DCs in comparison to OTUB1$^{fl/fl}$ mice already at 12h and 48h p.i. (Fig. 30). Additionally, CD11b$^+$ cDC2 of CD11c-Cre OTUB1$^{fl/fl}$ mice exhibited a reduced IL-12 production 48h but not 12h p.i. (Fig. 28).
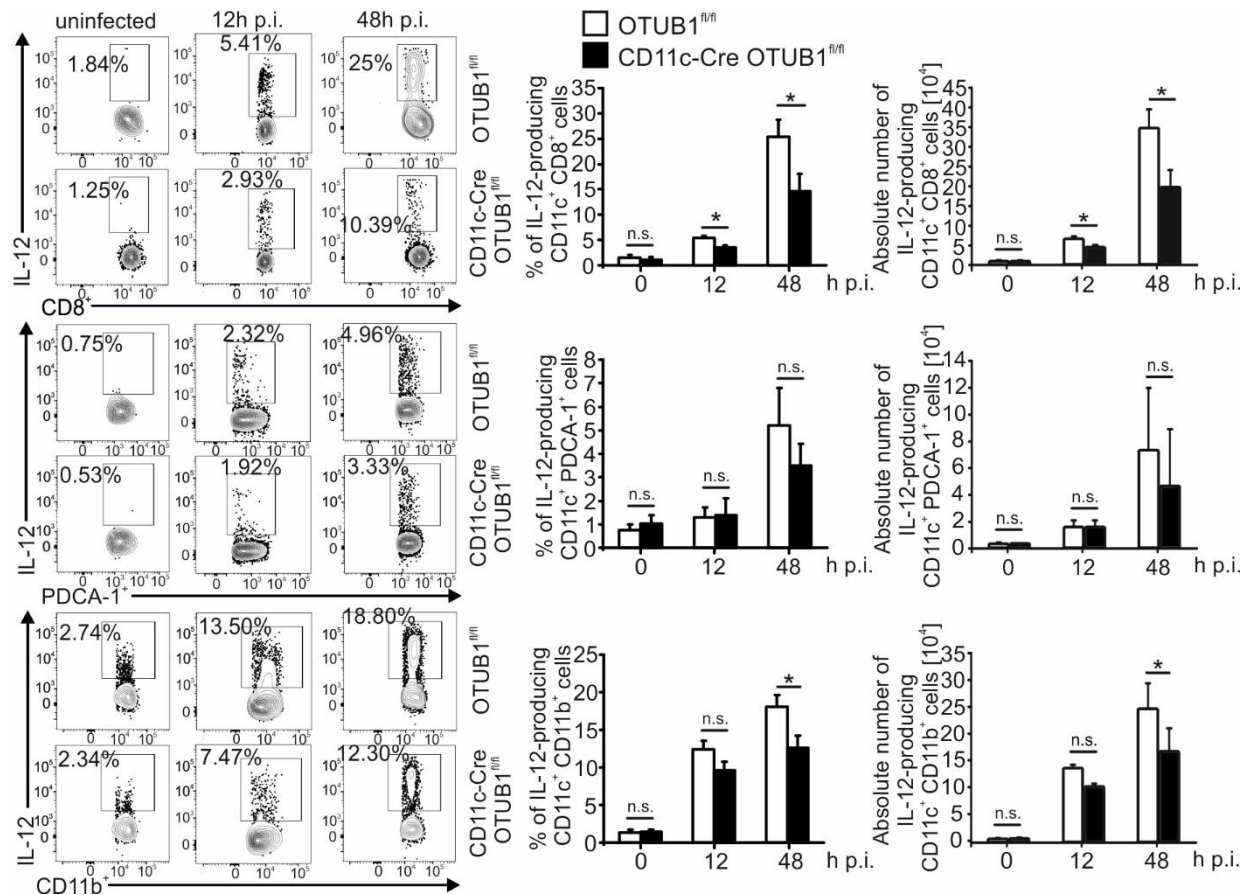

Figure 28 *Deletion of OTUB1 in DCs impairs cytokine response in toxoplasmosis. OTUB1$^{fl/fl}$ and CD11c-Cre OTUB1$^{fl/fl}$ mice were infected i.p. with 50.000 tachyzoites for 12 and 48 h, respectively. Peritoneal cells were collected by lavage of the peritoneal cavity and analysed by flow cytometry for IL-12 production in CD11c$^+$ CD8a+, CD11c$^+$ PDCA-1$^+$, and CD11c$^+$ CD11b$^+$ DCs.*

In contrast, IL-12 production of F4/80$^+$ macrophages was identical in both mouse strains (Fig. 29a). Additionally, the production of TNF and IL-6 was significantly reduced in all DC subtypes of CD11c-Cre OTUB1$^{fl/fl}$ mice at 2d p.i. (Fig. 29b and 29c).
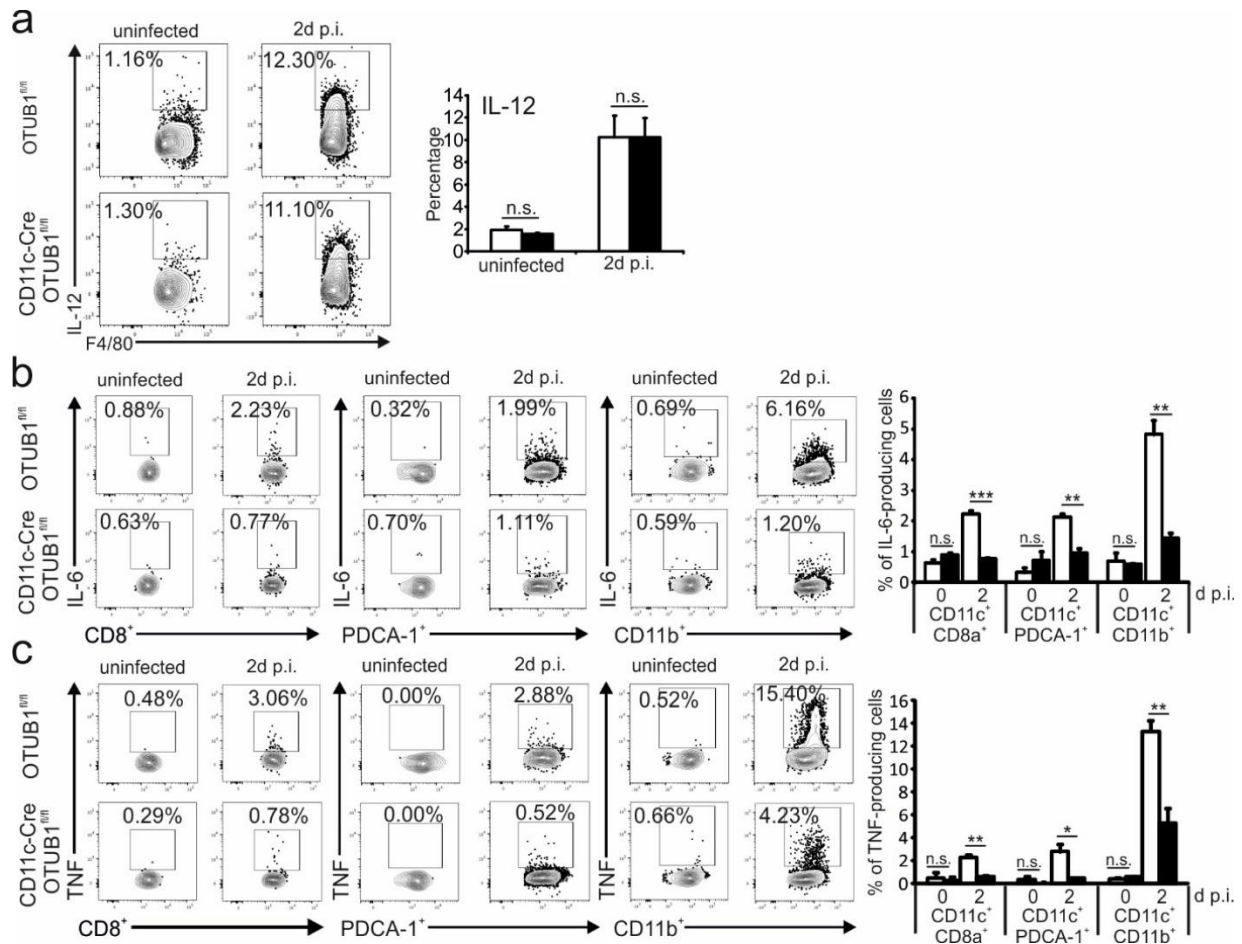
Figure 29 Deletion of OTUB1 in DCs impairs cytokine response in toxoplasmosis. *OTUB1$^{fl/fl}$ and CD11c-Cre OTUB1$^{fl/fl}$ mice were left untreated or infected i.p. with 50.000 tachyzoites for 48 h. Peritoneal cells were collected by lavage of the peritoneal cavity and analysed by flow cytometry for IL-12-producing macrophages (a), IL-6-producing DCs (b), and TNF-producing DCs (c). Representative flow cytometry plots and statistics are shown (n = 4). Representative flow cytometry plots (left panels) and statistics (right panels) are shown (n = 8). Data are shown as mean + SD. * p < 0.05, ** p < 0.01, *** p < 0.001.*

In good agreement with the UBC13 stabilizing function of OTUB1 in TgPFN-stimulated BMDCs (Fig. 30a), we detected an increased expression of UBC13 in CD8$^+$ cDC1, PDCA1$^+$ DC and CD11b$^+$ cDC2 isolated from OTUB1$^{fl/fl}$ mice after infection with *T. gondii* (Fig. 30, first top panel), confirming the critical role of OTUB1 in stabilizing UBC13 in DC *in vivo*. Beside induction of cytokines, NF-κB activity drives expression of immunologically important cell surface molecules such as MHC class II, CD40, CD80 and CD86, which regulate the interaction of DCs with T cells [220]. Here, we observed a significantly reduced expression of MHC II, CD80 and CD86 in CD8$^+$ cDC1 of CD11c-Cre OTUB1$^{fl/fl}$ mice 48h p.i. (Fig. 30), substantiating the role of OTUB1 in NF-κB activation particularly in this DC subtype.
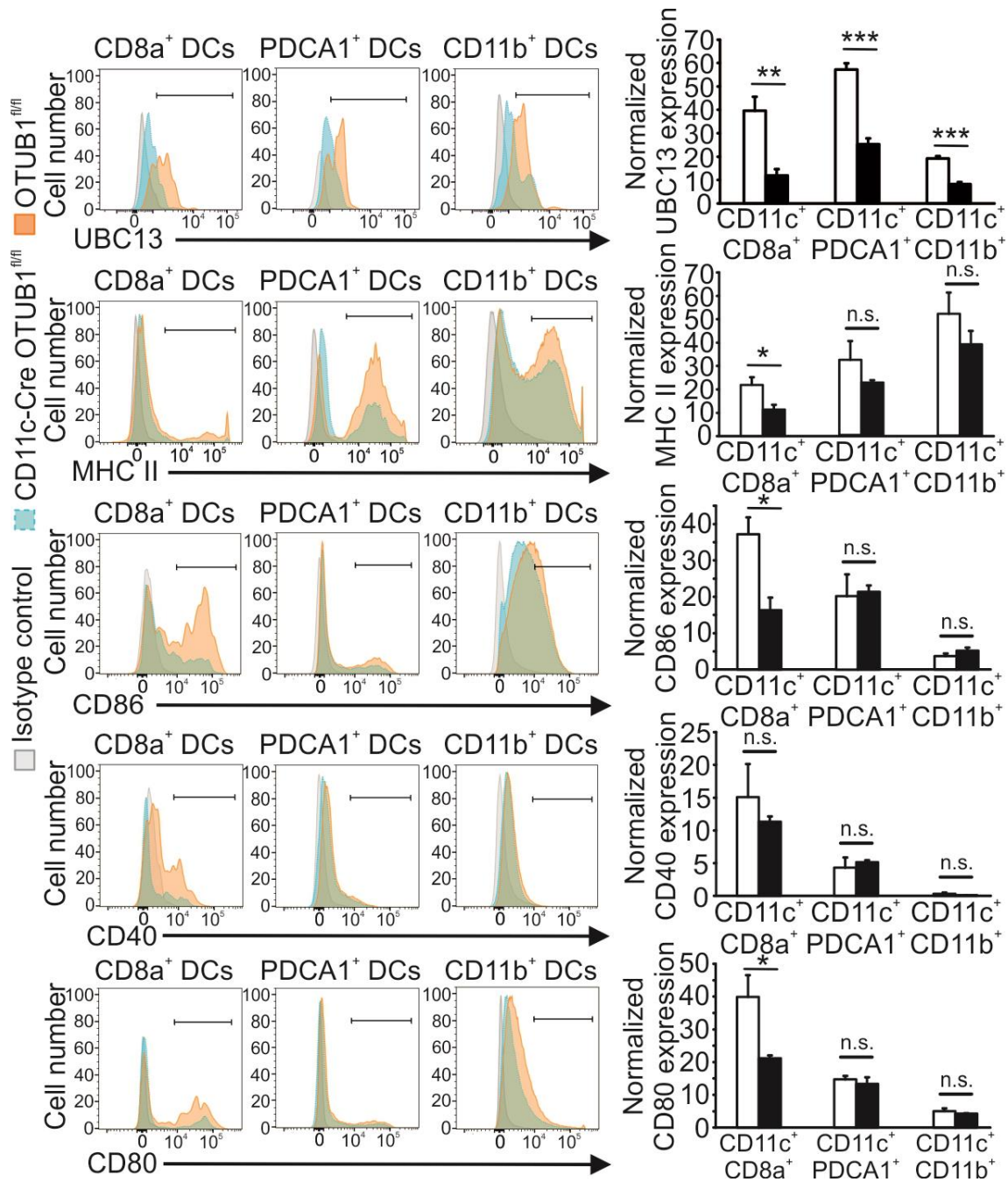
Figure 30 OTUB1-deficient DCs express reduced UBC13, MHC II, CD86 and CD80 during toxoplasmosis. OTUB1$^{fl/fl}$ and CD11c-Cre OTUB1$^{fl/fl}$ mice were infected i.p. with 50.000 tachyzoites for 48 h. Peritoneal cells were collected by lavage of the peritoneal cavity and analysed by flow cytometry for UBC13, MHC II, CD40, CD86 and CD80 expression in CD11c$^+$ CD8a$^+$, CD11c$^+$ PDCA-1$^+$, and CD11c$^+$ CD11b$^+$ DCs. Representative flow cytometry plots (left panels) and statistics (right panels) are shown (n = 8). Data are shown as mean + SD. * p < 0.05, ** p < 0.01, *** p < 0.001.

Given that CD8$^+$ cDC1-derived IL-12 is indispensable for the initiation of a potent IFN-γ response of NK cells upon *T. gondii* infection [172,221,222], the reduction of early produced IL-12 in CD8$^+$ cDC1 in CD11c-Cre OTUB1$^{fl/fl}$ mice was accompanied with a reduced IFN-γ response in NK cells but not in CD4$^+$ and CD8$^+$ T cells (Fig. 31). The strong OTUB1-dependent reduction of

IL-12 production in CD11b^{+} cDC2 at 48h p.i. is consistent with the observation that IFN-γ priming of these DC populations is required for their TLR11/12-dependet IL-12 production [197,223].
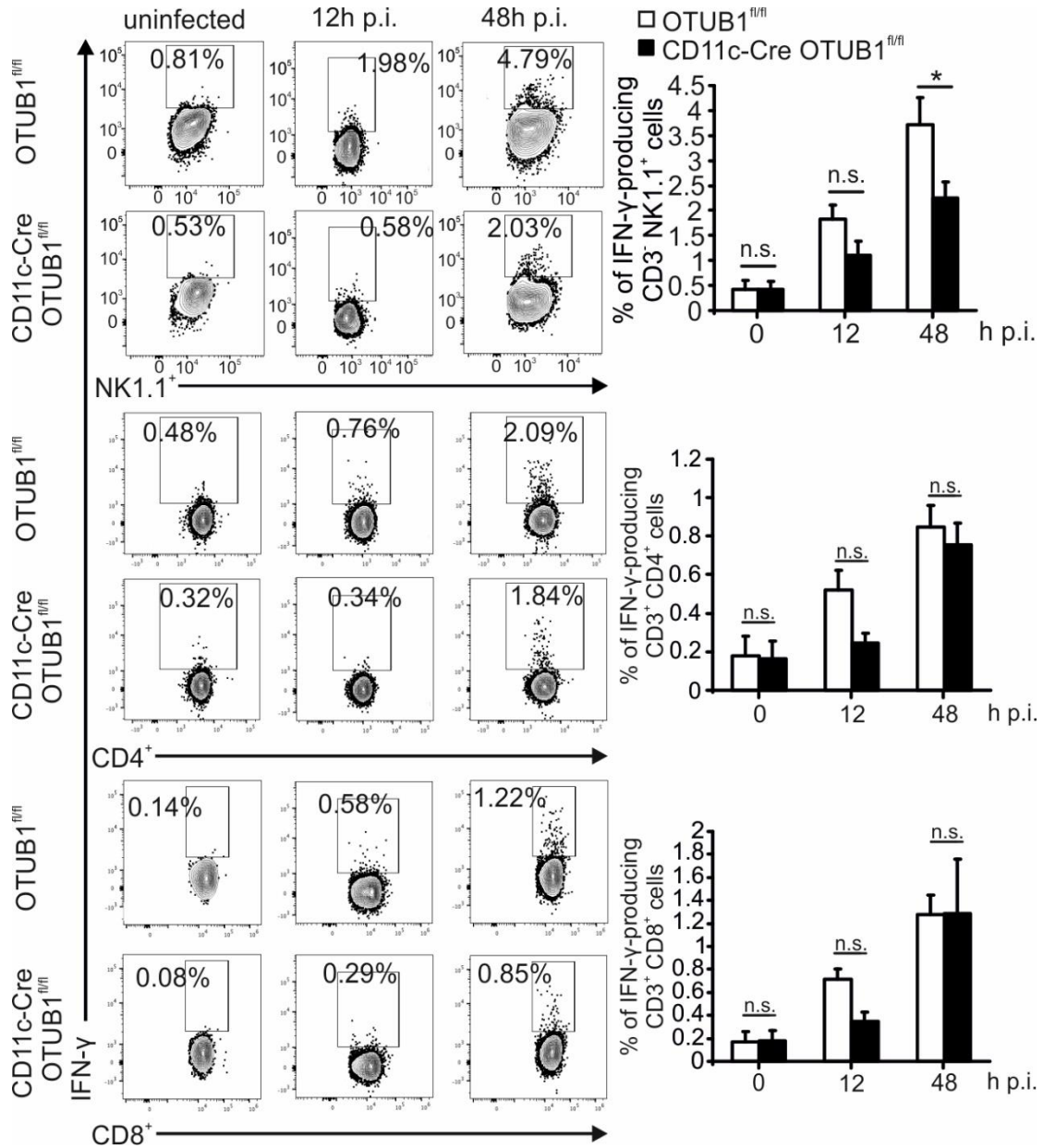

Figure 31 CD11c-Cre OTUB1^{fl/fl} mice have impaired IFNγ response. *OTUB1^{fl/fl} and CD11c-Cre OTUB1^{fl/fl} mice were infected i.p. with 50.000 tachyzoites for 12 and 48 h, respectively. Peritoneal cells were collected by lavage of the peritoneal cavity and analysed by flow cytometry IFN-γ production in NK cells (a) and T cells (b). Representative flow cytometry plots (left panels) and statistics (right panels) are shown (n = 8). Data are shown as mean + SD. * p < 0.05, ** p < 0.01, *** p < 0.001.*

The impaired immune response of OTUB1-deficient DCs resulted in a reduction of serum IL-12, IL-6 and to a lesser extent of TNF 48h p.i. (Fig. 32). Together, these data suggest a pivotal role for OTUB1 in driving NF-κB-dependent immune reactions in DCs including IL-12

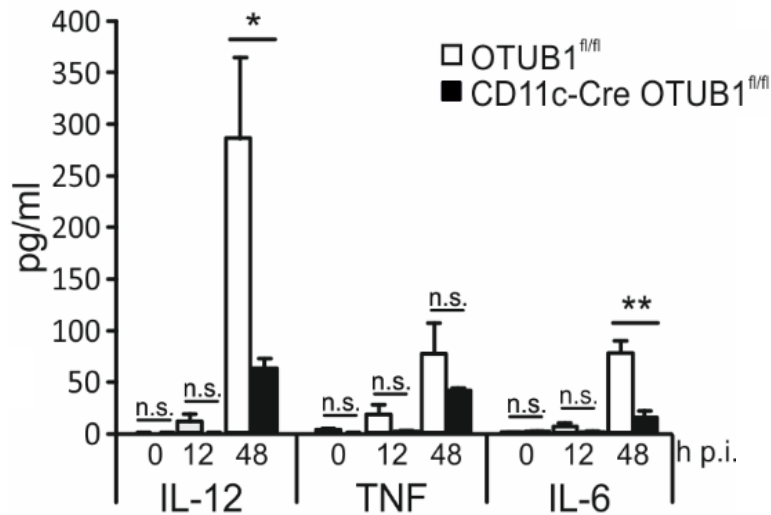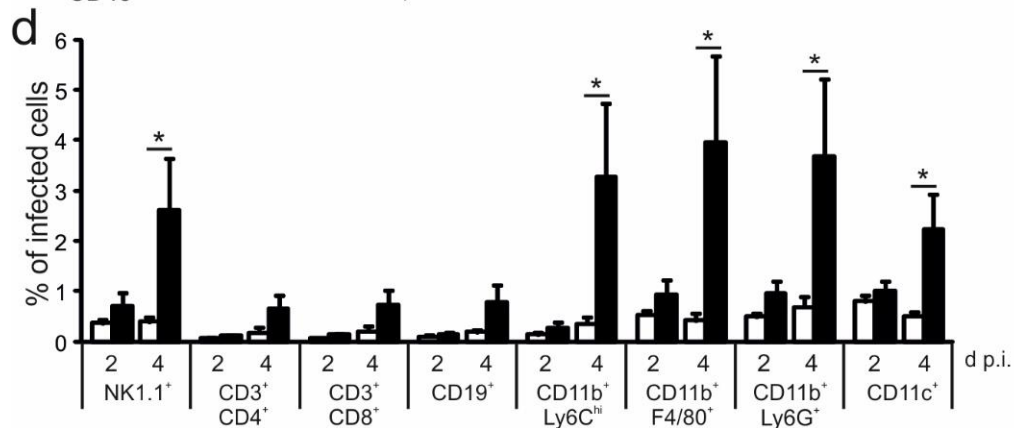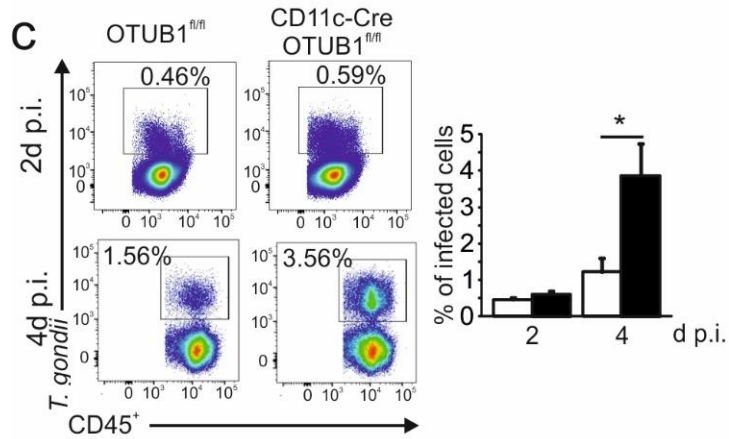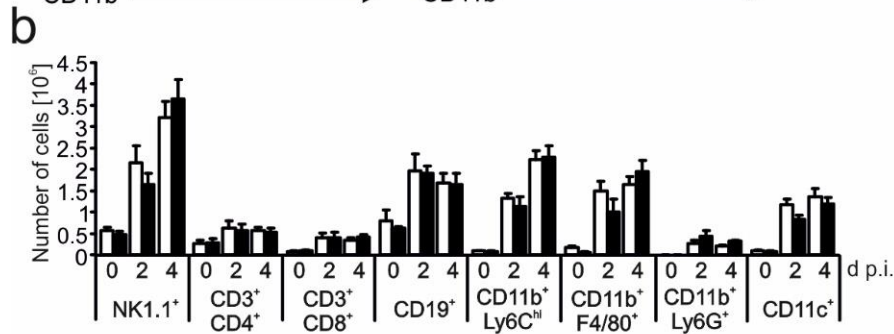production, which is critical for a potent NK cell-dependent IFN-γ response in toxoplasmosis [222].

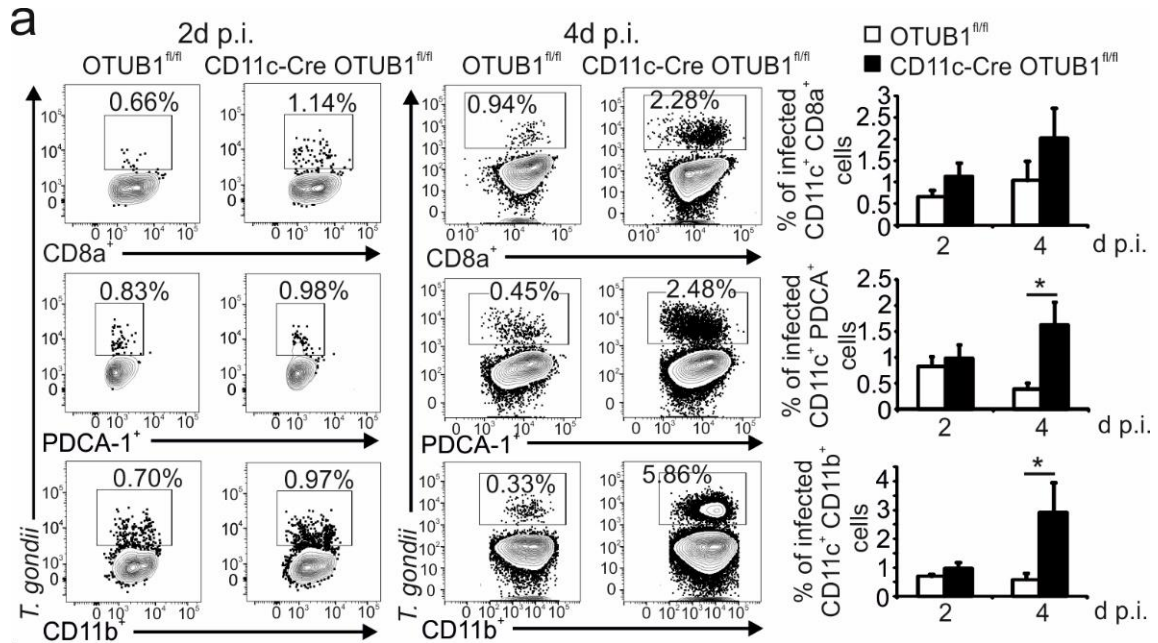*Figure 32 CD11c-Cre OTUB1fl/fl mice have reduced systemic cytokines in serum. OTUB1fl/fl and CD11c-Cre OTUB1fl/fl mice were left untreated or infected i.p. with 50.000 tachyzoites for indicated time points. Sera from infected mice were collected and cytokines were measured by ELISA (n = 4). Data are shown as mean + SD. * p < 0.05, ** p < 0.01, *** p < 0.00*

4.5 CD11c-Cre OTUB1fl/fl mice fail to control expansion of *T. gondii*

To investigate whether the diminished immune responses of OTUB1-deficient DCs affected the parasite control, we i.p. infected the mice with 50.000 GFP-expressing tachyzoites and determined the composition of leukocytes and parasite load in the peritoneal cavity at 2 and 4d p.i. The percentages of *T. gondii*-infected cDC2, pDC and to a lesser extent CD8+ cDC1, were increased in CD11c-Cre OTUB1fl/fl mice at day 4 p.i. (Fig. 33a). Numbers of leukocytes present at the site of infection were comparable between the two mouse strains (Fig. 33b) but the intracellular parasite load of total peritoneal cavity CD45+ leukocytes (Fig. 33c), as well as individual leukocyte subpopulations including NK1.1+ NK cells, CD11b+ Ly6Chi inflammatory monocytes, CD11b+ F4/80+ macrophages, and CD11b+ Ly6G+ neutrophils (Fig. 33d) was significantly increased in CD11c-Cre OTUB1fl/fl mice. This suggests that the early defect in immune activation of OTUB1-deficient DCs resulted in an insufficient control of the parasite at the early stage of infection. The massive release of *T. gondii* from infected cells may cause an augmented parasite dissemination to adjacent cells and, subsequently, to other organs.

Figure 33 *CD11c-Cre OTUB1$^{fl/fl}$ mice fail to control expansion of T. gondii.* *OTUB1$^{fl/fl}$ and CD11c-Cre OTUB1$^{fl/fl}$ mice were infected i.p. with 50.000 tachyzoites. Peritoneal cells were isolated from the peritoneal cavity and analysed by flow cytometry at day 2 and 4 p.i. (a) percentage of infected CD11c$^+$ CD8a$^+$, CD11c$^+$ PDCA-1$^+$, and CD11c$^+$ CD11b$^+$ DCs, respectively. (b) Number of recruited leukocytes in peritoneal cavity. (c) Percentages of infected peritoneal CD45$^+$ cells in OTUB1$^{fl/fl}$ and CD11c-Cre OTUB1$^{fl/fl}$ mice. (d) Percentages of infected peritoneal leukocyte subpopulations in OTUB1$^{fl/fl}$ and CD11c-Cre OTUB1$^{fl/fl}$ mice. Representative FACS plots (upper panel) and statistics (lower panel) are shown (n = 10 for each group).*

Indeed, quantitative analysis of *T. gondii* genomic DNA revealed that multiple organs of CD11c-Cre OTUB1$^{fl/fl}$ mice harbored significantly higher parasite loads compared as compared to OTUB1$^{fl/fl}$ control mice at day 10 p.i. (Fig. 34).
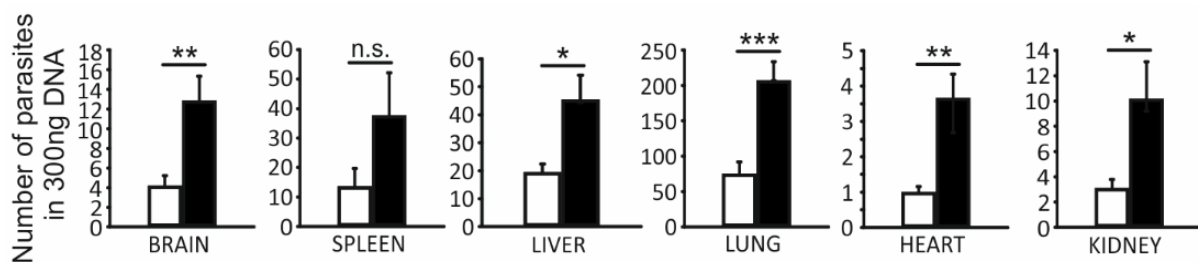

Figure 34 *CD11c-Cre OTUB1$^{fl/fl}$ mice harbour more parasite load in different organs.* *Mice were infected i.p. with 50.000 tachyzoites for 10 days. Parasite load in different organs was determined by semi-quantitative PCR on tissue DNA. (n = 5 for each group).*

Interestingly, *in vitro* infection with *T. gondii* resulted in similar parasite burden in OTUB1-sufficient and -deficient BMDCs with or without IFN-γ pre-stimulation, suggesting that OTUB1 does not interfere with the cell-intrinsic parasite killing mechanism in DCs (Fig. 35a). Consistently, the production of anti-parasitic effector molecules including iNOS, IGPT, and GBPs, was comparable between OTUB1-sufficient and -deficient BMDCs (Fig. 35b). *T. gondii* also promotes its systemic dissemination by hijacking the migratory properties of parasitized DCs [224–226]. To address whether OTUB1 has an impact on *Toxoplasma*-induced hypermigration of DCs, we performed motility analyses. Upon challenge with *T. gondii*, parasitized OTUB1-sufficient and -deficient BMDCs exhibited similar elevated velocities and unchallenged DCs exhibited non-significant differences in baseline velocity (Fig. 35c). Thus, *T. gondii*-induced DC hypermigration was OTUB1 independent. Collectively, these data suggest that OTUB1 has no impact on DC-intrinsic parasite control as well as DC-mediated *T. gondii* dissemination.
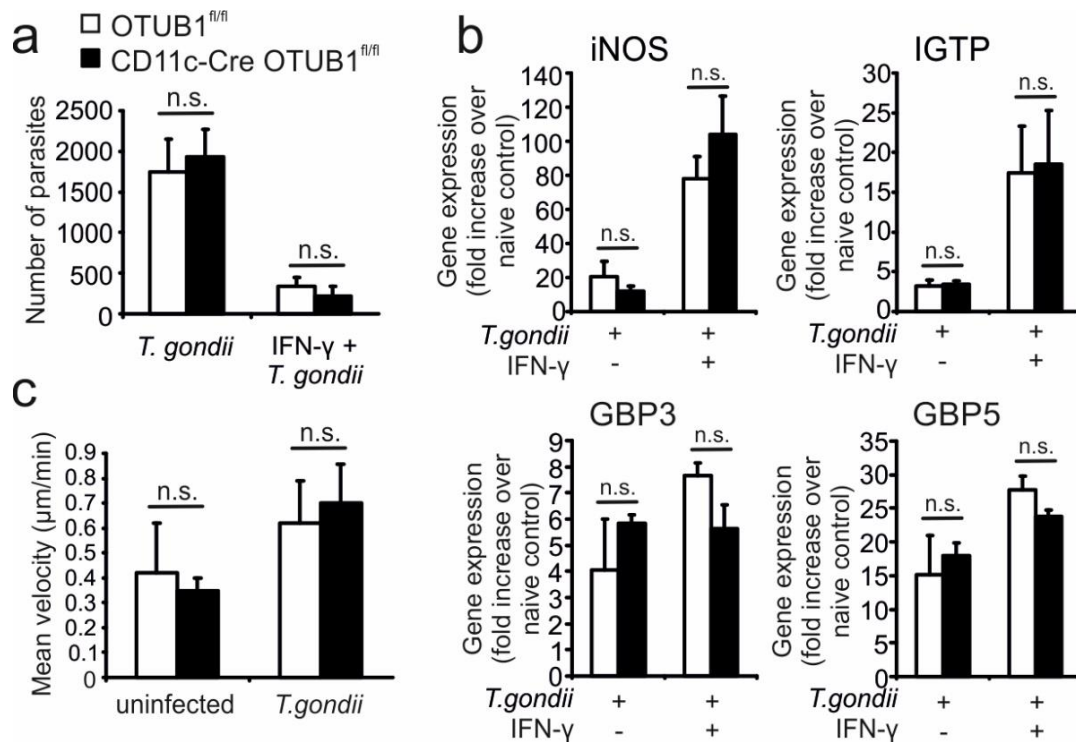
Figure 35 OTUB1 has no impact on DC-intrinsic parasite control as well as DC-mediated T. gondii dissemination.
OTUB1-sufficient and -deficient BMDCs were untreated or pre-treated with 10 ng/ml of IFN-γ for 24 h followed by infection with T. gondii tachyzoites (MOI = 3) for 24 h. Parasite load (b) and anti-parasitic gene expression (c) were determined by PCR (n = 4). Motility of OTUB1-sufficient and -deficient BMDCs was calculated before and after infection with T. gondii tachyzoites at an MOI of 3 (n = 3).

Hou et al. [221] demonstrated that an impaired IL-12 production by CD8^{+} cDC1 in acute toxoplasmosis results in a more severe course of chronic *Toxoplasma* encephalitis (TE) with increased intracerebral parasite load. To address whether DC-specific OTUB1 regulates the course of chronic TE, we infected CD11c-Cre OTUB1^{fl/fl} mice and control mice with 3 brain cysts of the type II DX strain. At day 30 p.i., the intracerebral parasite load in CD11c-Cre OTUB1^{fl/fl} mice was significantly higher than that in control mice (Fig. 36a). In addition, mortality of CD11c-Cre OTUB1^{fl/fl} mice during chronic TE was significantly increased (Fig. 36b). Of note, the intracerebral immune response of CD11c-Cre OTUB1^{fl/fl} mice was not impaired as illustrated by normal numbers of intracerebral leukocyte populations including DCs and T cells at day 30 p.i. (Fig. 36c-e). Additionally, IL-12 production of DCs and IFN-γ production of CD4^{+} and CD8^{+} T cells was equal in both genotypes (Fig. 36f and 36g, respectively). In parallel to the increased intracerebral load, production of anti-parasitic IGTP and iNOS as well as IL1β and IL-18 were

even increased in CD11c-Cre OTUB1$^{fl/fl}$ mice (Fig. 36h) further indicating that the aggravated

course of TE in CD11c-Cre OTUB1$^{fl/fl}$ mice is caused by an impaired DC immune response early

after infection but not by an insufficient intracerebral immune response.
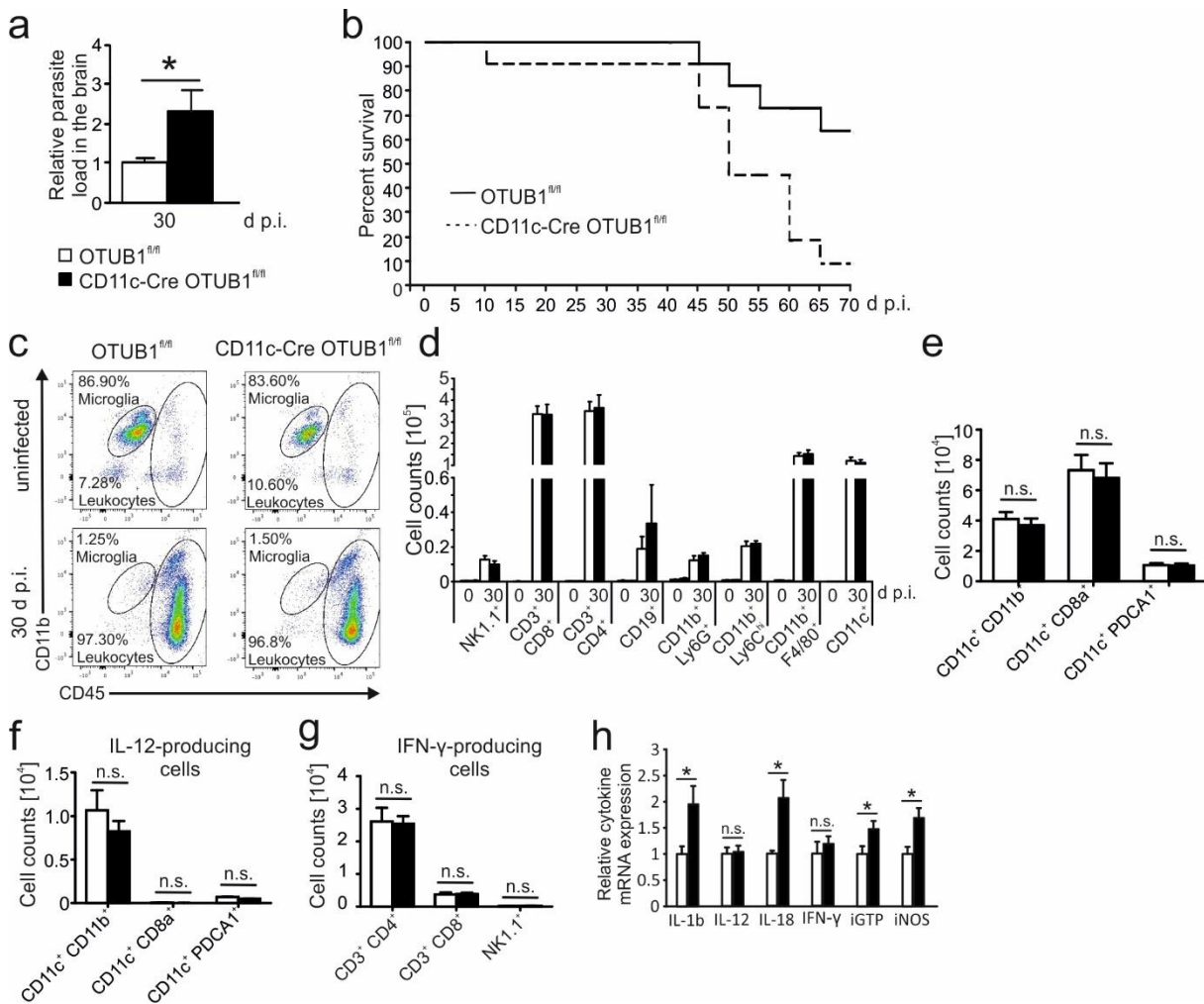
Figure 36 CD11c-Cre OTUB1$^{fl/fl}$ mice die early for TE. Mice were infected i.p. with 3 cysts. Parasite load in brains 30d p.i. was determined by semi-quantitative PCR on tissue DNA (n = 4 for each group) (a). Survival was monitored for 70d p.i. (b). Leukocytes were harvested from the brain and analysed by flow cytometry for percentages of CD45+ cells (c), absolute numbers of leukocyte (d) and DC (e) subsets, as well as absolute numbers of IL-12 (f) and IFN-γ (g) producing cells (n = 4). (h) Transcription of genes in the brain of OTUB1$^{fl/fl}$ and CD11c-Cre OTUB1$^{fl/fl}$ mice at day 30 p.i. was measured by qPCR (n = 4). Data are shown as mean + SD. * $p < 0.05$. (n = 10 for each group).

4.6 Supplementation of IL-12 improves the control *T. gondii* in CD11c-Cre OTUB1$^{fl/fl}$ mice

Mice selectively lacking CD8+ cDC1 are extremely susceptible to toxoplasmosis due to

impaired IL-12 and subsequent IFN-γ production [227]. Treatment of these *Batf3$^{-/-}$* mice with 0.5

μg IL-12 at days 0, 1, 2, 3 and 4 after infection restored resistance illustrating that IL-12

production by CD8$^+$ DCs is of central importance independent of all other protective immune reactions of this cell population [227]. To study whether the increased parasite expansion and dissemination in CD11c-Cre OTUB1$^{fl/fl}$ mice was caused by the early defect in IL-12 production by DCs, we administered 150 ng IL-12 i.p. to CD11c-Cre OTUB1$^{fl/fl}$ and control mice at days 0, 1, 2 and 3 after infection as shown in Fig. 37.

Figure 37 Experimental design scheme of IL-12 administration and analysis. *Mice were i.p. injected with either PBS or 150 ng IL-12 daily from 0 to 3d p.i.*

Here, although the defect in the production of cytokines by DCs was not limited only to IL-12, but also extended to TNF and IL-6, administration of IL-12 alone significantly reduced *T. gondii* load in both CD11c-Cre OTUB1$^{fl/fl}$ and control mice and abolished the differences in parasite load between the two genotypes at 4 days p.i. (Fig. 38a-d), indicating that the early deficit in IL-12 production by DCs is accountable for the uncontrolled parasite expansion in the acute infection.
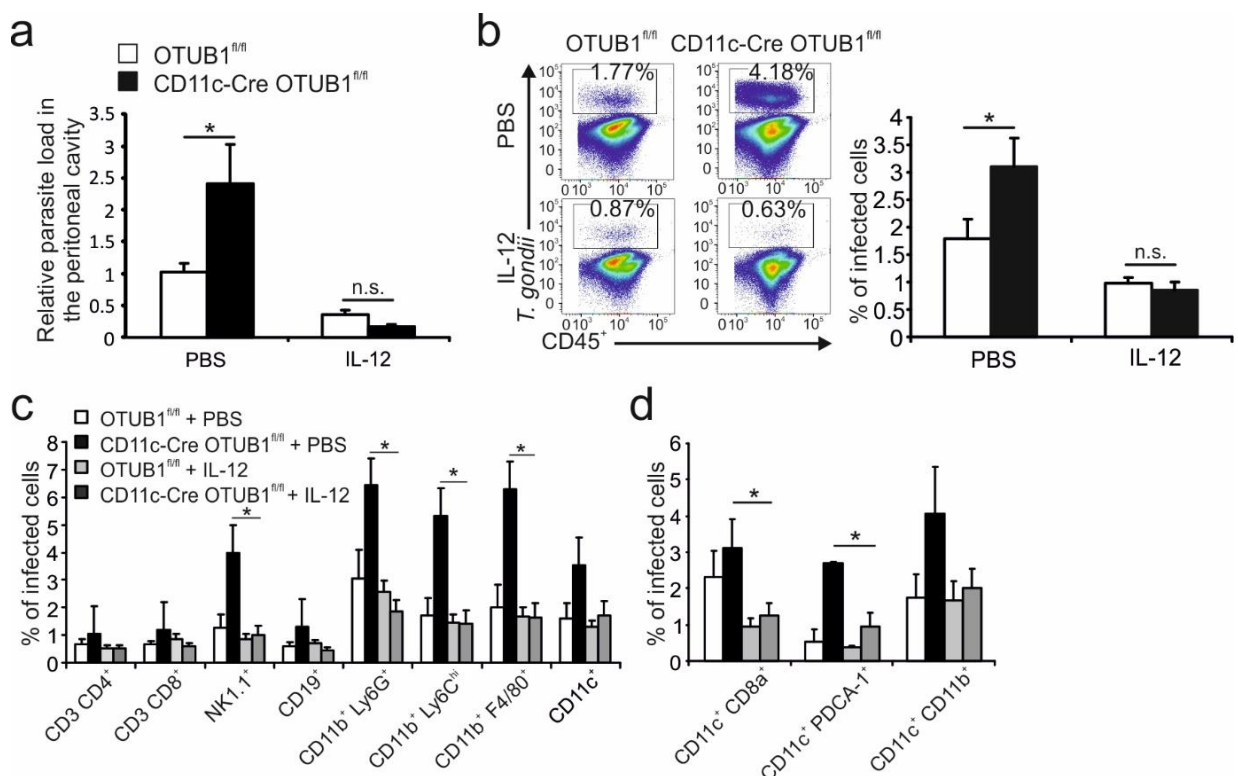
***Figure 38 IL-12 administration restores the capability of CD11c-Cre mice to control parasite replication in early stage of toxoplasmosis**. (a) Parasite load in peritoneal cells were determined by semi-quantitative PCR on tissue DNA after infection with 50.000 tachyzoites for 4 days (n = 8 for each group). (b) Percentages of infected peritoneal CD45+ cells were analysed by flow cytometry at day 4 after infection with 50.000 tachyzoites. Representative flow cytometry plots (left panel) and statistics (right panel) are shown (n = 8 for each group). (c and d) Percentages of infected peritoneal leukocyte subpopulations (c) and DC subsets (d) were analysed by flow cytometry at day 4 after infection with 50.000 tachyzoites (n = 8 for each group).*

Interestingly, IL-12 administration in acute toxoplasmosis was also able to dramatically reduce the intracerebral parasite load in the brain of chronically infected CD11c-Cre OTUB1$^{fl/fl}$ and OTUB1$^{fl/fl}$ mice, and, importantly, the intracerebral parasite load did no longer differ between the two genotypes (Fig. 39a). Histopathology confirmed that IL-12 treatment strongly reduced parasite numbers and abolished differences between the two mouse strains (Fig. 39b). Consistent with the finding that higher brain parasite loads are associated with increased mortality (Fig. 36a and 36b), supplementation of IL-12 dramatically increased the survival of CD11c-Cre OTUB1$^{fl/fl}$ mice (Fig. 39c). This suggests that the higher parasite burden and mortality of CD11c-Cre OTUB1$^{fl/fl}$ mice during chronic infection is caused by a failure to restrict parasite expansion in the early stage via innate immunity. Collectively, these results suggest that DC-specific OTUB1 contributes to parasite control in both acute and chronic toxoplasmosis by facilitating the early IL-12 production in DCs, which is indispensable for eliciting the protective IFN-γ response.
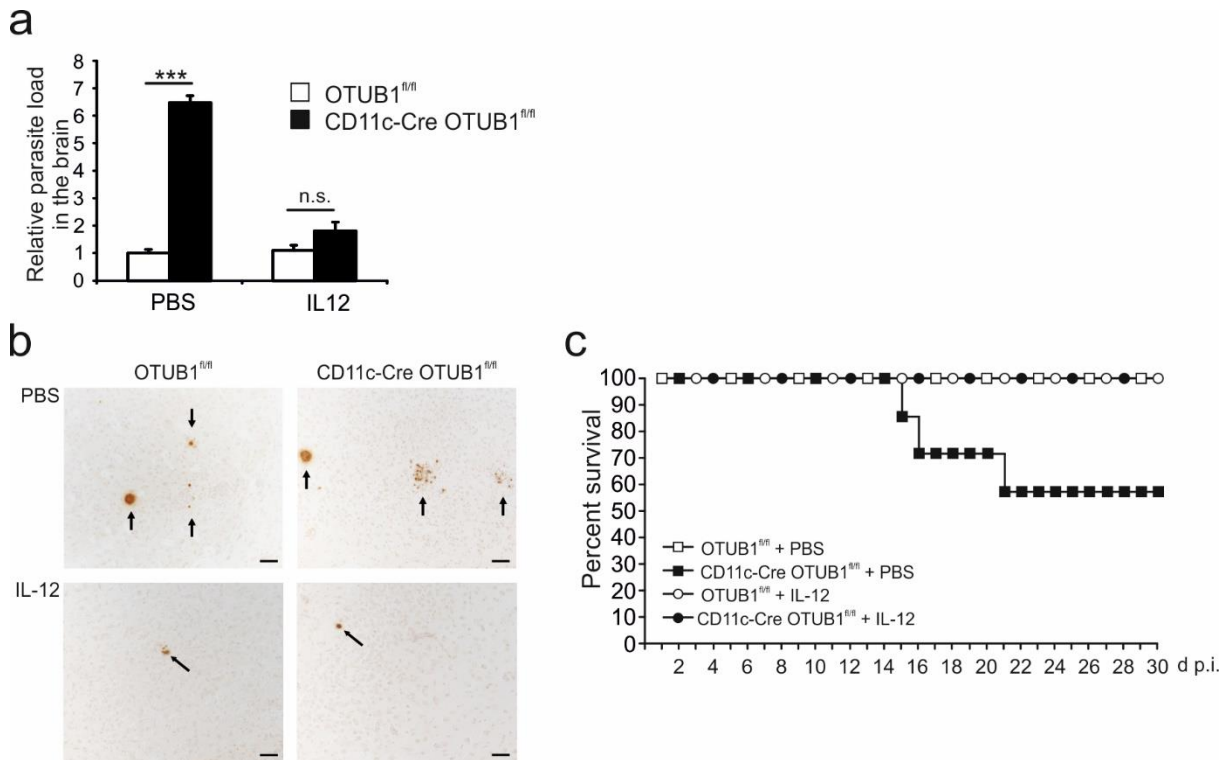
Figure 39 IIL-12 administration restores the capability of CD11c-Cre mice to control parasite replication in chronic stage of toxoplasmosis. *(a) Mice were i.p. infected with 5 cysts of the DX strain. At day 30 p.i., parasite load in the brain of surviving mice was determined by semi-quantitative PCR. Two independent experiments with comparable results were performed. One representative experiment is shown (n = 4 for each group). (b) Intracerebral parasites in the brains of T. gondii-infected OTUB1$^{fl/fl}$ and CD11c-Cre OTUB1$^{fl/fl}$ mice at 30d p.i. A PBS-treated OTUB1$^{fl/fl}$ mouse (top left) shows a single focus consisting of a few T. gondii cysts and some tachyzoites in the white matter of the frontal lobe. The brain of a PBS-treated CD11c-Cre OTUB1$^{fl/fl}$ mouse (top right) shows an increased number of parasitic foci (arrows) with T. gondii cysts and tachyzoites in the white matter of the frontal lobe. In both an OTUB1$^{fl/fl}$ and a CD11c-Cre OTUB1$^{fl/fl}$ mouse, IL-12 application reduced the intracerebral parasitic load with only single cysts scattered throughout the frontal lobe (arrows). Immunohistochemistry with polyclonal rabbit anti-T. gondii (BioGenex, Fremont, CA, USA) and slight counterstaining with hemalum; original magnification x200; scale bar (A-D): 50 µm. The photomicrographs shown are representative for three mice per experimental group. Similar results were obtained in a second independent experiment. (c) The survival of mice was monitored daily up to 30 days after infection with 5 DX strain cysts (n = 8 for each group). Data are displayed as mean + SD. * p < 0.05, ** p < 0.01, *** p < 0.001.*

4.7 OTUB1 regulates cytokine production in LPS-induced sepsis and death

As shown in Fig. 8b, 9e and 9f, in addition to TgPFN, LPS stimulation upregulated OTUB1 expression *in vivo* and *in vitro*. Additionally, OTUB1 amplified NF-κB activation in LPS stimulated BMDCs (Fig. 15c and 17) and interacted with UBC13 (Fig. 21c and 21d) showing that OTUB1 also augment LPS-induced signaling and cellular responses. To investigate the functional role of DC-specific OTUB1 in LPS challenge, we injected lethal doses of LPS to CD11c-Cre OTUB1$^{fl/fl}$ and OTUB1$^{fl/fl}$ mice. As compared with OTUB1$^{fl/fl}$ mice, CD11c-Cre OTUB1$^{fl/fl}$ mice

produced significantly less IL-12 and TNF upon stimulation with LPS (Fig. 40a), indicating that, in opposite to A20 [228], OTUB1 in DCs sensitizes mice to LPS by enhancing cytokine production in DCs. In good agreement, CD11c-Cre OTUB1^{fl/fl} mice survived significantly longer as OTUB1^{fl/fl} mice (Fig. 40b) due to reduced systemic inflammation.
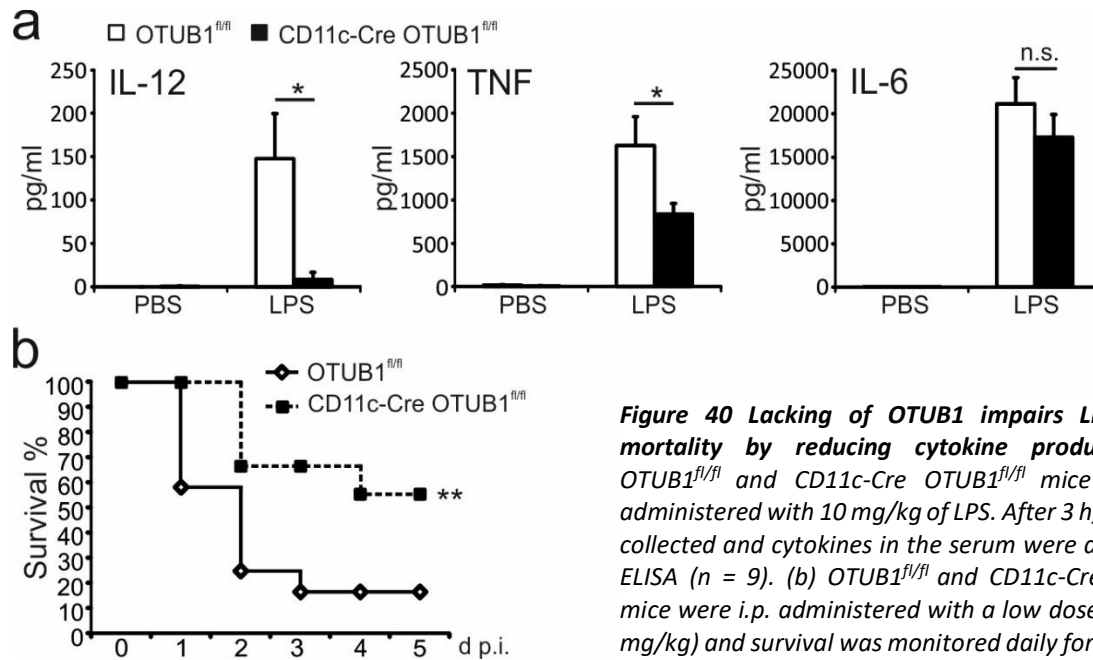
Figure 40 Lacking of OTUB1 impairs LPS-induced mortality by reducing cytokine production. *(a) OTUB1^{fl/fl} and CD11c-Cre OTUB1^{fl/fl} mice were i.p. administered with 10 mg/kg of LPS. After 3 h, blood was collected and cytokines in the serum were analysed by ELISA (n = 9). (b) OTUB1^{fl/fl} and CD11c-Cre OTUB1^{fl/fl} mice were i.p. administered with a low dose of LPS (10 mg/kg) and survival was monitored daily for 6 days (n = 10). Data are displayed as mean + SD. * p < 0.05, ** p < 0.01.*

To explore the role of DC-specific OTUB1 in viral infection, we infected mice with murine Cytomegalovirus (MCMV), which induces a strong IL-12 response in various DC subtypes [186]. In MCMV infection, induction of IL-12 in DCs is mediated by TLR3 [229], TLR7 [188], TLR9 [230,231], RIG-I-like Receptors (RLR) [187], and cGAS/STING [187], which may compensate each other with respect to IL-12 production. In contrast to toxoplasmosis and LPS challenge, MCMV infection resulted in comparable DC response in CD11c-Cre OTUB1^{fl/fl} and OTUB1^{fl/fl} control mice, in both the liver (Fig. 41a-41c) and spleen (Fig. 41d-41f). Numbers of DC subpopulations (Fig. 41b and 41e) and IL-12 producing DC subsets (Fig. 41c and 41f) were not regulated by DC-specific OTUB1. In addition, serum levels of IL-12, TNF and IL-6 (Fig. 41g) and the viral load in the liver, spleen, lung and lymph nodes (Fig. 41h) were equal between both infected mouse strains.
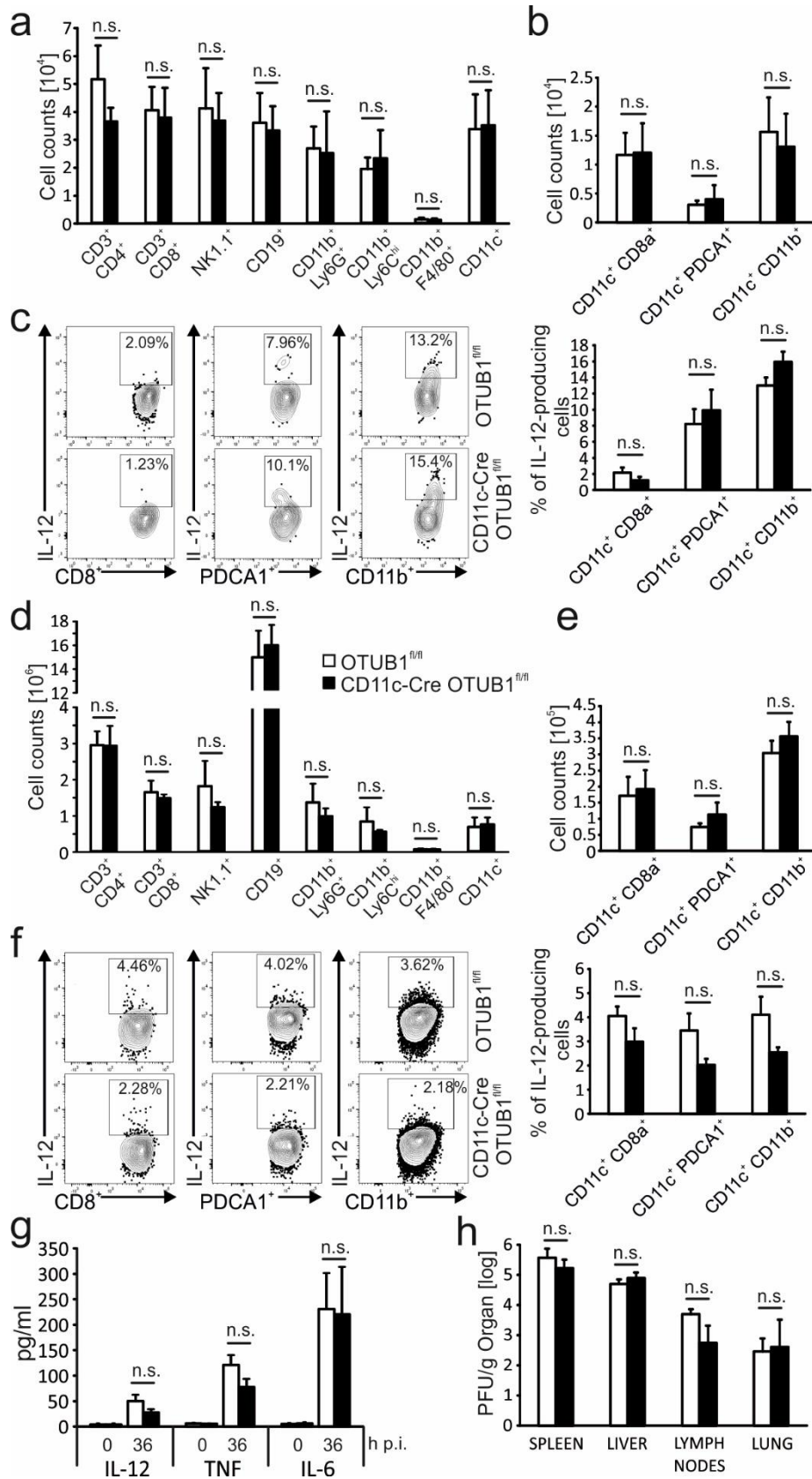
Figure 41 DC response to MCMV is independent of OTUB1. *(a to h) OTUB1^(fl/fl) and CD11c-Cre OTUB1^(fl/fl) mice were infected i.v. with 106 MCMV and after 36 h mice were sacrificed for the collection of livers, spleens, lungs and lymph nodes (n = 4). (a to c) Flow cytometry analysis of leukocytes isolated from the liver. (d to f) Flow cytometry analysis of leukocytes isolated from the spleen. (g) Cytokines in the serum were measured by ELISA. (h) Organ homogenates were plated in serial log10 dilutions on primary murine embryonic fibroblasts. Plaques were counted after 4 days of culture under a light microscope (Zeiss).*

5. DISCUSSION

The swift sensing of invading pathogens by DCs plays a critical role in the defense against infections. In this process, TLR-mediated activation of NF-κB is essential for the rapid induction of immune responses. However, hyperactivation of the NF-κB signaling may lead to immunopathology and diseases, as observed in LPS-mediated TLR4 activation during Gram-negative sepsis [232]. Results presented in the present study provide evidence that the DUB OTUB1 critically supports canonical NF-κB activation in DCs and mediates DC-dependent protection in infectious disease but augments immunopathology upon LPS challenge.

Mechanistically, we identified that UBC13 interacts with OTUB1 upon TgPFN and LPS stimulation, extending a previous study showing that, in the cell nucleus, OTUB1 binds to UBC13 in response to DNA double-strand breaks [205]. With respect to TLR signaling, UBC13 is a key molecule bolstering MyD88-mediated NF-κB activity by cooperating with the E3 ligases Pellino and TRAF6, respectively. First, engagement of TLR11/12 and TLR4, respectively, induces recruitment and interaction with MyD88, which is followed by the recruitment of IRAK4 to MyD88. This oligomeric Myddosome acts as a platform for the binding of IRAK1, IRAK2, and IRAK3 [233]. Activated IRAK1 catalyzes the phosphorylation of Pellino, which is a prerequisite for its activity as an E3 ubiquitin ligase [52,206]. In collaboration with the cognate E2 ubiquitin-conjugating enzyme UBC13, active Pellino acts back on IRAK1 by enabling its K63-specific ubiquitination [206] and subsequent activation of NEMO. Second, even without K63 ubiquitination, IRAK1 can also activate the IKK complex via inducing the association and activation of TRAF6. As an E3 ligase, TRAF6 adds K63 polyubiquitin chains on itself with UBC13 acting as the E2 conjugase [210]. This two-fold ubiquitination-regulating function places UBC13 as a pivotal molecule bolstering MyD88-mediated NF-κB activity. In good agreement with this

dual function of UBC13 in the MyD88/NF-κB signaling, K63 ubiquitination of both IRAK1 and TRAF6 was augmented in TgPFN-stimulated OTUB1-competent BMDCs. Additionally, OTUB1 increased the amount of free ubiquitin in MyD88-activated DCs, which may further contribute to augmented NF-kB activation, since free ubiquitin can directly stimulate TAK1 [215]. The stimulatory role of OTUB1 on TAK1/ NF-κB activation upon TNFR and TLR3 engagement may also be mediated by increased activation of TAK1 by unanchored ubiquitin chains and, additionally, by UBC13 mediate K63 polyubiquitination of RIP1, which also contributes to TAK1 activation [199–201,211].

Interestingly, UBC13 is also a target of ubiquitination and its protein stability is compromised by K48-linked polyubiquitin chains added by A20 [207]. Here, we identify that K48 ubiquitination of UBC13 is counteracted by OTUB1. Since K48 ubiquitination is associated with protein degradation, OTUB1 increases the stability of UBC13. In this way, OTUB1 preserves the E2 activity of UBC13 and thereby enhances K63 ubiquitination of IRAK1 and TRAF6, leading to increased NF-κB activation. We found that UBC13 protein is not stable and can be degraded even in the presence of OTUB1 (Fig. 25a, 25c and Fig. 26). However, OTUB1 can significantly delay the degradation of UBC13, showing that OTUB1 serves as a fine-tuning mechanism in protein ubiquitination and degradation. Interestingly, transfection with OTUB1 mutants revealed that prevention of UBC13 degradation required both the N-terminus and the catalytic domain of OTUB1, given that only wild type but not the OTUB1-C91S-GFP and the OTUB1-ΔN-GFP mutants, rescued UBC13 from degradation (Fig. 26). Interestingly, consistent with our finding, both the C91 residue and the N-terminus of OTUB1 are required for its effect on SMAD3 [147].

Both the canonical NF-κB pathway, which is induced by engagement of TLRs and is dependent on degradation of the NF-κB inhibitor IκBα, and the non-canonical NF-κB pathway, which is

dependent on the degradation of the IκB-like inhibitor p100, play fundamental roles in immune responses. Due to the central importance of NF-κB pathways, several DUBs including TNFAIP3 (A20) and CYLD critically regulate NF-κB pathways and each of these DUBs modulates various signaling molecules [234]. With respect to OTUB1, Li et al. [235] recently identified that OTUB1 prevented B cell-mediated autoimmunity not only by suppressing p100 degradation and non-canonical NF-κB activation but also by preserving p100 in the steady-state preventing aberrant NF-κB activation in the canonical pathway. In combination with our data demonstrating that OTUB1 supports canonical NF-κB activation in DCs upon stimulation with various proinflammatory stimuli, OTUB1 qualifies as a critical regulator of both canonical and non-canonical NF-kB pathways and their crosstalks depending on the environment, the stimuli and potentially also the cell type.

In this regard, we identified that OTUB1 played a central protective role in the UBC13-mediated activation of the NF-κB pathway of CD11c$^+$ DCs in response to TLR11/12-dependent activation by the protozoal parasite *T. gondii* but contributes to immunopathology upon TLR4-dependent LPS challenge. Of note, both TgPFN and LPS also induced a stronger activation of MAPKs in OTUB1-competent BMDCs, which is in accordance with supportive role of UBC13 in LPS-induced MAPK activation [204]. Thus, these pathways may also contribute to the pro-inflammatory phenotype of OTUB1$^{fl/fl}$ mice in toxoplasmosis and LPS challenge, although the strong reduction of IL-12 production and the abolishment of OTUB1-dependent increased IL-12 production upon NF-κB inhibition may argue for a superior role of the NF-κB pathway. Since OTUB1-competent BMDCs showed a stronger activation of TAK1 and production of cytokines IL-12, TNF, and IL-6 upon engagement of TLR2, TLR7, TLR9 and IL-1R, which all signal via MyD88, as well as upon TNF stimulation and Poly I:C-induced TLR3 activation, which both induce MyD88-independent signaling, OTUB1 may contribute to pro-inflammatory DC

responses in a wide range of infections and inflammatory disorders. However, our data on OTUB1-independent cytokine production of DCs and pathogen control in MCMV infection illustrate that the underlying pathogen determines the importance of OTUB1 in DC activation. MCMV activates several pattern recognition receptors including TLR3 [229], TLR7 [188], TLR9 [230,231], RLR [187] and cGAS/STING [187] in DCs and these receptors can compensate each other with respect to protective DC functions in MCMV infection [187,231,236]. Additionally, MCMV actively manipulates IRF3 and NF-κB activation to promote viral spread [237–239]. These data extent previous *in vitro* studies on the inhibition of Sendai virus-induced IRF3 and NF-κB signaling by OTUB1 [145], and further indicate that the DC-specific function of OTUB1 interplays with pathogen-mediated modulation of host cell signaling.

To address the *in vivo* importance of OTUB1-mediated NF-κB activation, we studied the murine model of toxoplasmosis, because protection against *T. gondii* is critically dependent on TgPFN-mediated activation of TLR11/12 in DCs. Engagement of TLR11/12 by TgPFN activates CD8+ cDC1 in a MyD88-dependent manner to produce IL-12, which drives protection against *T. gondii* independent of other relevant DC functions including cross-presentation of antigens and production of chemokines and other cytokines [221]. IL-12 production of CD8+ cDC1, which cannot be compensated by other IL-12-producing cell populations, is critical for the induction of IFN-γ production by NK cells and anti-parasitic effector molecules in infected host cells resulting in the early containment of parasite multiplication, restriction of the intracerebral parasite load and survival of chronic TE [221]. Here, we demonstrate that OTUB1 enables DCs to fulfill these critical immunoregulatory functions in toxoplasmosis by enhancing TgPFN/MyD88-induced IL-12 transcription via NF-κB but not via IRF8, which also supports IL-12 production of DCs in toxoplasmosis [196,197]. This assumption was further substantiated by the inhibition of IL-12 production in both OTUB1-competent and -deficient BMDCs upon NF-

κB inhibitor treatment. Likewise, OTUB1 promoted LPS-induced TLR4/MyD88-dependent NF-κB activation and cytokine production. Since DCs also play an important role in sepsis and contribute to LPS-induced immunopathology [228], mice with intact OTUB1 function in DCs produced significantly more pro-inflammatory disease-promoting cytokines and succumbed significantly earlier to LPS challenge. It will be of interest to explore in more details the *in vivo* role of OTUB1 in other PRR-MyD88-dependent and -independent signaling pathways, cell types and infectious diseases.

The balanced activation of DCs in response to invading pathogens is important to ensure pathogen control and to limit immunopathology. DUBs including A20 and Trabid have emerged as an important group of enzymes absolutely required for this balanced DC activation [228,240–242]. In this study, we identified OTUB1 as a novel DUB that regulates TLR-induced DC activation via deubiquitinating and stabilizing UBC13, thereby providing a potential target for the treatment of infectious and inflammatory diseases.

Open questions and future prospects

Despite in this work we were able to address important knowledge gaps in DC activation introducing OTUB1 as a new regulator of TLR/MyD88-mediated NF-κB activation, some open points persist and additionally studies are required to better understand the exact mechanism behind OTUB1-mediated deubiquitination of UBC13.

Interaction between OTUB1 and UBC13 has already been reported in the context of DNA damage [150,214,219]. In that context OTUB1 has been shown to interact to UBC13 in the nucleus after DNA damage and to inhibit the E2 function of UBC13 in a non-catalytic way, blocking DNA repair mechanisms. In our study, we proved that OTUB1 and UBC13 can also interact in the cytoplasm of TLR-stimulated DCs, resulting in UBC13 stabilization, and therefore enhanced

NF-κB activation. Inflammation increases oxidative DNA damage [244,245], therefore, after TLR stimulations and NF-κB activation, pathways for DNA repair are activated [246]. In our work, we did not focus on the regulatory role of OTUB1 in DNA repair but we do not exclude that in the same inflammatory context OTUB1 could play two different roles: in the cytoplasm as inflammation initiator and in the nucleus as suppressor of DNA repair. Next studies will focus on this double function of OTUB1 and how the switch between pro-inflammatory molecule and inhibitor of DNA repair is regulated.

Our work gives the basis for a better understanding of the fine regulation of the NF-κB pathway. Accumulating evidence suggests that the DUBs play a critical role in the regulation of this and other pathways, indispensable for the activation and regulation of the immune system. Thus, DUBs are raising the attention for the development of specific inhibitors, through which activate or suppress the immune response. Although progress has been made in our understanding of DUB biology/mechanisms, there is considerable work to be done in order to move DUB activating or inhibiting drugs into the clinic [247,248]. Basic research is crucial to discover the natural regulatory mechanism in a cell in order to identify candidate pathways and targets which are required for regulation of DUB expression and activity that may be modulated pharmacologically. Due to the canonical and noncanonical activities of OTUB1, it represents a complex target. Currently the only known inhibitors of OTUB1 are unspecific inhibitors of catalytic activity of a broad range of cysteine-dependent DUBs (such as N-ethylmaleimide), but are not able to block the non-catalytic activity of OTUB1. Therefore, further studies are required to better understand the biochemical basis of OTUB1 and to develop specific drugs suitable for the treatment of several disease and cancer.

Graphical summary of the study
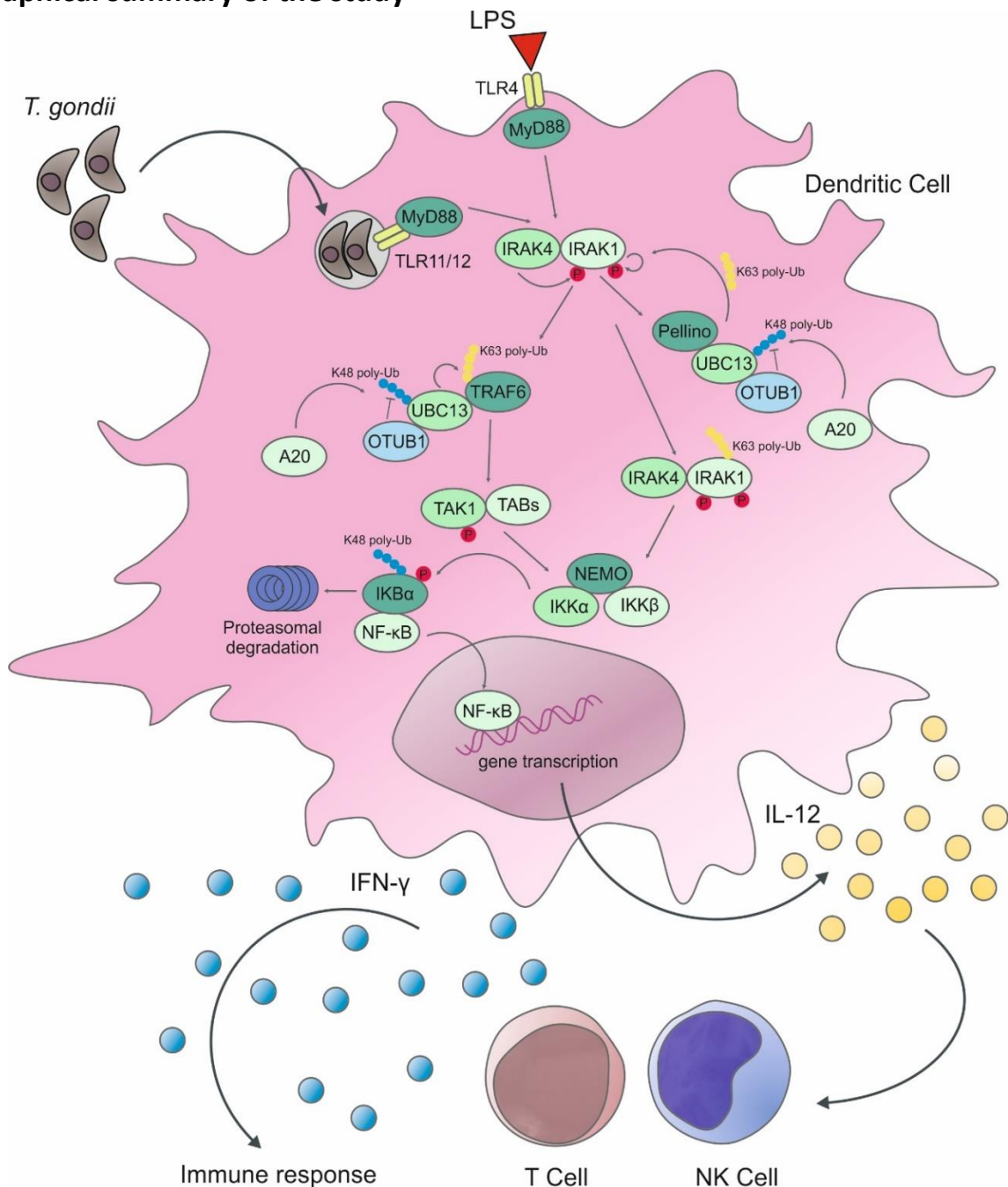
Figure 42 Graphical summary of the project. *When T. gondii, LPS or other ligands are recognized by their specific TLRs, MyD88, IRAK1 and IRAK4 are recruited to the receptors. This leads to the phosphorylation of IRAK1 by IRAK4 and by itself. Then two pathways which lead to the activation of IKK complex and NEMO are activated. IKK complex phosphorylates IKBα, that is fastly degraded. NF-κB consequently, is not distrained in the cytoplasm anymore and can translocate in the nucleus to activated gene transcription. In the first pathway, phosphorylated IRAK1 activated the E3 TRAF6, which, with the collaboration of the E2 UBC13, K63-polyubiquitinates itself. K63-polyubiquitinated TRAF6, activated then TABs and TAK1, which eventually activated NEMO and IKK complex. On the other hand, phosphorylated IRAK1 can also activate TRAF6, which, together with UBC13, transfer K63-polyubiquitination back on IRAK1. K63-polyubiquitinated IRAK1 is now able to activate the IKK complex. The activity of UBC13 is counter-regulated by K48-polyubiquitination. Indeed, after stimulation, A20 rapidly add K48-polyubiquitin chains on UBC13, which is soon proteasomal degraded. OTUB1, otherwise, blocks UBC13 degradation by reducing its K48-polyubiquitination levels. As a result of that, DC can produce increased and effective amount of IL-12, which stimulated NK cells and T cells to produce IFN-γ and ultimately activates the immune response.*

BIBLIOGRAPHY

1. Steinman, R. M. Identification of a novel cell type in peripheral organs of mice. *Jem* **137**, 1142–1162 (1973).

2. Mckenna, K., Beignon, A. & Bhardwaj, N. MINIREVIEW Plasmacytoid Dendritic Cells : Linking Innate and Adaptive Immunity. **79**, 17–27 (2005).

3. Sichien, D., Lambrecht, B. N., Guilliams, M. & Scott, C. L. Development of conventional dendritic cells : from common bone marrow progenitors to multiple subsets in peripheral tissues. **10**, 831–844 (2017).

4. Eisenbarth, S. C. Dendritic cell subsets in T cell programming: location dictates function. *Nat. Rev. Immunol.* **19**, 89–103 (2019).

5. Rodrigues, P. F. *et al.* Distinct progenitor lineages contribute to the heterogeneity of plasmacytoid dendritic cells. *Nat. Immunol.* **19**, 711–722 (2018).

6. Schlitzer, A., Zhang, W., Song, M. & Ma, X. Recent advances in understanding dendritic cell development, classification, and phenotype. *F1000Research* **7**, (2018).

7. Merad, M., Sathe, P., Helft, J., Miller, J. & Mortha, A. The Dendritic Cell Lineage: Ontogeny and Function of Dendritic Cells and Their Subsets in the Steady State and the Inflamed Setting. *Annu. Rev. Immunol.* **31**, 563–604 (2013).

8. Colonna, M., Trinchieri, G. & Liu, Y. J. Plasmacytoid dendritic cells in immunity. *Nat. Immunol.* **5**, 1219–1226 (2004).

9. Segura, E. & Amigorena, S. Inflammatory dendritic cells in mice and humans. *Trends Immunol.* **34**, 440–445 (2013).

10. Mildner, A. & Jung, S. Review Development and Function of Dendritic Cell Subsets. *Immunity* **40**, 642–656 (2014).

11. O'Keeffe, M., Mok, W. H. & Radford, K. J. Human dendritic cell subsets and function in health and disease. *Cell. Mol. Life Sci.* **72**, 4309–4325 (2015).

12. Kubach, J. *et al.* Dendritic Cells: Sentinels of Immunity and Tolerance. *Int. J. Hematol.* **81**, 197–203 (2005).

13. Villadangos, J. A. & Schnorrer, P. Intrinsic and cooperative antigen-presenting functions of dendritic-cell subsets in vivo. *Nat. Rev. Immunol.* **7**, 543–555 (2007).

14. Heath, W. R. *et al.* Subsets , and the Generation of Immunity To Cellular Antigens. *Immunol. Rev.* **199**, 9–26 (2004).

15. Rock, K. L. & Shen, L. Cross-presentation: Underlying mechanisms and role in immune surveillance. *Immunol. Rev.* **207**, 166–183 (2005).

16. Vargas, P., Barbier, L., Sáez, P. J. & Piel, M. Mechanisms for fast cell migration in complex environments. *Curr. Opin. Cell Biol.* **48**, 72–78 (2017).

17. Worbs, T., Hammerschmidt, S. I. & Förster, R. Dendritic cell migration in health and disease. *Nat. Rev. Immunol.* **17**, 30–48 (2017).

18. Weber, M. *et al.* Interstitial Dendritic Cell Guidance by Haptotactic Chemokine Gradients. *Science (80-.).* **339**, 328–332 (2019).

19. Wendland, M. *et al.* Lymph Node T Cell Homeostasis Relies on Steady State Homing of Dendritic Cells. *Immunity* **35**, 945–957 (2011).

20. Qu, C. *et al.* Role of CCR8 and Other Chemokine Pathways in the Migration of Monocyte-derived Dendritic Cells to Lymph Nodes. *J. Exp. Med.* **200**, 1231–1241 (2004).

21. Seyfizadeh, N. N., Muthuswamy, R., Mitchell, D. A., Nierkens, S. & Seyfizadeh, N. N. Migration of dendritic cells to the lymph nodes and its enhancement to drive anti-tumor responses. *Crit. Rev. Oncol. Hematol.* **107**, 100–110 (2016).

22. Steinman, R. M., Hemmi, H. & Hemmi, R. M. S. H. Dendritic Cells: Translating Innate to Adaptive Immunity. *From Innate Immun. to Immunol. Mem.* 17–58 (2006). doi:10.1007/3-540-32636-7_2

23. Korn, T., Bettelli, E., Oukka, M. & Kuchroo, V. K. IL-17 and Th17 Cells. *Annu. Rev. Immunol.* **27**, 485–517 (2009).

24. Min, W.-P. *et al.* Inhibitory Feedback Loop Between Tolerogenic Dendritic Cells and Regulatory T Cells in Transplant Tolerance. *J. Immunol.* **170**, 1304–1312 (2003).

25. Kim, J. M., Rasmussen, J. P. & Rudensky, A. Y. Regulatory T cells prevent catastrophic autoimmunity throughout the lifespan of mice. *Nat. Immunol.* **8**, 191–197 (2007).

26. Austyn, J. M. Dendritic Cells in the Immune System—History, Lineages, Tissues, Tolerance, and Immunity. *Microbiol. Spectr.* **79**, 25–32 (2016).

27. Waisman, A., Lukas, D., Clausen, B. E. & Yogev, N. Dendritic cells as gatekeepers of tolerance. *Semin. Immunopathol.* **39**, 153–163 (2017).

28. Qian, C. & Cao, X. Dendritic cells in the regulation of immunity and inflammation. *Semin. Immunol.* **35**, 3–11 (2018).

29. Craxton, A., Magaletti, D., Ryan, E. J. & Clark, E. A. Macrophage-and dendritic cell-dependent regulation of human B-cell proliferation requires the TNF family ligand BAFF. (2003). doi:10.1182/blood-2002-10-3123

30. Balázs, M., Martin, F., Zhou, T. & Kearney, J. Blood dendritic cells interact with splenic marginal zone B cells to initiate T-independent immune responses. *Immunity* **17**, 341–52 (2002).

31. Banchereau, J. *et al.* Mmunobiology of. *Annu. Rev. Immunol.* 767–811 (2000). doi:10.1146/annurev.immunol.18.1.767

32. Song, L., Dong, G., Guo, L. & Graves, D. T. The function of dendritic cells in modulating the host response. *Mol. Oral Microbiol.* **33**, 13–21 (2018).

33. Ohnmacht, C. *et al.* Constitutive ablation of dendritic cells breaks self-tolerance of CD4 T cells and results in spontaneous fatal autoimmunity. *J. Exp. Med.* **206**, 549–559 (2009).

34. Birnberg, T. *et al.* Lack of Conventional Dendritic Cells Is Compatible with Normal Development and T Cell Homeostasis, but Causes Myeloid Proliferative Syndrome. *Immunity* **29**, 986–997 (2008).

35. Hemmi, H. & Akira, S. TLR Signalling and the Function of Dendritic Cells. *Mech. Epithel. Def.* **86**, 120–135 (2005).

36. Takeuchi, O. & Akira, S. Pattern recognition receptors and inflammation. *Cell* **140**, 805–20 (2010).

37. Hou, B., Reizis, B. & DeFranco, A. L. Toll-like Receptors Activate Innate and Adaptive Immunity by using Dendritic Cell-Intrinsic and -Extrinsic Mechanisms. *Immunity* **29**, 272–282 (2008).

38. Medzhitov, R., Preston-Hurlburt, P. & Janeway, C. A. A human homologue of the Drosophila Toll protein signals activation of adaptive immunity. *Nature* **388**, 394–397 (1997).

39. Takeda, K. & Akira, S. Toll-Like Receptors. in *Current Protocols in Immunology* **77**, 14.12.1-14.12.13 (John Wiley & Sons, Inc., 2007).

40.   Barton, G. M. & Medzhitov, R. Toll-like receptors and their ligands. *Curr. Top. Microbiol. Immunol.* **270**, 81–92 (2002).

41.   Arnold-schrauf, C., Berod, L. & Sparwasser, T. Dendritic cell specific targeting of MyD88 signalling pathways in vivo. 32–39 (2015). doi:10.1002/eji.201444747

42.   Adachi, O. *et al.* Targeted disruption of the MyD88 gene results in loss of IL-1- and IL-18-mediated function. *Immunity* **9**, 143–50 (1998).

43.   Sakai, J. *et al.* Lipopolysaccharide-induced NF-κB nuclear translocation is primarily dependent on MyD88, but TNFα expression requires TRIF and MyD88. *Sci. Rep.* **7**, 1428 (2017).

44.   Arnold-Schrauf, C. *et al.* Dendritic cells coordinate innate immunity via MyD88 signaling to control Listeria monocytogenes infection. *Cell Rep.* **6**, 698–708 (2014).

45.   Sen, R. & Baltimore, D. Multiple nuclear factors interact with the immunoglobulin enhancer sequences. *Cell* **46**, 705–16 (1986).

46.   Reinhard, K., Huber, M., Lohoff, M. & Visekruna, A. International Journal of Medical Microbiology The role of NF- B activation during protection against Leishmania infection. *Int. J. Med. Microbiol.* **302**, 230–235 (2012).

47.   Perkins, N. D. Regulation of NF-kappaB by atypical activators and tumour suppressors. *Biochem. Soc. Trans.* **32**, 936–9 (2004).

48.   Mitchell, S., Vargas, J. & Hoffmann, A. Signaling via the NF κ B system. **8**, 227–241 (2016).

49.   Kanarek, N. & Ben-Neriah, Y. Regulation of NF-κB by ubiquitination and degradation of the IκBs. *Immunol. Rev.* **246**, 77–94 (2012).

50.   Ordureau, A. *et al.* The IRAK-catalysed activation of the E3 ligase function of Pellino isoforms induces the Lys63-linked polyubiquitination of IRAK1. *Biochem. J.* **409**, 43–52 (2008).

51.   Kawai, T. & Akira, S. Signaling to NF-kappaB by Toll-like receptors. *Trends Mol. Med.* **13**, 460–9 (2007).

52.   Schauvliege, R., Janssens, S. & Beyaert, R. Pellino proteins are more than scaffold proteins in TLR/IL-1R signalling: a role as novel RING E3-ubiquitin-ligases. *FEBS Lett.* **580**, 4697–702 (2006).

53.   Lawrence, T. The Nuclear Factor NF- k B Pathway in Inflammation. 1–11 (2019).

54.   Bonizzi, G. & Karin, M. The two NF-κB activation pathways and their role in innate and adaptive immunity. *Trends Immunol.* **25**, 280–288 (2004).

55.   Moynagh, P. N. The NF- B pathway The NF- B Pathway. **2005**, 4589–4592 (2005).

56.   Hoesel, B. & Schmid, J. A. The complexity of NF- κ B signaling in inflammation and cancer. 1–15 (2013).

57.   Baker, R. G., Hayden, M. S. & Ghosh, S. Review NF- k B , Inflammation , and Metabolic Disease. 11–22 (2011). doi:10.1016/j.cmet.2010.12.008

58.   Beinke, S. *et al.* NF-kappaB1 p105 negatively regulates TPL-2 MEK kinase activity. *Mol. Cell. Biol.* **23**, 4739–52 (2003).

59.   Sun, S. C. The non-canonical NF-κB pathway in immunity and inflammation. *Nat. Rev. Immunol.* **17**, 545–558 (2017).

60.   Shishodia, S. & Aggarwal, B. B. Nuclear factor-κB: a friend or a foe in cancer? *Biochem. Pharmacol.* **68**, 1071–1080 (2004).

61.   Patel, M., Horgan, P. G., McMillan, D. C. & Edwards, J. NF-κB pathways in the development and progression of colorectal cancer. *Transl. Res.* **197**, 43–56 (2018).

62. Williams, R. O., Paleolog, E. & Feldmann, M. Cytokine inhibitors in rheumatoid arthritis and other autoimmune diseases. *Curr. Opin. Pharmacol.* **7**, 412–417 (2007).

63. Allenspach, E. & Torgerson, T. R. Autoimmunity and Primary Immunodeficiency Disorders. *J. Clin. Immunol.* **36**, 57–67 (2016).

64. Mulero, M. C. *et al.* Chromatin-bound IκBα regulates a subset of polycomb target genes in differentiation and cancer. *Cancer Cell* **24**, 151–66 (2013).

65. Basak, S. *et al.* A fourth IkappaB protein within the NF-kappaB signaling module. *Cell* **128**, 369–81 (2007).

66. Vallabhapurapu, S. & Karin, M. Regulation and Function of NF-κB Transcription Factors in the Immune System. *Annu. Rev. Immunol.* **27**, 693–733 (2009).

67. Fiorini, E. *et al.* Peptide-induced negative selection of thymocytes activates transcription of an NF-kappa B inhibitor. *Mol. Cell* **9**, 637–48 (2002).

68. Kuwata, H. *et al.* IκBNS Inhibits Induction of a Subset of Toll-like Receptor-Dependent Genes and Limits Inflammation. *Immunity* **24**, 41–51 (2006).

69. Wesche, H. *et al.* IRAK-M is a novel member of the Pelle/interleukin-1 receptor-associated kinase (IRAK) family. *J. Biol. Chem.* **274**, 19403–10 (1999).

70. Hubbard, L. L. N. & Moore, B. B. IRAK-M regulation and function in host defense and immune homeostasis. *Infect. Dis. Rep.* **2**, (2010).

71. Schroder, K. & Tschopp, J. The inflammasomes. *Cell* **140**, 821–32 (2010).

72. Burns, K. *et al.* Inhibition of interleukin 1 receptor/Toll-like receptor signaling through the alternatively spliced, short form of MyD88 is due to its failure to recruit IRAK-4. *J. Exp. Med.* **197**, 263–8 (2003).

73. Bhaumik, D. *et al.* Expression of microRNA-146 suppresses NF-κB activity with reduction of metastatic potential in breast cancer cells. *Oncogene* **27**, 5643–5647 (2008).

74. Sheedy, F. J. *et al.* Negative regulation of TLR4 via targeting of the proinflammatory tumor suppressor PDCD4 by the microRNA miR-21. *Nat. Immunol.* **11**, 141–147 (2010).

75. Tili, E. *et al.* Modulation of miR-155 and miR-125b Levels following Lipopolysaccharide/TNF-α Stimulation and Their Possible Roles in Regulating the Response to Endotoxin Shock. *J. Immunol.* **179**, 5082–5089 (2007).

76. Carballo, E., Lai, W. S. & Blackshear, P. J. Feedback Inhibition of Macrophage Tumor Necrosis Factor-α Production by Tristetraprolin. *Science (80-.).* **281**, 1001–1005 (1998).

77. Ziembik, M. A., Bender, T. P., Larner, J. M. & Brautigan, D. L. Functions of protein phosphatase-6 in NF-κB signaling and in lymphocytes. *Biochem. Soc. Trans.* **45**, 693–701 (2017).

78. Abdul-Sada, H. *et al.* The PP4R1 sub-unit of protein phosphatase PP4 is essential for inhibition of NF-&#x3BA;B by merkel polyomavirus small tumour antigen. *Oncotarget* **8**, 25418–25432 (2017).

79. Lu, T. & Stark, G. R. NF- k B : Regulation by Methylation. **75**, 3692–3696 (2015).

80. Zinngrebe, J., Montinaro, A., Peltzer, N. & Walczak, H. Ubiquitin in the immune system. *EMBO Rep.* **15**, 28–45 (2014).

81. George, A. J., Hoffiz, Y. C., Charles, A. J., Zhu, Y. & Mabb, A. M. A Comprehensive Atlas of E3 Ubiquitin Ligase Mutations in Neurological Disorders. *Front. Genet.* **9**, 29 (2018).

82. Davis, M. E. & Gack, M. U. Ubiquitination in the antiviral immune response. *Virology* **479–480**, 52–65

(2015).

83.   McDowell, G. S. & Philpott, A. Non-canonical ubiquitylation: Mechanisms and consequences. *Int. J. Biochem. Cell Biol.* **45**, 1833–1842 (2013).

84.   Akutsu, M., Dikic, I. & Bremm, A. Ubiquitin chain diversity at a glance. *J. Cell Sci.* **129**, 875–880 (2016).

85.   Yau, R. & Rape, M. The increasing complexity of the ubiquitin code. *Nat. Cell Biol.* **18**, 579–586 (2016).

86.   Stolz, A. & Dikic, I. Heterotypic Ubiquitin Chains: Seeing is Believing. *Trends Cell Biol.* **28**, 1–3 (2018).

87.   Michel, M. A., Swatek, K. N., Hospenthal, M. K. & Komander, D. Ubiquitin Linkage-Specific Affimers Reveal Insights into K6-Linked Ubiquitin Signaling. *Mol. Cell* **68**, 233-246.e5 (2017).

88.   Michel, M. A. *et al.* Assembly and Specific Recognition of K29- and K33-Linked Polyubiquitin. *Mol. Cell* **58**, 95–109 (2015).

89.   Gatti, M. *et al.* RNF168 Promotes Noncanonical K27 Ubiquitination to Signal DNA Damage. *Cell Rep.* **10**, 226–238 (2015).

90.   Kulathu, Y. & Komander, D. Atypical ubiquitylation — the unexplored world of polyubiquitin beyond Lys48 and Lys63 linkages. *Nat. Rev. Mol. Cell Biol.* **13**, 508–523 (2012).

91.   Elia, A. E. H. *et al.* Quantitative Proteomic Atlas of Ubiquitination and Acetylation in the DNA Damage Response. *Mol. Cell* **59**, 867–81 (2015).

92.   Kim, W. *et al.* Systematic and Quantitative Assessment of the Ubiquitin-Modified Proteome. *Mol. Cell* **44**, 325–340 (2011).

93.   Wickliffe, K. E., Williamson, A., Meyer, H.-J., Kelly, A. & Rape, M. K11-linked ubiquitin chains as novel regulators of cell division. *Trends Cell Biol.* **21**, 656–663 (2011).

94.   Boname, J. M. *et al.* Efficient Internalization of MHC I Requires Lysine-11 and Lysine-63 Mixed Linkage Polyubiquitin Chains. *Traffic* **11**, 210–220 (2010).

95.   Goto, E. *et al.* Contribution of Lysine 11-linked Ubiquitination to MIR2-mediated Major Histocompatibility Complex Class I Internalization. *J. Biol. Chem.* **285**, 35311 (2010).

96.   Dynek, J. N. *et al.* c-IAP1 and UbcH5 promote K11-linked polyubiquitination of RIP1 in TNF signalling. *EMBO J.* **29**, 4198–4209 (2010).

97.   Wang, Q. *et al.* The E3 Ubiquitin Ligase AMFR and INSIG1 Bridge the Activation of TBK1 Kinase by Modifying the Adaptor STING. *Immunity* **41**, 919–933 (2014).

98.   Fei, C. *et al.* Smurf1-mediated Lys29-linked nonproteolytic polyubiquitination of axin negatively regulates Wnt/β-catenin signaling. *Mol. Cell. Biol.* **33**, 4095–105 (2013).

99.   Yang, M. *et al.* K33-linked polyubiquitination of Zap70 by Nrdp1 controls CD8+ T cell activation. *Nat. Immunol.* **16**, 1253–1262 (2015).

100. Huang, H. *et al.* K33-Linked Polyubiquitination of T Cell Receptor-ζ Regulates Proteolysis-Independent T Cell Signaling. *Immunity* **33**, 60–70 (2010).

101. Yuan, W.-C. *et al.* K33-Linked Polyubiquitination of Coronin 7 by Cul3-KLHL20 Ubiquitin E3 Ligase Regulates Protein Trafficking. *Mol. Cell* **54**, 586–600 (2014).

102. Xu, P. *et al.* Quantitative proteomics reveals the function of unconventional ubiquitin chains in proteasomal degradation. *Cell* **137**, 133–45 (2009).

103. Peth, A., Uchiki, T. & Goldberg, A. L. ATP-dependent steps in the binding of ubiquitin conjugates to the 26S proteasome that commit to degradation. *Mol. Cell* **40**, 671–81 (2010).

104. Kanarek, N. & Ben-Neriah, Y. Regulation of NF-κB by ubiquitination and degradation of the IκBs. *Immunol. Rev.* **246**, 77–94 (2012).

105. Chen, J. & Chen, Z. J. Regulation of NF-κB by ubiquitination. *Curr. Opin. Immunol.* **25**, 4–12 (2013).

106. Zhou, W. & Yuan, J. Necroptosis in health and diseases. *Semin. Cell Dev. Biol.* **35**, 14–23 (2014).

107. Zhao, X. *et al.* The HECT-domain ubiquitin ligase Huwe1 controls neural differentiation and proliferation by destabilizing the N-Myc oncoprotein. *Nat. Cell Biol.* **10**, 643–53 (2008).

108. Hirata, Y. *et al.* TRIM48 Promotes ASK1 Activation and Cell Death through Ubiquitination-Dependent Degradation of the ASK1-Negative Regulator PRMT1. *Cell Rep.* **21**, 2447–2457 (2017).

109. Fernández-Majada, V. *et al.* The tumour suppressor CYLD regulates the p53 DNA damage response. *Nat. Commun.* **7**, 12508 (2016).

110. Mallette, F. A. & Richard, S. K48-linked ubiquitination and protein degradation regulate 53BP1 recruitment at DNA damage sites. *Cell Res.* **22**, 1221–1223 (2012).

111. Jin, W., Chang, M. & Sun, S.-C. Peli: a family of signal-responsive E3 ubiquitin ligases mediating TLR signaling and T-cell tolerance. *Cell. Mol. Immunol.* **9**, 113–122 (2012).

112. Jarome, T. J. & Devulapalli, R. K. The Ubiquitin-Proteasome System and Memory: Moving Beyond Protein Degradation. *Neurosci.* **24**, 639–651 (2018).

113. Ohtake, F., Saeki, Y., Ishido, S., Kanno, J. & Tanaka, K. The K48-K63 Branched Ubiquitin Chain Regulates NF-κB Signaling. *Mol. Cell* **64**, 251–266 (2016).

114. Wang, Y. *et al.* Hepatitis B e Antigen Inhibits NF-κB Activity by Interrupting K63-Linked Ubiquitination of NEMO. *J. Virol.* **93**, (2018).

115. Liu, P. *et al.* K63-linked polyubiquitin chains bind to DNA to facilitate DNA damage repair. *Sci. Signal.* **11**, eaar8133 (2018).

116. Lee, B. L., Singh, A., Mark Glover, J. N., Hendzel, M. J. & Spyracopoulos, L. Molecular Basis for K63-Linked Ubiquitination Processes in Double-Strand DNA Break Repair: A Focus on Kinetics and Dynamics. *J. Mol. Biol.* **429**, 3409–3429 (2017).

117. Meng, J. *et al.* ARRDC4 regulates enterovirus 71-induced innate immune response by promoting K63 polyubiquitination of MDA5 through TRIM65. *Cell Death Dis.* **8**, e2866 (2017).

118. Ordureau, A. *et al.* Defining roles of PARKIN and ubiquitin phosphorylation by PINK1 in mitochondrial quality control using a ubiquitin replacement strategy. *Proc. Natl. Acad. Sci.* **112**, 6637–6642 (2015).

119. Lauwers, E., Jacob, C. & André, B. K63-linked ubiquitin chains as a specific signal for protein sorting into the multivesicular body pathway. *J. Cell Biol.* **185**, 493–502 (2009).

120. Nathan, J. A., Tae Kim, H., Ting, L., Gygi, S. P. & Goldberg, A. L. Why do cellular proteins linked to K63-polyubiquitin chains not associate with proteasomes? *EMBO J.* **32**, 552–565 (2013).

121. Pugh, D. *et al.* DWNN, a novel ubiquitin-like domain, implicates RBBP6 in mRNA processing and ubiquitin-like pathways. *BMC Struct. Biol.* **6**, 1 (2006).

122. Nanduri, P., Hao, R., Fitzpatrick, T. & Yao, T.-P. Chaperone-mediated 26S Proteasome Remodeling Facilitates Free K63 Ubiquitin Chain Production and Aggresome Clearance. *J. Biol. Chem.* **290**, 9455–9464 (2015).

123. Kirisako, T. *et al.* A ubiquitin ligase complex assembles linear polyubiquitin chains. *EMBO J.* **25**, 4877–87 (2006).

124. Tokunaga, F. *et al.* Involvement of linear polyubiquitylation of NEMO in NF-κB activation. *Nat. Cell Biol.* **11**, 123–132 (2009).

125. Belgnaoui, S. M. *et al.* Linear Ubiquitination of NEMO Negatively Regulates the Interferon Antiviral Response through Disruption of the MAVS-TRAF3 Complex. *Cell Host Microbe* **12**, 211–222 (2012).

126. Rivkin, E. *et al.* The linear ubiquitin-specific deubiquitinase gumby regulates angiogenesis. *Nature* **498**, 318–24 (2013).

127. Ndubaku, C. & Tsui, V. Inhibiting the Deubiquitinating Enzymes (DUBs). (2015). doi:10.1021/jm501061a

128. Hanpude, P., Bhattacharya, S., Dey, A. K. & Maiti, T. K. Deubiquitinating enzymes in cellular signaling and disease regulation. *IUBMB Life* **67**, 544–555 (2015).

129. Komander, D., Clague, M. J. & Urbé, S. Breaking the chains: structure and function of the deubiquitinases. *Nat. Rev. Mol. Cell Biol.* **10**, 550 (2009).

130. Collins, G. A. & Goldberg, A. L. Leading Edge The Logic of the 26S Proteasome. (2017). doi:10.1016/j.cell.2017.04.023

131. Mevissen, T. E. T. *et al.* Molecular basis of Lys11-polyubiquitin specificity in the deubiquitinase Cezanne. *Nature* **538**, 402–405 (2016).

132. Wertz, I. E. *et al.* De-ubiquitination and ubiquitin ligase domains of A20 downregulate NF-κB signalling. *Nature* **430**, 694–699 (2004).

133. Shembade, N., Ma, A. & Harhaj, E. W. Inhibition of NF-kB Signaling by A20 Through Disruption of Ubiquitin Enzyme Complexes. *Science (80-.).* **327**, 1135–1140 (2010).

134. Kovalenko, A. *et al.* The tumour suppressor CYLD negatively regulates NF-κB signalling by deubiquitination. *Nature* **424**, 801–805 (2003).

135. Enesa, K. *et al.* NF-kappaB suppression by the deubiquitinating enzyme Cezanne: a novel negative feedback loop in pro-inflammatory signaling. *J. Biol. Chem.* **283**, 7036–45 (2008).

136. Hu, H. *et al.* OTUD7B controls non-canonical NF-κB activation through deubiquitination of TRAF3. *Nature* **494**, 371–374 (2013).

137. Borodovsky, A. *et al.* Chemistry-Based Functional Proteomics Reveals Novel Members of the Deubiquitinating Enzyme Family. **9**, 1149–1159 (2002).

138. Fagerberg, L. *et al.* Analysis of the Human Tissue-specific Expression by Genome-wide Integration of Transcriptomics and Antibody-based Proteomics. *Mol. Cell. Proteomics* **13**, 397–406 (2014).

139. Schwanhäusser, B. *et al.* Global quantification of mammalian gene expression control. *Nature* **473**, 337–342 (2011).

140. Pasupala, N. *et al.* OTUB1 non-catalytically stabilizes the E2 ubiquitin- conjugating enzyme UBE2E1 by preventing its autoubiquitination. *J. Biol. Chem.* **293**, 18285–18295 (2018).

141. Edelmann, M. J. *et al.* Structural basis and specificity of human otubain 1-mediated deubiquitination. **390**, 379–390 (2009).

142. Sato, Y. *et al.* Molecular basis of Lys-63-linked polyubiquitination inhibition by the interaction between human deubiquitinating enzyme OTUB1 and ubiquitin- conjugating enzyme UBC13. *J. Biol. Chem.* **287**, 25860–25868 (2012).

143. Mevissen, T. E. T. & Komander, D. Mechanisms of Deubiquitinase Specificity and Regulation. *Annu. Rev. Biochem.* **86**, 159–192 (2017).

144. Soares, L. *et al.* Two isoforms of otubain 1 regulate T cell anergy via GRAIL. *Nat. Immunol.* **5**, 45–54 (2004).

145. Li, S. *et al.* Regulation of virus-triggered signaling by OTUB1- and OTUB2-mediated deubiquitination of TRAF3 and TRAF6. *J. Biol. Chem.* **285**, 4291–4297 (2010).

146. Wiener, R., Zhang, X., Wang, T. & Wolberger, C. The mechanism of OTUB1-mediated inhibition of ubiquitination. *Nature* **483**, 618–622 (2012).

147. Herhaus, L., Al-salihi, M., Macartney, T., Weidlich, S. & Sapkota, G. P. OTUB1 enhances TGFβ signalling by inhibiting the ubiquitylation and degradation of active SMAD2/3. *Nat. Commun.* **4**, 1–13 (2013).

148. Karunarathna, U. *et al.* OTUB1 inhibits the ubiquitination and degradation of FOXM1 in breast cancer and epirubicin resistance. *Oncogene* **35**, 1433–1444 (2016).

149. Stanišić, V., Malovannaya, A., Qin, J., Lonard, D. M. & O'Malley, B. W. OTU Domain-containing Ubiquitin Aldehyde-binding Protein 1 (OTUB1) Deubiquitinates Estrogen Receptor (ER) α and Affects ERα Transcriptional Activity. *J. Biol. Chem.* **284**, 16135–16145 (2009).

150. Edelmann, M. J., Kramer, H. B., Altun, M. & Kessler, B. M. Post-translational modification of the deubiquitinating enzyme otubain 1 modulates active RhoA levels and susceptibility to Yersinia invasion. *FEBS J.* **277**, 2515–2530 (2010).

151. Goncharov, T. *et al.* OTUB1 modulates c-IAP1 stability to regulate signalling pathways. *EMBO J.* **32**, 1103–1114 (2013).

152. Sun, X. & Dai, M. Deubiquitinating enzyme regulation of the p53 pathway: A lesson from Otub1. *World J. Biol. Chem.* **5**, 75–85 (2014).

153. Saldana, M. *et al.* Otubain 1: A non-canonical deubiquitinase with an emerging role in cancer. *Endocr. Relat. Cancer* **26**, R1–R14 (2019).

154. Black, M. W. & Boothroyd, J. C. Lytic Cycle of Toxoplasma gondii. *Microbiol. Mol. Biol. Rev.* **64**, 607–623 (2003).

155. DUBEY, J. P., LINDSAY, D. S. & SPEER, A. Structures of Toxoplasma gondii Tachyzoites, Bradyzoites, and Sporozoites and Biology and Development of Tissue Cysts. *Clin. Microbiol. Rev.* **94**, 426–434 (1998).

156. Haldar, K. Protein trafficking in apicomplexan parasites: crossing the vacuolar Rubicon. *Curr. Opin. Microbiol.* **32**, 38–45 (2016).

157. Lüder, C. G. K., Rahman, T., Lueder, C. G. K. & Rahman, T. Impact of the host on Toxoplasma stage differentiation. *Microb. Cell* **4**, 203–211 (2017).

158. White, M. W., Radke, J. R. & Radke, J. B. Toxoplasma development - turn the switch on or off? *Cell. Microbiol.* **16**, 466–472 (2014).

159. Tenter, A. M., Heckeroth, A. R. & Weiss, L. M. Toxoplasma gondii: from animals to humans. *Int. J. Parasitol.* **30**, 1217–1258 (2000).

160. Saeij, J. P. J., Boyle, J. P. & Boothroyd, J. C. Differences among the three major strains of Toxoplasma gondii and their specific interactions with the infected host. *Trends Parasitol.* **21**, 476–481 (2005).

161. Orr, G. *et al.* Distinct Strains of Toxoplasma gondii Feature Divergent Transcriptomes Regardless of Developmental Stage. *PLoS One* **9**, e111297 (2014).

162. Sabin-Feldman dye test - Learn Microbiology Online. Available at: https://microbeonline.com/sabin-feldman-dye-test/. (Accessed: 12th February 2020)

163.   d1210-1 : USDA ARS. Available at: https://www.ars.usda.gov/oc/images/photos/sep08/d1210-1/. (Accessed: 12th February 2020)

164.   Parasitology 07 Toxoplasma gondii, Pneumocystic carinii Flashcards - Cram.com. Available at: https://www.cram.com/flashcards/parasitology-07-toxoplasma-gondii-pneumocystic-carinii-933531. (Accessed: 12th February 2020)

165.   Hill, D. & Dubey, J. P. Toxoplasma gondii : transmission , diagnosis and prevention. *Clin. Microbiol. Infect.* **8**, 634–640 (2002).

166.   Halonen, S. K. & Weiss, L. M. Toxoplasmosis. in **114**, 125–145 (2013).

167.   Innes, E. A. A brief history and overview of toxoplasma gondii. *Zoonoses and Public Health* **57**, 1–7 (2010).

168.   Montoya, J. & Liesenfeld, O. Toxoplasmosis. *Lancet* **363**, 1965–1976 (2004).

169.   Pereira-Chioccola, V. L., Vidal, J. E. & Su, C. *Toxoplasma gondii* infection and cerebral toxoplasmosis in HIV-infected patients. *Future Microbiol.* **4**, 1363–1379 (2009).

170.   Cohen, S. B. & Denkers, E. Y. The gut mucosal immune response to Toxoplasma gondii. *Parasite Immunol.* **37**, 108–117 (2015).

171.   Dupont, C. D., Christian, D. A. & Hunter, C. A. Immune response and immunopathology during toxoplasmosis. *Semin. Immunopathol.* **34**, 793–813 (2012).

172.   Liu, C.-H. *et al.* Cutting edge: dendritic cells are essential for in vivo IL-12 production and development of resistance against Toxoplasma gondii infection in mice. *J. Immunol.* **177**, 31–5 (2006).

173.   Hou, B., Benson, A., Kuzmich, L., DeFranco, A. L. & Yarovinsky, F. Critical coordination of innate immune defense against Toxoplasma gondii by dendritic cells responding via their Toll-like receptors. *Proc. Natl. Acad. Sci.* **108**, 278–283 (2011).

174.   Andrade, W. A. *et al.* Combined action of nucleic acid-sensing Toll-like receptors and TLR11/TLR12 heterodimers imparts resistance to Toxoplasma gondii in mice. *Cell Host Microbe* **13**, 42–53 (2013).

175.   Yarovinsky, F. *et al.* TLR11 Activation of Dendritic Cells by a Protozoan Profilin-Like Protein. *Science (80-.).* **308**, 1626–1629 (2005).

176.   Pittman, K. J. & Knoll, L. J. Long-Term Relationships: the Complicated Interplay between the Host and the Developmental Stages of Toxoplasma gondii during Acute and Chronic Infections. *Microbiol. Mol. Biol. Rev.* **79**, 387–401 (2015).

177.   Filisetti, D. & Candolfi, E. Immune response to Toxoplasma gondii. *Ann. Ist. Super. Sanita* **40**, 71–80 (2004).

178.   Scanga, C. A. *et al.* Cutting Edge: MyD88 Is Required for Resistance to Toxoplasma gondii Infection and Regulates Parasite-Induced IL-12 Production by Dendritic Cells. *J. Immunol.* **168**, 5997–6001 (2002).

179.   Yarovinsky, F. Innate immunity to Toxoplasma gondii infection. *Nat. Rev. Immunol.* **14**, 109–121 (2014).

180.   Weidner, J. M. *et al.* Migratory activation of parasitized dendritic cells by the protozoan *Toxoplasma gondii* 14-3-3 protein. *Cell. Microbiol.* **18**, 1537–1550 (2016).

181.   DUBEY, J. P. Bradyzoite-Induced Murine Toxoplasmosis: Stage Conversion, Pathogenesis, and Tissue Cyst Formation in Mice Fed Bradzoites of - Different Strains of Toxoplasma gondii. *J. Eukaryot. Microbiol.* **44**, 592–602 (2007).

182.   Reddehase, M. J. & Lemmermann, N. A. W. Mouse model of cytomegalovirus disease and immunotherapy in the immunocompromised host: Predictions for medical translation that survived the

"test of time". *Viruses* **10**, (2018).

183.   Krmpotic, A., Bubic, I., Polic, B., Lucin, P. & Jonjic, S. Pathogenesis of murine cytomegalovirus infection. *Microbes Infect.* **5**, 1263–1277 (2003).

184.   Slavuljica, I. *et al.* Immunobiology of congenital cytomegalovirus infection of the central nervous system - The murine cytomegalovirus model. *Cell. Mol. Immunol.* **12**, 180–191 (2015).

185.   Alexandre, Y. O., Cocita, C. D., Ghilas, S. & Dalod, M. Deciphering the role of DC subsets in MCMV infection to better understand immune protection against viral infections. *Front. Microbiol.* **5**, 1–20 (2014).

186.   Dalod, M. *et al.* Dendritic cell responses to early murine cytomegalovirus infection: Subset functional specialization and differential regulation by interferon α/β. *J. Exp. Med.* **197**, 885–898 (2003).

187.   Tegtmeyer, P. K. *et al.* STING induces early IFN-β in the liver and constrains myeloid cell-mediated dissemination of murine cytomegalovirus. *Nat. Commun.* **10**, (2019).

188.   Zucchini, N. *et al.* Cutting edge: Overlapping functions of TLR7 and TLR9 for innate defense against a herpesvirus infection. *J. Immunol.* **180**, 5799–803 (2008).

189.   Wang, X. *et al.* OTUB1 inhibits CNS autoimmunity by preventing IFN-γ-induced hyperactivation of astrocytes. *EMBO J.* (2019). doi:10.15252/embj.2018100947

190.   Caton, M. L., Smith-Raska, M. R. & Reizis, B. Notch-RBP-J signaling controls the homeostasis of CD8-dendritic cells in the spleen. *J. Exp. Med.* **204**, 1653–64 (2007).

191.   Gilda, J. E. *et al.* Western blotting inaccuracies with unverified antibodies: Need for a Western Blotting Minimal Reporting Standard (WBMRS). *PLoS One* **10**, (2015).

192.   Hjerpe, R. *et al.* Efficient protection and isolation of ubiquitylated proteins using tandem ubiquitin-binding entities. *EMBO Rep.* **10**, 1250–1258 (2009).

193.   Mashayekhi, M. *et al.* CD8α+ Dendritic Cells Are the Critical Source of Interleukin-12 that Controls Acute Infection by Toxoplasma gondii Tachyzoites. *Immunity* **35**, 249–259 (2011).

194.   Peng, Y., Xu, R. & Zheng, X. HSCARG Negatively Regulates the Cellular Antiviral RIG-I Like Receptor Signaling Pathway by Inhibiting TRAF3 Ubiquitination via Recruiting OTUB1. *PLoS Pathog.* **10**, 1–10 (2014).

195.   Baietti, M. F. *et al.* OTUB1 triggers lung cancer development by inhibiting RAS monoubiquitination. *EMBO Mol. Med.* **8**, 288–303 (2016).

196.   Koblansky, A. A. *et al.* Recognition of Profilin by Toll-like Receptor 12 Is Critical for Host Resistance to Toxoplasma gondii. *Immunity* **38**, 119–130 (2013).

197.   Raetz, M. *et al.* Cooperation of TLR12 and TLR11 in the IRF8-Dependent IL-12 Response to Toxoplasma gondii Profilin. *J. Immunol.* **191**, 4818–4827 (2013).

198.   Shi, J. H. & Sun, S. C. Tumor necrosis factor receptor-associated factor regulation of nuclear factor κB and mitogen-activated protein kinase pathways. *Frontiers in Immunology* **9**, (2018).

199.   Cusson-Hermance, N., Khurana, S., Lee, T. H., Fitzgerald, K. A. & Kelliher, M. A. Rip1 mediates the trif-dependent Toll-like receptor 3- and 4-induced NF-κB activation but does not contribute to interferon regulatory factor 3 activation. *J. Biol. Chem.* **280**, 36560–36566 (2005).

200.   Shim, J. H. *et al.* TAK1, but not TAB1 or TAB2, plays an essential role in multiple signaling pathways in vivo. *Genes Dev.* **19**, 2668–2681 (2005).

201.   Hamidi, A. *et al.* Polyubiquitination of transforming growth factor β(TGFβ)- associated kinase 1

mediates nuclear factor-κB activation in response to different inflammatory stimuli. *J. Biol. Chem.* **287**, 123–133 (2012).

202. Arthur, J. S. C. & Ley, S. C. Mitogen-activated protein kinases in innate immunity. *Nature Reviews Immunology* **13**, 679–692 (2013).

203. Yamamoto, M. *et al.* Key function for the Ubc13 E2 ubiquitin-conjugating enzyme in immune receptor signaling. *Nat. Immunol.* **7**, 962–970 (2006).

204. Fukushima, T. *et al.* Ubiquitin-conjugating enzyme Ubc13 is a critical component of TNF receptor-associated factor (TRAF)-mediated inflammatory responses. *Proc. Natl. Acad. Sci. U. S. A.* **104**, 6371–6376 (2007).

205. Nakada, S. *et al.* Non-canonical inhibition of DNA damage-dependent ubiquitination by OTUB1. *Nature* **466**, 941–6 (2010).

206. Ordureau, A. *et al.* The IRAK-catalysed activation of the E3 ligase function of Pellino isoforms induces the Lys 63 -linked polyubiquitination of IRAK1. *Biochem. J.* **409**, 43–52 (2008).

207. Shembade, N., Ma, A. & Harhaj, E. W. Inhibition of NF-kappaB signaling by A20 through disruption of ubiquitin enzyme complexes. *Science* **327**, 1135–9 (2010).

208. Edelmann, M. J. J. *et al.* Structural basis and specificity of human otubain 1-mediated deubiquitination. *Biochem. J.* **418**, 379–390 (2008).

209. Zhang, Y. *et al.* Uev1A-Ubc13 catalyzes K63-linked ubiquitination of RHBDF2 to promote TACE maturation. *Cell. Signal.* **42**, 155–164 (2018).

210. Deng, L. *et al.* Activation of the Iκb kinase complex by TRAF6 requires a dimeric ubiquitin-conjugating enzyme complex and a unique polyubiquitin chain. *Cell* **103**, 351–361 (2000).

211. Hodge, C. D. *et al.* Ubc13: the Lys63 ubiquitin chain building machine. *Oncotarget* **7**, 64471–64504 (2016).

212. Carlile, C. M., Pickart, C. M., Matunis, M. J. & Cohen, R. E. Synthesis of free and proliferating cell nuclear antigen-bound polyubiquitin chains by the RING E3 ubiquitin ligase Rad5. *J. Biol. Chem.* **284**, 29326–29334 (2009).

213. Pasupala, N. *et al.* OTUB1 non-catalytically stabilizes the E2 ubiquitin-conjugating enzyme UBE2E1 by preventing its autoubiquitination. *J. Biol. Chem.* **293**, 18285–18295 (2018).

214. Cui, W. *et al.* -TrCP-Mediated IRAK1 Degradation Releases TAK1-TRAF6 from the Membrane to the Cytosol for TAK1-Dependent NF- B Activation. *Mol. Cell. Biol.* **32**, 3990–4000 (2012).

215. Xia, Z. P. *et al.* Direct activation of protein kinases by unanchored polyubiquitin chains. *Nature* **461**, 114–119 (2009).

216. Kimura, Y. *et al.* An Inhibitor of a Deubiquitinating Enzyme Regulates Ubiquitin Homeostasis. *Cell* **137**, 549–559 (2009).

217. Pertel, T. *et al.* TRIM5 is an innate immune sensor for the retrovirus capsid lattice. *Nature* **472**, 361–365 (2011).

218. Hu, L. *et al.* Oligomerization-primed coiled-coil domain interaction with Ubc13 confers processivity to TRAF6 ubiquitin ligase activity. *Nat. Commun.* **8**, (2017).

219. Koblansky, A. A. *et al.* The Innate Immune Receptor NLRX1 Functions as a Tumor Suppressor by Reducing Colon Tumorigenesis and Key Tumor-Promoting Signals. *Cell Rep.* **14**, 2562–75 (2016).

220. Yoshimura, S., Bondeson, J., Foxwell, B. M. J., Brennan, F. M. & Feldmann, M. Effective antigen

presentation by dendritic cells is NF-κB dependent: coordinate regulation of MHC, co-stimulatory molecules and cytokines. *Int. Immunol.* **13**, 675–683 (2001).

221. Hou, B., Benson, A., Kuzmich, L., DeFranco, A. L. & Yarovinsky, F. Critical coordination of innate immune defense against Toxoplasma gondii by dendritic cells responding via their Toll-like receptors. *Proc. Natl. Acad. Sci.* **108**, 278–283 (2011).

222. Ge, Y. *et al.* Natural killer cell intrinsic toll-like receptor MyD88 signaling contributes to IL-12-dependent IFN-γ production by mice during infection with Toxoplasma gondii. *Int. J. Parasitol.* **44**, 475–484 (2014).

223. Trinchieri, G. Interleukin-12 and the regulation of innate resistance and adaptive immunity. *Nat. Rev. Immunol.* **3**, 133–46 (2003).

224. Lambert, H., Hitziger, N., Dellacasa, I., Svensson, M. & Barragan, A. Induction of dendritic cell migration upon Toxoplasma gondii infection potentiates parasite dissemination. *Cell. Microbiol.* **8**, 1611–23 (2006).

225. Lachenmaier, S. M., Deli, M. A., Meissner, M. & Liesenfeld, O. Intracellular transport of Toxoplasma gondii through the blood-brain barrier. *J. Neuroimmunol.* **232**, 119–30 (2011).

226. Kanatani, S. *et al.* Voltage-dependent calcium channel signaling mediates GABAA receptor-induced migratory activation of dendritic cells infected by Toxoplasma gondii. *PLOS Pathog.* **13**, e1006739 (2017).

227. Mashayekhi, M. *et al.* CD8α+Dendritic Cells Are the Critical Source of Interleukin-12 that Controls Acute Infection by Toxoplasma gondii Tachyzoites. *Immunity* **35**, 249–259 (2011).

228. Xuan, N. T. *et al.* A20 expression in dendritic cells protects mice from LPS-induced mortality. *Eur. J. Immunol.* **45**, 818–28 (2015).

229. Tabeta, K. *et al.* Toll-like receptors 9 and 3 as essential complonents of innate immune defense against mouse cytomegalovirus infection. *Proc. Natl. Acad. Sci. U. S. A.* **101**, 3516–3521 (2004).

230. Puttur, F. *et al.* Conventional Dendritic Cells Confer Protection against Mouse Cytomegalovirus Infection via TLR9 and MyD88 Signaling. *Cell Rep.* **17**, 1113–1127 (2016).

231. Krug, A. *et al.* TLR9-dependent recognition of MCMV by IPC and DC generates coordinated cytokine responses that activate antiviral NK cell function. *Immunity* **21**, 107–119 (2004).

232. Rosadini, C. V & Kagan, J. C. Early innate immune responses to bacterial LPS. *Curr. Opin. Immunol.* **44**, 14–19 (2017).

233. Motshwene, P. G. *et al.* An Oligomeric Signaling Platform Formed by the Toll-like Receptor Signal Transducers MyD88 and IRAK-4. *J. Biol. Chem.* **284**, 25404–25411 (2009).

234. Lork, M., Verhelst, K. & Beyaert, R. CYLD, A20 and OTULIN deubiquitinases in NF-κB signaling and cell death: so similar, yet so different. *Cell Death Differ.* **24**, 1172–1183 (2017).

235. Li, Y. *et al.* Preventing abnormal NF-κB activation and autoimmunity by Otub1-mediated p100 stabilization. *Cell Res.* **29**, 474–485 (2019).

236. Ishikawa, H., Ma, Z. & Barber, G. N. STING regulates intracellular DNA-mediated, type i interferon-dependent innate immunity. *Nature* **461**, 788–792 (2009).

237. Stempel, M., Chan, B. & Brinkmann, M. M. Coevolution pays off: Herpesviruses have the license to escape the DNA sensing pathway. *Medical Microbiology and Immunology* **208**, 495–512 (2019).

238. Chan, B. *et al.* The murine cytomegalovirus M35 protein antagonizes type I IFN induction downstream of pattern recognition receptors by targeting NF-κB mediated transcription. *PLoS Pathog.* **13**, (2017).

239. Stempel, M. *et al.* The herpesviral antagonist m152 reveals differential activation of STING -dependent IRF and NF -κB signaling and STING 's dual role during MCMV infection . *EMBO J.* **38**, (2019).

240. Kool, M. *et al.* The Ubiquitin-Editing Protein A20 Prevents Dendritic Cell Activation, Recognition of Apoptotic Cells, and Systemic Autoimmunity. *Immunity* **35**, 82–96 (2011).

241. Hammer, G. E. *et al.* Expression of A20 by dendritic cells preserves immune homeostasis and prevents colitis and spondyloarthritis. *Nat. Immunol.* **12**, 1184–1193 (2011).

242. Jin, J. *et al.* Epigenetic regulation of the expression of Il12 and Il23 and autoimmune inflammation by the deubiquitinase Trabid. *Nat. Immunol.* **17**, 259–68 (2016).

243. Juang, Y. C. *et al.* OTUB1 Co-opts Lys48-Linked Ubiquitin Recognition to Suppress E2 Enzyme Function. *Mol. Cell* **45**, 384–397 (2012).

244. Wunderlich, R. *et al.* Interconnection between DNA damage, senescence, inflammation, and cancer. *Front. Biosci. (Landmark Ed.* **22**, 348–369 (2017).

245. Neves-Costa, A. & Moita, L. F. Modulation of inflammation and disease tolerance by DNA damage response pathways. *FEBS J.* **284**, 680–698 (2017).

246. Kraft, D. *et al.* NF-κB-dependent DNA damage-signaling differentially regulates DNA double-strand break repair mechanisms in immature and mature human hematopoietic cells. *Leukemia* **29**, 1543–1554 (2015).

247. D'Arcy, P., Wang, X. & Linder, S. Deubiquitinase inhibition as a cancer therapeutic strategy. *Pharmacol. Ther.* **147**, 32–54 (2015).

248. Wang, Y. *et al.* OTUB1-catalyzed deubiquitination of FOXM1 facilitates tumor progression and predicts a poor prognosis in ovarian cancer. *Oncotarget* **7**, 36681–36697 (2016).

Erklärung

Hiermit erkläre ich, dass ich die von mir eingereichte Dissertation zum Thema:

Dendritic cell-specific function of OTUB1 in inflammation and infection

selbstständig verfasst, nicht schon als Dissertation verwendet habe und die benutzten Hilfsmittel und Quellen vollständig angegeben wurden.

Weiterhin erkläre ich, dass ich weder diese noch eine andere Arbeit zur Erlangung des akademischen Grades doctor rerum naturalium (Dr. rer. nat.) an anderen Einrichtungen eingereicht habe.

Magdeburg, den

20.02.2020 Floriana Mulas